1989

Ablation on Barpu glacier, Karakoram Himalaya, Pakistan a study of melt processes on a faceted, debris-covered ice surface

Mohammad Inamullah Khan
Wilfrid Laurier University

NOTICE

The quality of this microform is heavily dependent upon the quality of the original thesis submitted for microfilming. Every effort has been made to ensure the hig' iest quality of reproduction possible.

If pages are missing, contact the university which granted the degree.

Some pages may have indistinct print especially if the original pages were typed with a poor typewriter ribbon or if the university sent us an inferior photocopy.

Reproduction in full or in part of this microform is governed by the Canadian Copyright Act, R.S.C. 1970, c. C-30, and subsequent amendments.

AVIS

La qualité de cette microforme dépend grandement de la qualité de la thèse soumise au microfilmage. Nous avons tout fait pour assurer une qualité supérieure de reproduction.

S'il manque des pages, veuillez communiquer avec l'université qui a conféré le grade.

La qualité d'impression de certaines pages peut laisser à désirer, surtout si les pages originales ont été dactylographiées à l'aide d'un ruban usé ou si l'université nous a fait parvenir une photocopie de qualité inférieure.

La reproduction, même partielle, de cette microforme est soumise à la Loi canadienne sur le droit d'auteur, SRC 1970, c. C-30, et ses amendements subséquents.

ABLATION ON BARPU GLACIER, KARAKORAM HIMALAYA, PAKISTAN; A STUDY OF MELT PROCESSES ON A FACETED, DEBRIS-COVERED ICE SURFACE

By

Mohammad Inamullah Khan

B.E. (CIVIL),

N.E.D. University of Engineering and Technology

Karachi, Pakistan, 1984

THESIS

Submitted to the Department of Geography

in partial fulfilment of the requirements

for the Master of Arts degree

Wilfrid Laurier University

1989

ISBN 0-315-50091-3

Preface

Pakistan is dependent on the main Indus River and its westerly tributaries for power generation, irrigation, and fresh water supply. The Indus tributaries are primarily fed by the melting of snow and ice in the high mountains -- Karakoram and Himalaya.

A Snow and Ice Hydrology Project (S.I.H.P) was established in 1985 to investigate the hydrology of the mountain headwaters of the Indus, and especially of snow and ice conditions above 2,500 m. a.s.l. This is a collaborative project funded jointly by the Water and Power Development Authority (WAPDA), the Canadian International Development Reasearch Centre (IDRC), and Wilfrid Laurier University. In Pakistan, the project is coordinated by the Hydrology Research Directorate of WAPDA in Lahore. In Canada, the project coordination is undertaken by the Cold Regions Research Centre at Wilfrid Laurier University in Waterloo, Ontario. A total project budget of some $1.6 million (Canadian) is shared about equally by Pakistan and Canada.

The basic aim of this project is to improve our understanding of the

hydrology of the Upper Indus Basin (U.I.B). It has involved fieldwork, with applications of remote sensing, analysis of existing river discharge and meteorological observations to provide the basis for improved seasonal streamflow forecasting for water management through effective reservoir operation to control/manage floods to enable Pakistan to make effective use of water. Both Pakistani engineers and Canadian scientists are involved in all phases of the work.

Field work has been concentrated in two main areas; the Biafo - Hispar and Barpu - Bualtar glacier areas of the Central Karakoram, and the Nanga Parbat/Kaghan Valley area. In both areas basic data are being collected on meteorology, hydrology, and glaciology. Glaciology has mainly involved the study of melting and flow rate in combination with depth of the glacier. The effects of debris cover on ice melting have been studied for a long time, but the local topography of the glacier has not been taken into account. The small differently oriented slope surfaces, termed facets, occupy a significant area in the ablation zones of a glacier especially in the Central Karakoram and Himalaya glaciers which positively affect the overall ablation of a glacier. In essence the present study is the first one in which both of these factors were involved in estimating ablation. The credit goes to Dr. Gordon Young, who gave me this idea during the summer field season 1986 in Pakistan, which was further encouraged by Dr. Kenneth Hewitt.

I wish to express my deep appreciation to Dr. Gordon Young, Dr. Kenneth Hewitt, and Dr. Jim Gardner for their guidance and assistance in the field and in the office. Many thanks to all WAPDA and Canadian members of the project for their help in various phases of this research.

I am particularly grateful to the Geography department and Computing service at WLU as a whole for excellent working facilities and cooperation in all aspects. Special thanks to Dr. Barry Boots and Dr. H. C. Bezner who helped in computing data and Pam Schauss who helped in making maps and photographs.

I would like to acknowledge Mr. Mike Stone and Mr. Eric Mattson for valuable discussion and comments.

The study was supported financially by IDRC (Canada) and WAPDA (Pakistan).

ABSTRACT

Snowfall at high elevations in the Central Karakoram mountain range is the major source of moisture for the Upper Indus Basin. The snowfall is reflected in the high percentage of glacier cover in this region. These glaciers act as natural regulators of streamflow; storing water in winter and releasing it in summer.

Since the climatic conditions can be considered as nearly uniform in a small area, the local topography and debris conditions on the glaciers are some of the more predominant factors in controlling melting of glacier ice. In Karakoram glaciers, heavy debris loads generally protect the ice beneath by reducing melting; whereas facets of bare ice generally melt faster by absorbing greater amounts of solar radiation due to slope aspect, angle, and a thin layer of sediment which accelerates ablation. Furthermore, in faceted areas, more ice is exposed to the atmosphere than in other parts of the glacier. Thus a higher ablation rate can be expected in highly faceted ice.

The aim of this thesis is to evaluate the importance of debris cover and surface ruggedness in explaining the pattern of ablation in the Central Karakoram on the Barpu Glacier.

Average flat surface ablation rate measured in the study area, is estimated at 2.7 cm/day. The ablation rate is reduced to 2.3 cm/day when the debris cover thickness distribution over the entire study area is taken into account. The average debris cover thickness was 12.4 cm, which greatly decelerates ablation. Facets, which accounted for 8.5% of the study area, were dominated by SW and W orientations. The highest facet ablation rate (6.7 cm/day) was measured on SW facets which cover almost 45% of the total facet area. The weighted facet ablation is estimated at 5.7 cm/day. The net ablation rate, based on unweighted debris covered ablation (2.7 cm/day) and facet ablation (5.7 cm/day), is estimated at 3 cm/day (i.e. 11.1% increase due to facets), whereas the net ablation rate, based on weighted debris covered ablation (2.3 cm/day) and facet ablation, is estimated at 2.6 cm/day (i.e. 13% increase due to facets). Radiation and air temperature were the most significant factors as far as the external meteorological conditions are concernd. Almost 71% variation in ablation is explaind by these two parameters.

Contents

CHAPTER 2

CHAPTER 3

CHAPTER 4

CHAPTER 5

LIST OF TABLES

LIST OF FIGURES

LIST OF PLATES

Chapter 1

Introduction

1.1 PREAMBLE

Pakistan is primarily dependent upon irrigated agriculture in the Indus Basin. In fact, the world's largest contiguous irrigation system is found in the Indus Plains. This irrigation system includes inter-river link canals and two major storage reservoirs at Mangla and Tarbela that regulate as well as supplement the water supplies. The Indus River is Pakistan's main source of water for irrigation, power generation, and water supply for urban and industrial units.

The waters of the Indus derive largely from high-altitude snowfalls and the glaciers of the northern mountain ranges, the Karakoram; Kohistan; and Himalaya. About 12% of the Upper Indus Basin (U.I.B.) is covered by perennial snow and ice (Hewitt, 1985a and 1988b). The hydrology of the U.I.B. is affected by the snow and ice conditions in the Karakoram Mountains which extend some 480 km Northwest to Southeast and supply the main stem of the Indus with most of its water. These mountains are heavily glacierized (see Figure 1.1).

Figure 1.1
GLACIERS AND DRAINAGE in the KARAKORAM-HIMALAYA RANGES

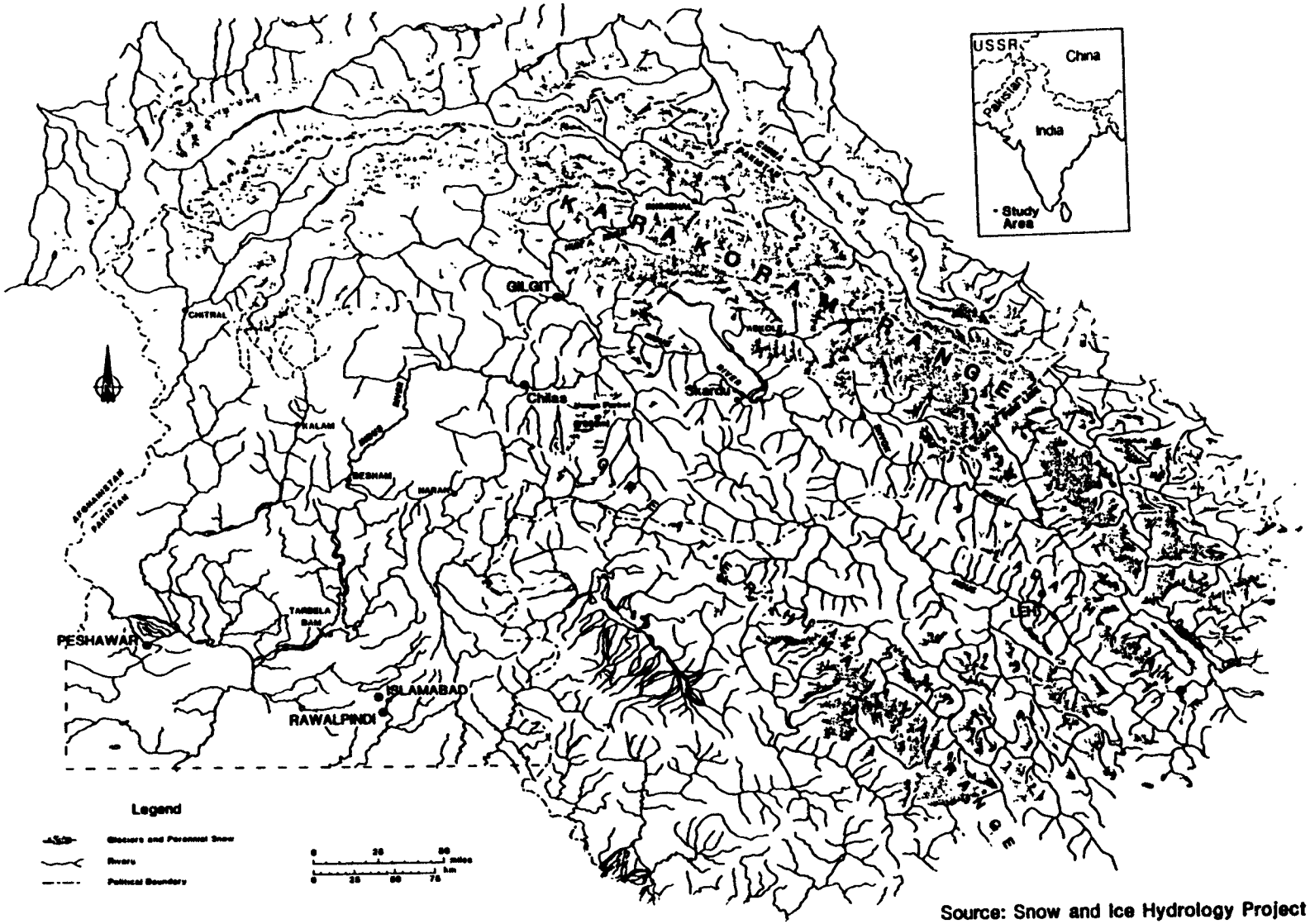

Source: Snow and Ice Hydrology Project

About 37% of their area is glacier covered (Tarar, 1982) compared to the Greater Himalaya (17% glacier covered) and the Alps (2.2% glacier covered) (Wissman, 1959, cited Mercer, 1975). The main stem of the Indus contributes more than half the total flow of the Indus system.

The glaciers of the Indus Basin originate in high snowfall areas, generally above 4,000 m a.s.l. About 70-80% of the total annual streamflow from the U.I.B. originates as snow and ice melt in the Karakoram (Hewitt, 1988a and Wake, 1987), compared to 50% in Himachal Pradesh, between Kashmir and Nepal, and 30% from the Ganges tributaries in Nepal. Most of the melt water yield is derived from glacier ice that has flowed to lower altitudes, mainly in the range 3000-5000 m. a.s.l., and has melted during an intense period of melting that usually dominates river flow from mid-July until early September.

The hydrology of glacier-fed rivers is strongly influenced by glacier behaviour. Glaciers have a regulatory effect on streamflow. In years of low precipitation (winter or summer snowfall) the glacier component of streamflow is large (Young, 1981). The principal influences of glaciers on streamflow are often unexpected contributions to streamflow volume, a delay of the maximum seasonal flow, and a decrease in annual and monthly variation of runoff (Fountain and Tangborn, 1985).

The melting (rates and variability) of Karakoram glaciers is one of the most important hydrological components influencing streamflow and is greatly affected by supraglacial debris cover and local topography on the glacier. These two factors may play a significant role in fluctuations in water yield from the whole U.I.B. That, in turn, reflects the predominent role of solar insolation in high mountain

snow and ice melt.

The melting of relatively smooth and clean ice surfaces is relatively easy to measure, as surface lowering translates into a volume of meltwater produced and an ablation rate. In rugged ice ablation zones the situation is not so simple as such surfaces ablate at different rates within a small area due to differential amounts of incoming solar radiation. The situation becomes more complicated when the rugged ice surface is covered by a debris layer, thus presenting all types of surfaces (i.e. slope, horizontal, clean ice, and debris covered etc.) in their full contrast within a small region.

Small slope surfaces having different orientations are common surficial features of ablation zones. These slopes are generally referred to as Ice Cliffs or Facets, which have different and interesting chracteristics due to their aspects and slope gradient. Between 25% and 90% of the ablation zones of Karakoram glaciers are covered with variable amounts of ablation moraine (Wake, 1985) and more than 15% of ablation zones are faceted (Inoue and Yoshida, 1980). According to Hewitt (1985b) about one-fifth of the ablation zone of Biafo glacier is debris covered. The Hispar glacier has some 30 km of its ablation zone covered, while the Baltoro has a still higher ratio. In Khumbu Region, Nepal, the debris covered type glaciers are 15 times larger in area and 5 times longer in length than clean ice type glaciers (Fujii and Higuchi, 1977).

The surface debris cover largely controls the rates of ice melt which, in turn, affects the mode of formation of glacially deposited land forms (Young, 1981). It has long been recognized that a thin layer accelerates the ablation rate of the underlying ice, whereas a thick layer retards it (Nakawo and Takahashi, 1982). On

the other hand facets tend to increase the overall ablation rate by absorbing greater amounts of solar radiation, depending on their concentration and distribution with respect to orientation and area. The southern facets, for example, receive greater insolation resulting in significantly higher melting rates of ice as compared to northern facets. This suggests that facet ablation is mainly controlled by its physical features, i.e. aspect, and gradient. While debris composition and concentration are the main controlling factors for flat surface ablation.

The present research in the Karakoram, therefore, has two different components. The basis of this study is to understand facet ablation as a fundamental component of the hydrology of the U.I.B. and to understand the behaviour of ice melting under a debris layer. In essence, this study attempts to apply a unique technique to estimate representative ice ablation under variable topographical, morphological, and meteorological conditions. This is accomplished by developing an ablation stake network that covers a range of differently oriented facets and varying thicknesses of debris covers in the ablation zone of Barpu glacier at Sumaiyar Bar.

1.2 RESEARCH OBJECTIVES

The goal of this research is to determine the facet and flat surface ice surface ablation on Barpu glacier at about 3,500 m a.s.l. This is done by selecting the facets on geometrical basis (i.e. orientation and slope angle). The stakes for measuring the facet ablation were also used for flat surface ablation measurements under their existing debris conditions, in addition ablation was measured on one stake profile denoted by P, and on one stake diamond (established for strain rate measurements) denoted by S.

The main objectives were:

1. to provide an estimate of ablation rate, in the U.I.B., while accounting for facet contribution;

2. to determine the debris cover effect on ablation rates, and to estimate the ablation over a large area on the basis of debris concentrations;

3. to compare the ablation rate or runoff from facets having different aspects and slope angles;

4. to estimate the percentage of debris-free (facets) and debris-covered area per unit area (i.e. 1 km^2);

5. to estimate the percentage of the facet area on the basis of their orientation;

6. to provide an estimate of the debris budget, i.e. size distribution and percentage of debris thicknesses per unit area (1 km^2);

7. to study the effects of meteorological conditions (Radiation, Temperature, and Relative humidity etc.) on ablation rates.

1.3 ORGANIZATION OF RESEARCH

Members of the Snow and Ice Hydrology Project (S.I.H.P.) spent the 1987 summer season in the Barpu Glacier Basin. Major field activities were performed during late spring and early summer, since this period represents a large runoff from snow and ice. Meteorological and hydrological conditions on Barpu glacier at Sumaiyar Bar (3,500 m a.s.l.) were measured. The focus of the measurements was on:

i) facet melting and its physical characteristics,

ii) ablation under debris cover,

iii) debris thickness percentage and size distribution, and

iv) meteorological conditions affecting ablation.

1.4 LITERATURE REVIEW

The effect of facets on ice ablation has not been extensively reported in the literature. Some researchers, for example, Young (1971) and Lewkowicz (1986), have measured the incoming solar radiation on large areas considering the surface geometry. But in their studies they considered surface in an attempt to get the appropriate value of incoming short wave radiation on different slopes. Furthermore, they considered the whole plot (e.g. up to 1.5 km^2) as one slope or surface. Whereas in the present study; there were hundreds of small and large (e.g. 1 to 400 m^2) differently oriented facets within a small area (say 1 km^2) which are contrasted from their surrounding debris covered area. Consequently the facet contribution to the ablation rate is never taken into account. The present study, therefore, is one of the first attempts to consider the role of facets on the overall rate of ablation.

1.4.1 Facet Studies

Wushiki (1977) indirectly studied facets on the Kongma Glacier in Khumbu, Nepal. The primary focus of his work was to study the stratigraphy of the glacier. Inoue Jiro (1978) completed mass balance studies on the Kongma Glacier from 1973 to 1976. He measured the ablation rate of a few facets, but his study was limited to observing the collapse of facets only. The interesting part of that work relevant here, how photographs taken in 1970 by Inoue and in 1977 by Wushiki, show a similar arrangement of facets. These photographs suggest that recession of the facet is compensated by flow of the glacier.

In 1978 Inoue and Yoshida (1980) measured the ablation of a few facets in one of their classified areas during the ablation study on Khumbu glacier. The

average facet ablation rate was found to be 2.3 cm/day (highest was 4.5 cm/day) compared to flat surface ablation of 0.15 cm/day under a debris cover 1.2 m thick. The mean ablation rate was 0.3 cm/day, knowing the facet area a 15%. Ablation was not compared on the basis of slope aspect and angle, since the purpose of their ablation study was not to investigate the effects of facets and their co· ·bution to overall ablation. It was treated only as a minor portion of the main study.

1.4.2 Debris Co··er Effect on Ablation

The effect of debris cover on ablation rates has been investigated by a number of researchers. The following is a review of some of these studies. Fujii (1974) studied the ablation of snow under a debris cover varying in thickness from 0.5 to 8 cm, scattered on nine test fields on a snowpatch just beside the Rikha Samba Glacier in Hidden Valley, Mukut Himalaya. The greatest acceleration of ablation was found under a debris cover of 0.5 cm thick, with a critical thickness of 1.6 cm. Ablation was retarded under debris layers thicker than 1.6 cm. A similar phenomenon was observed on Khumbu Glacier by Inoue (1977). He found that the scattered debris on the glacier surface promotes melting of ice by absorption of solar radiation, while thicker debris near the glacier terminus reduces the melting of ice.

Inoue and Yoshida (1980) studied the characteristics of the ablation process in connection with properties of supra‹ lacial debris and micrometeorological conditions during the summer monsoon of 1978 in Nepal on the Khumbu ‚lacier. According to the characteristics of supraglacial debris they classified the ablation zone of glacier into 4 areas. The average ablation rate of 2.5 cm/day was obtained in the upper half of the ablation zone where glacier flow was active, while in the lower stagnant area it was less than 0.4 cm/day due to the heavy debris load. In the area

with thick debris cover (1.2 m) and ablation lakes, the ablation rate was only 0.15 cm/day. An average ablation of 1.9 cm/day was measured in the ogive (debris free) zone while in the lower part (ice pinnacle zone), with supraglacial debris deposits as a dispersed bouldery veneer around ice pinnacles, it was 2.5 cm/day. The schist zone (where dark colored schistose debris with low concentration and albedo enhanced ablation) melted more rapidly than in the granitic zone (where light colored granitic debris was the major component). The ablation rate here ranged from 0.8 to 3.7 cm/day, and differed from site to site according to the thickness and lithology of the debris cover.

Nakawo and Young (1981 and 1982) investigated the effect of surface debris of known properties (i.e. thermal conductivity and resistance, specific heat, density etc.) on rates of ice melt at Peyto Glacier in the Rocky Mountains of Alberta, Canada, in 1979. Six plots of varying thicknesses (0.01 to 0.1 m) of artificial debris layers were prepared near the snout of the glacier. External variables including radiation and air temperature, as well as the physical characteristics of the debris layers were studied. The results indicate a general asymptotic decrease in the ablation rate as thermal resistance of layer increases. Thermal resistance is a function of thickness and the thermal conductivity of the debris surface. Results also indicate a slightly higher ablation rate, on average, for a dry surface as compared to a wet surface.

Hewitt (1985c) found that debris covers have a profound effect upon melting on the Biafo Glacier, Northern Pakistan. He studied the effects of varying thicknesses as well as the different types of material of debris cover. Five experimental sites were set up. Three of the sites were examples of differing natural situations, the first on almost clear ice, the second on a medial moraine and the

third on an area of multiple small debris cover. Two other sites were artificially prepared by material derived from well-sorted deposits on the glacier. At one of them, five experimental plots were set up with layers of fine debris varying in thickness from a film of grains to 5 cm. At the other plot, rock fragments varying in size from small cobbles to boulders 40 cm in diameter were set out. Results show that fine-grained and thin veneers greatly magnify rates of melting while thicker and coarser covers serve to insulate the ice and reduce rates of melting.

Gardner (1986) observed the same tendency on Rakhiot Glacier in Pakistan. An ablation rate of 7 cm/day was observed on a clean ice surface, while under a debris cover of 40 cm, it was found to be only 0.8 cm/day. The highest ablation (11.3 cm/day) occurred beneath a debris cover about 1 cm thick.

Watanabe, Iwata, and Fushimi (1986) studied the ablation under 11 morphologically classified debris-covered surfaces (classified by Iwata et. al., 1980) on Khumbu glacier, Nepal. In the highest part of the ablation area, the ablation occurred at constant rates. Below this, dominant ablation around the supraglacial lakes and streams occurred, in addition to inactive ice melting under the debris cover. Further down, the ablation rates reduce because of thicker debris cover. At the terminus the thicker debris cover protects the glacier ice from melting, though slight melting occurs in subglacial or englacial channels.

1.4.3 Summary

There is a positive impact of the facets on ablation rate. They generally melt faster than the surrounding debris covered surfaces. The net facet effect on overall ablation rate depends on the average facet ablation rate and the areal concentration

in the ablation zone.

Concerning the effect of debris cover on ablation, previous studies have shown that ablation is a function of the thickness and lithology of the debris cover in addition to the external meteorological conditions. Debris layers less than 3 cm in thickness, dark colored, dry, and fine-grained materials, all magnify the ablation rate. Whereas thicker, light colored, and coarser debris cover serves to insulate the ice.

Chapter 2

Geography and Climate

2.1 OVERVIEW

Pakistan is an arid to semi-arid region with surface waters derived mainly from the River Indus and its tributaries. It has an extensive network of irrigation canals, the largest in the world (Abbas, 1967). The irrigation system in the Indus plains is fed through 16 diversion dams and 580 km of inter-river link canals. In addition, the system has three major storage reservoirs: namely Mangla, Tarbela, and Chashma (Tarar, 1982).

Much of Pakistan is mountainous. Its northernmost territories consist of tangled mountains notably, the western Himalayas, Karakoram, and Hindu Kush ranges. The headwaters of the Indus River originate in these mountains and flow through wild gorges to the plains. The lives of more than a hundred million people depend on the waters of this huge river system, together with its glacier sources in High Asia (Kick, 1978). Its drainage basin covers almost the whole of Pakistan as well as parts of India, China, and Afghanistan (Figure 2.1).

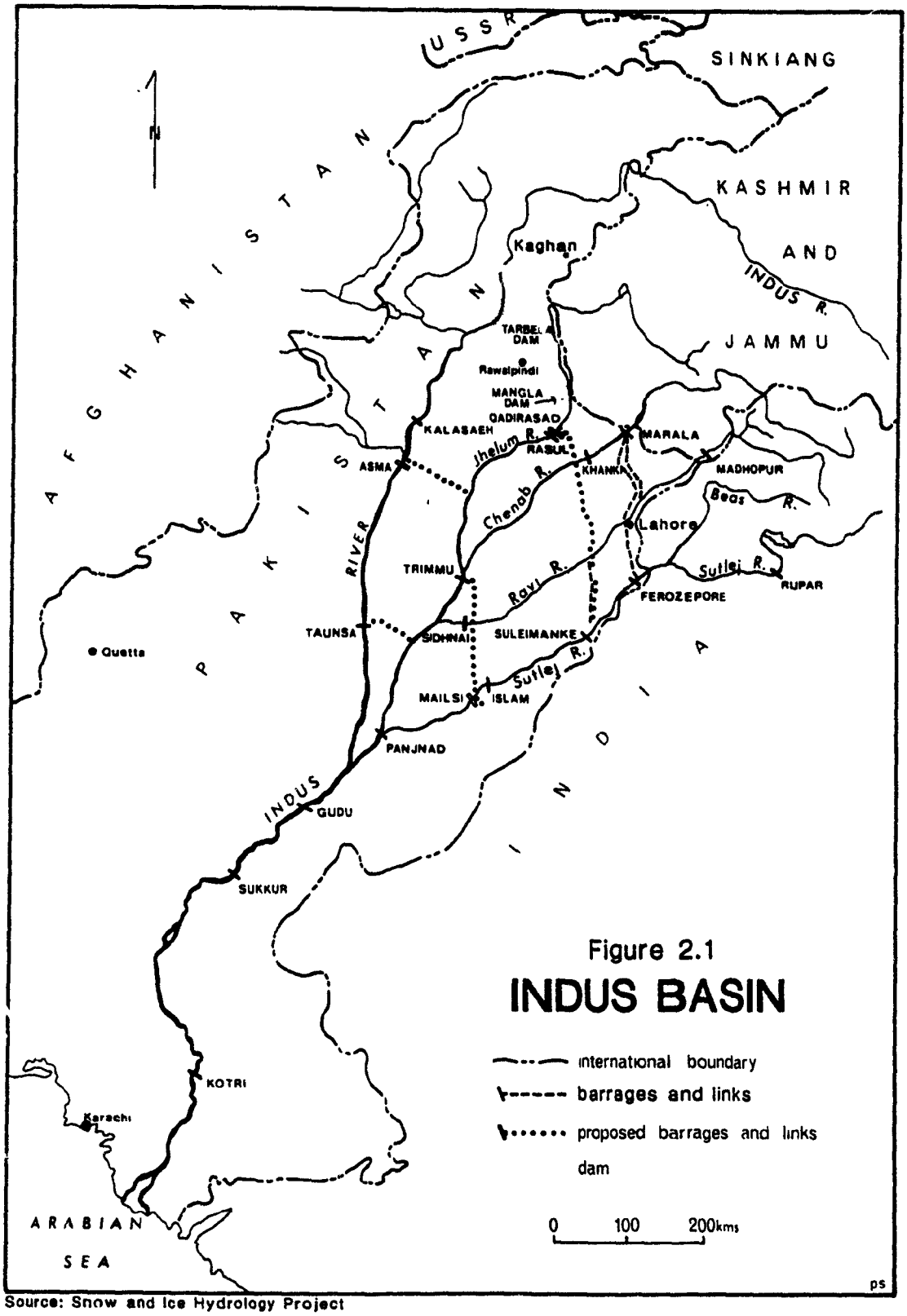

Figure 2.1

INDUS BASIN

Source: Snow and Ice Hydrology Project

The Upper Indus Basin (U.I.B.) serves as a watershed above the Tarbela Reservoir, and comprises an area of approximately 250,000 km^2. Thirteen percent of it is covered by perennial snow and ice. At the end of the winter season, an area of about approximately 200,000 km^2 in the mountainous regions of the U.I.B. is extensively snowcovered. For the Indus main stem, snow may cover more than 90% of the catchment above Tarbela Dam, and commonly more than 70% (Hewitt, 1985a).

The Karakoram Range in northern Pakistan is one of the most heavily glacierised regions outside of the polar realms, and holds some of the world's longest valley glaciers (Schultz, 1974). The water supply of the Upper Indus System depends on the hydrological behaviour of these glaciers.

With the independence and partitioning of India in 1947, most of the Indus Valley became the territory of Pakistan. The international boundary between India and Pakistan cut the irrigation system of the Bari Doab and the Sutluj Valley projects, originally designed as one scheme, into two parts (Figure 2.1). The Indus Waters Treaty, signed in 1960, is the basis of water sharing between the two countries. The treaty gives India full control of the eastern tributary streams, Ravi, Beas, and Sutlej; and allows Pakistan to utilize exclusively the flow of the Indus and most of the waters of the Chenab and Jhelum. India has use of the Chenab and Jhelum for needs within Jammu and Kashmir.

Pakistan, through this Treaty, has become largely dependent on water from the snow and ice sources in the northern mountains for the Tarbela and Mangla Reservoirs. Just at the time of greatest water need in summer, the supply of meltwater is most plentiful. In recent decades, mainly under the direction of the

Water and Power Development Authority (WAPDA), huge projects have been undertaken to harness the waters of the Indus.

WAPDA conducted snow surveys on a limited scale in the Kaghan Valley in 1961 through 1968 which were limited in area and extent. The snow surveys continued in 1976, with use of the Landsat Imagery. The results were utilized to determine the areal extent of snow cover and a relationship developed for the prediction of snowmelt runoff in the Indus River at Besham and the Jhelum River at Kohala.

In 1974 the World Meteorological Organization (WMO), United Nations Development Programme (UNDP), Pakistan Meteorological Department (PMD), and WAPDA jointly completed a project titled "Improvement of River Flow Forecasting and Flood Warning System for the Indus River Basin in Pakistan" (WAPDA, 1982). Under this project, in addition to Radar and automatic picture transmission (APT) facilities, reporting stream gauges and precipitation gauges with telemarks have been installed at 41 stations. The network of gauging stations in the U.I.B. is shown in figure 2.2.

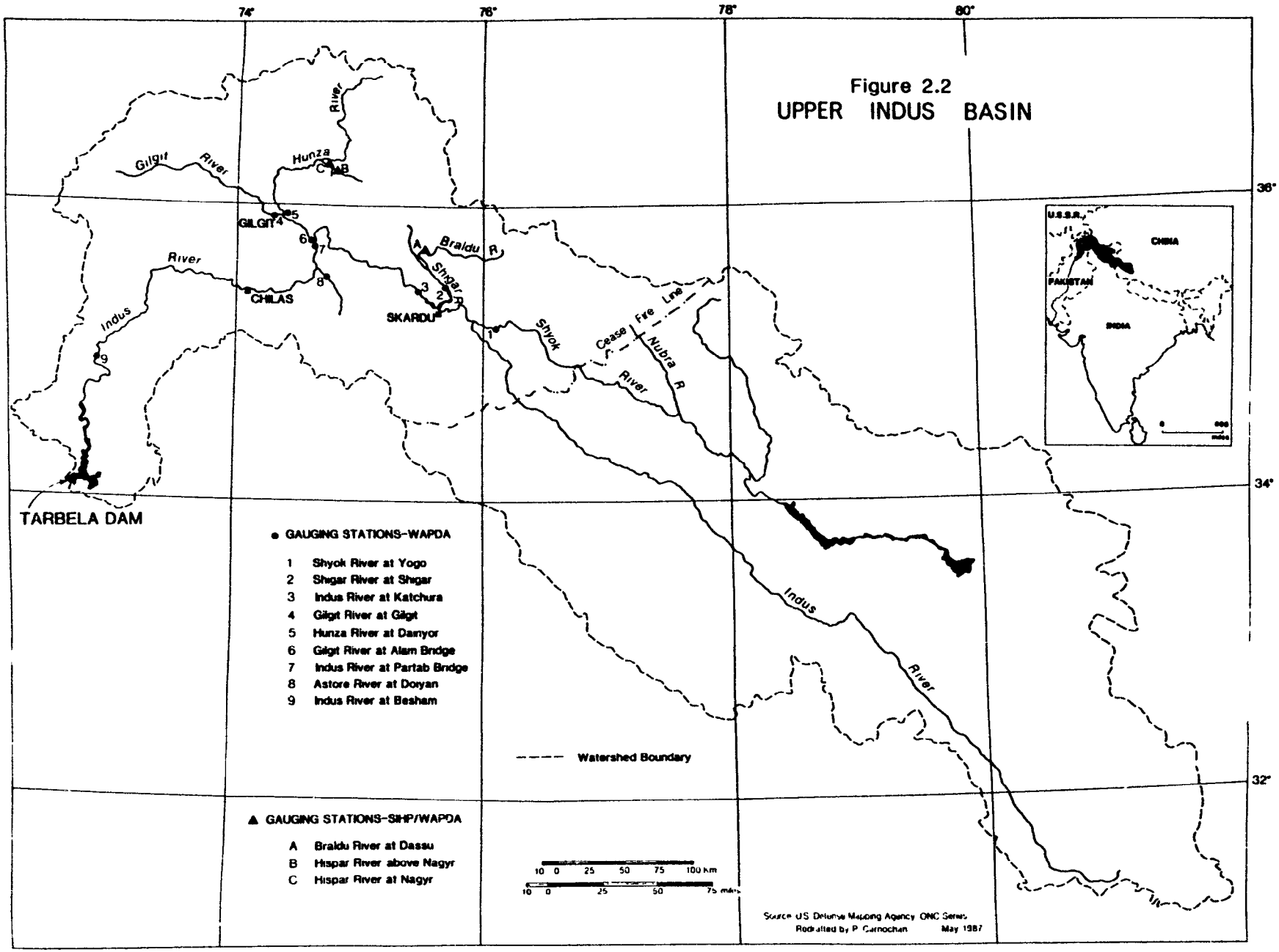
Figure 2.2
UPPER INDUS BASIN
74°
76°
78°
80°
36°
34°
32°
Gilgit River
Hunza River
GILGIT
CHILAS
SKARDU
Braldu R
Shigar R
Indus River
Shyok River
Cease Fre Line
Nubra R
TARBELA DAM
U.S.S.R.
CHINA
PAKISTAN
INDIA
GAUGING STATIONS-WAPDA
1 Shyok River at Yogo
2 Shigar River at Shigar
3 Indus River at Katchura
4 Gilgit River at Gilgit
5 Hunza River at Danyor
6 Gilgit River at Alam Bridge
7 Indus River at Partab Bridge
8 Astore River at Doyan
9 Indus River at Besham
Watershed Boundary
GAUGING STATIONS-SIHP/WAPDA
A Braldu River at Dassu
B Hispar River above Nagyr
C Hispar River at Nagyr
10 0 25 50 75 100 km
10 0 25 50 75 miles
Source: US Defense Mapping Agency ONC Series
Redrafted by P. Carnochan May 1987

2.2 GEOGRAPHY OF THE KARAKORAM

2.2.1 Regional Setting

The Karakoram Mountains are situated in the interior of Central Asia (around 74° - 76.25° E and 35.6° - 36.42° N). The Karakoram consists of a series of mountain ranges that extends over 2500 km from the eastern Ladak to the Hindu Kush (see Figure 2.3). They are bordered by the Great Himalaya to the south and southeast, the Aghil Range and Kun Lun to the north and northeast, the Pamirs to the northwest, and the Hindu Kush to the west. The Upper Chitral River forms the western boundary and the upper Shyok the eastern. Both are tributaries of the Indus.

The Karakoram Range forms the watershed between the Indus and Yarkand rivers. Eighteen of its peaks rise to more than 7,600 m and six to more than 7,900 m. The six highest are K2 (8,611 m), Broad Peak (8,047 m), Gasherbrum-I also known as Hidden Peak (8,086 m), Gasherbrum-II (8,035 m), Gasherbrum-III (7,952 m), and Gasherbrum-IV (7,925 m).

The Karakoram is divided into sections called mustaghs (ice mountains). In the greater Karakoram Range from northwest to southeast, these are the Batura, Hispar, Panmah, Baltoro, Siachen, and Saser mustaghs. North of the Great Karakoram the Lupghar group and the Ghunjerab Mountains lie on either side of the Hunza River. The range south of this crest is known as the Lesser Karakoram and contains Rakaposhi, Haramosh, Masherbrum, and Saltoro groups (Tahirkheli and Jan, 1984) (see Figure 2.3).

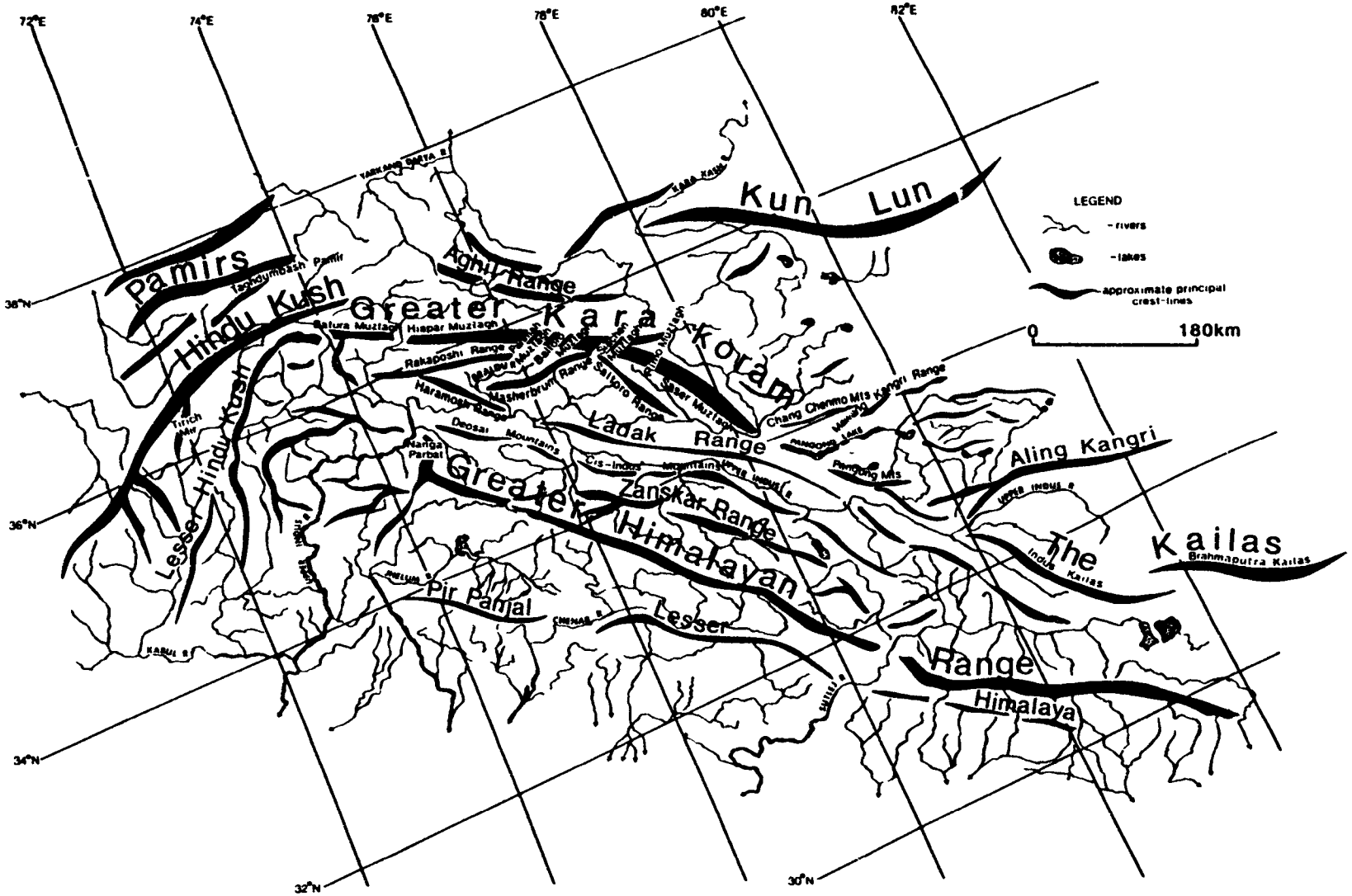

Figure 2.3

Geographical Map of the Karakoram-Himalaya Ranges

source: Snow and Ice Hydrology Project

The elevation of the snowline ranges from 5,100 m in the south to 5,600 m in the main ranges. In the north the snow line lies at 4,700 - 5,300 m (Goudie, Jones, and Brunsden, 1984). Most of the melt water from this almost 760 km continuous high mountain belt of glaciers flows into tributaries of the Indus: the Nubra, Shyok, Shigar, Hunza, and Gilgit. The Shaksgam and the Yarkand drain the northern regions and flow northward into China, where they are dissipated in the Takla Makan desert of Sinkiang. Since the sources of the Indus and its tributaries lie high up in the Himalaya, Karakoram, and Hindu Kush mountains, they are generally situated under the ice of more than a thousand glaciers.

2.2.2 The Upper Indus: Course and Tributaries

The Indus, extends more than 3,000 km, rises in the southwestern part of the Tibetan Plateau and flows to the north of the Vale of Kashmir in arid valleys between the Himalaya and the Karakoram mountain ranges. From its origin in Tibet to its terminus in the Arabian Sea, the Indus drains a total catchment of 933,632 km^2 (Ringenoldus, 1975).

In the north-western Himalaya, the ranges on both sides of the Indus River are aligned from west-north-west to east-south-east. The crest of the Ladakh ranges about 5400-5700 m a.s.l. (Burbank and Fort, 1985). The parallel ridge crest of the north eastern flank of the Zaskar Range rises to similar heights on the south-western side of the Indus. Eighteen kilometers beyond Leh, in Ladakh, the Indus is joined on its left by its first tributary, the Zaskar. Continuing for 240 km in the same direction the Indus is joined by the Shyok on the right bank. After its confluence with the Shyok, and up to the Kohistan Mountains, it is fed by large glaciers on the Karakoram Range, the Nanga Parbat Massif, and the Kohistan

Ranges. There is an immense gorge over 4,600 m deep and 20 to 26 km wide around the Nanga Parbat Massif. The Shyok, Shigar, Hunza, Gilgit and other streams carry the glacial water into the Indus. The Basin layout is shown in Figure 2.4, while the major Lower Indus tributaries are shown in Figure 2.1.

Figure 2.4 BASIN LAYOUT

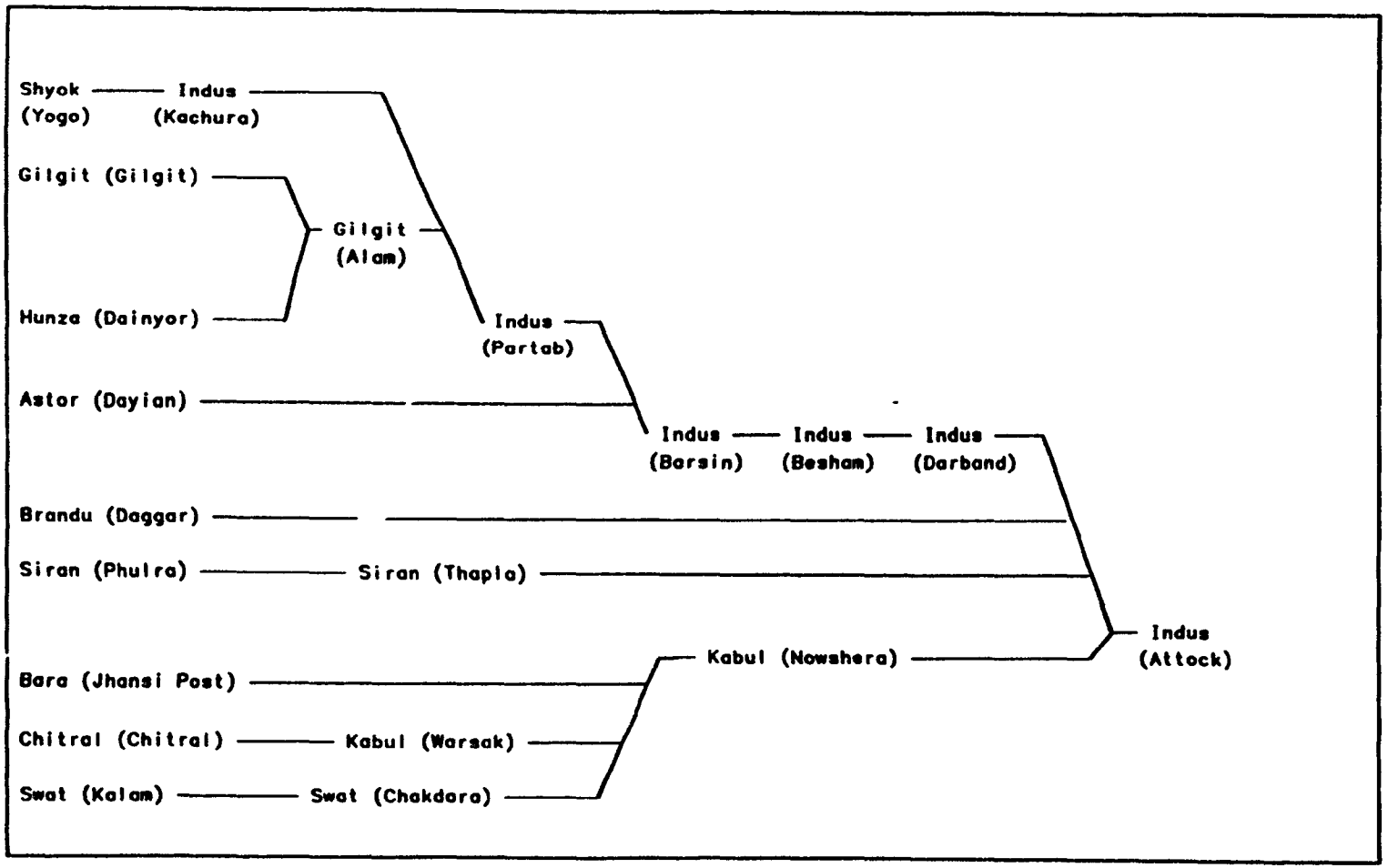

(Young and Hewitt, 1988)

2.2.3 Geomorphology

Topography of the Karakoram system is characterized by craggy peaks and steep slopes. The southern slope is long and very steep, the northern slope steep and short. Cliffs and talus slopes occupy a vast area. Transverse valleys usually have the appearance of narrow, deep, steep ravines.

Structurally, the Karakoram originated from folding in the Cenozoic Era (up to 65 × 10^6 years ago). The mountains rose gradually in a series of parallel folds during the Tertiary period. In some cases, huge blocks were overthrust and lie on younger sedimentary rocks. Erosion over thousands of years completed the process of shaping the mountains in their present form.

The Greater Karakoram is composed of some sedimentary or metasedimentary rocks, igneous, and metamorphic rocks. Granite, gneiss, crystallized slate, and phyllite dominate the geological composition.

In the east are Jurassic and Tertiary rocks of continental origin and Cretaceous marine deposits. To the south and north, the crystalline core of the Karakoram is edged by region of Triassic limestones and micaceous slates of the Paleozoic and partly of the Mesozoic eras (from 190 to 570 × 10^6 years old). To the south, sedimentary rock is sometimes cut by intrusion of plutonic rocks (formed deep down from a molten state), including granites and granodiorites of pre-Micocene age (Encyclopaedia Britannica, V-10, 1984).

2.2.4 Glaciers

The Karakoram mountain glaciers store large volumes of water and are responsible for a larger share of freshwater supply to the Indus. The glacier cover of the Greater Karakoram Range, most of which drains to the Indus, is about 15,000 km^2 (Hewitt, 1988a). This Range contains some of the largest glaciers in the world. According to Hewitt (1988a) between 40 to 50 glacier basins dominate the supply of meltwater within the range. These include basins of a dozen glaciers in excess of 250 km^2 in area of which the three largest are Siachen (1,200 km^2), Baltoro (760 km^2), and Biafo (640 km^2). Numerous glaciers have steep icefalls and many of their tongues are covered with debris (Finsterwalder, 1960). The area and length of major valley glaciers are given in Table 2.1.

Table 2.1. THE MAJOR VALLEY GLACIERS IN THE KARAKORAM (after Von Wissman, 1959)

Name	Area (sq km)	Length (km)
Siachen	1182.5	75.0
Baltoro	757.5	62.2
Biafo	627.5	68.0
Hispar	622.3	53.1
Rimo	510.8	45.1
Skamri *	427.9	41.1
Panmah	410.0	44.0
Chogo Lungma	331.9	47.0
Kondus	311.2	32.0
Te Rong	295.6	27.4
Batura	290.4	59.6
Khurdopin	280.1	41.1
Sarpo Laggo *	230.8	33.0
Braldu *	202.3	35.1
Virjerab	189.3	36.1
Kero Lungma	150.4	20.9
Bilafond	150.4	22.5
Yazghil	145.2	30.1
Riong *	140.0	--
Barpu	136.1	33.8
K2 (Depsang) *	135.4	17.7
Karambar	132.2	27.4
Staghar *	129.7	29.0
	7789.2	

* Glaciers not within the Indus Basin.

(Young and Hewitt, 1988)

In the Gilgit-Hunza Basin, some glaciers penetrate well below 3,000 m a.s.l. The Batura Glacier terminus is at about 2,400 m, the Minapin 2,200 m, and Hopar 2,300 m. In the far east of the Karakoram, glacier termini lie above 4,300 m a.s.l.

Thermal regimes of Karakoram glaciers are varied and influenced by the slope aspect. Small and intermediate size glaciers descending from steep northerly

slopes are largely "Cold" (well below the melting temperature); those on southerly slopes, at least for much of their ablation zone areas, are "Warm" (at or close to pressure melting point). The majority of the larger glaciers have intermediate orientations and a mixture of Warm and Cold regions.

Visser (1938) divides the valley glaciers into two main types: "firnmulden" or Alpine-type glaciers, with bowl-shaped accumulation areas separated from the ablation area by the firn limit; and "firnkessel" or Mustagh-type glacier, occupying narrow, steep-sided troughs and fed by avalanches (cited by Mercer, 1975). Avalanching plays a great part in the direct nourishment of many glaciers. It is also a widespread factor in redistribution of snow from higher to lower altitudes and transport of debris onto glaciers.

The erosional debris of varying composition and thickness is observed to cover the ablation zones of most of the Karakoram glaciers, which has a marked effect on the hydrology of the U.I.B. Some hundreds of square kilometres of glacier ablation zones are more or less heavily blanketed with moraine (Hewitt, 1988a). The quantity of ablation moraine on lower glacier areas is probably strongly related to the amount of avalanche nourishment of the upper reaches.

The glaciers of Batura Mustagh (Hunza-Karakoram) are very important for agriculture in the valleys. Irrigation channels lead run-off water to the very dry valley bottoms. These channels begin as near as possible to the end of the glaciers.

Glacier Dams and Dam Burst Floods: The damming of the major tributaries and then bursting of such glacier dams has an effect on hydrology of the U.I.B. These hazardous hydrologic events affect run-off, flood, low flow problems and erosion. Thirty-five destructive outburst floods have been recorded for the Karakoram region

in the past two hundred years (Hewitt, 1985d). Thirty glaciers are known to have advanced across major headwater streams of the Indus and Yarkand Rivers. Outbursts from a series of dams on the Upper Shyok between 1926 and 1932 brought devastating floods along more than 1200 km of the Indus (Hewitt, 1982).

Geographically, glacier dams in main river valleys have occurred from the far western to the far eastern parts of the Karakoram Range; and in the Lesser Hindu Kush, Nanga Parbat, Haramosh, Aghil, and far northeast Hindu Kush Range.

The high, humid, glacial areas not only provide most of the water, but also most of the erosional debris transported in most years. In the Upper Indus some 90% of the annual sediment yield is carried in just over two months (Hewitt, 1985c). These mostly occur in mid- to late-summer when melting is concentrated in the high snowfields and glacier basins where precipitation is greatest.

When floods occur, they reach and scour exceptional quantities of sediment from the terraces, valley walls, and old glacial deposits of the fluvial zone. These erosional events increase the rate of sedimentation in artificial dams on rivers and reduce their economic lifetimes.

Surging Glaciers: Glaciers, being dynamic, are constantly changing their size and shape in response to both climatic changes and to their internal dynamic regime (Young, 1977 and 1980). Glacier surging is one of the most dramatic phenomena of glacier motion. A surging-type glacier, after flowing along in an apparently normal manner for years, speeds up for a relatively short time to flow rates as much as hundred times the normal rate and then drops back to an apparently normal flow state (Kamb, Raymond and others,1985).

At least 11 surges of exceptional scale have been recorded within the U.I.B. which have had an important influence on the glacial hydrology in the region (Hewitt, 1985c). A surge is commonly accompanied by increased water and sediment discharge. Glacier surging also bears a relation to overthrust faulting and gravity tectonics in the earth and landsliding.

2.3 STUDY AREA

The Barpu Glacier rises on the north-east flanks of Chogo Lungma Group of the Rakaposhi Range. The glacier stretches some 33.8 km with an average slope gradient of about 9°, and is located at latitude 36.05° - 36.23° N, longitude 74.79° - 74.91° E, on the eastern slope of the Karakoram Mountains (see Figure 2.5 and Plates 2.1 & 2.2, also see the Plates B.1 & B.2 in Appendix B). Its terminus hangs directly above the Hopar or Bualtar Glacier in Nagar. The ablation area covers 27.7 km^2 of the total area of 136.1 km^2 at an altitude from 2,835 to 7,460 m (see Appendix A).

The study location Sumaiyar Bar lies in middle of the glacier at latitude 36.15° N and longitude 74.86° E at about 3,500 m a.s.l., which is also the mean ablation area elevation of Barpu Glacier. The stretch of glacier from its point of origin to the junction with Miar Glacier is also sometimes referred to as Sumaiyar Bar Glacier. On the extreme right there is a range of ice pinnacles which diminishes at its junction to the Miar glacier. The particular site was selected mainly due to the representativeness of the debris covered glaciers of the Central Karakoram and the easy excessibilty.

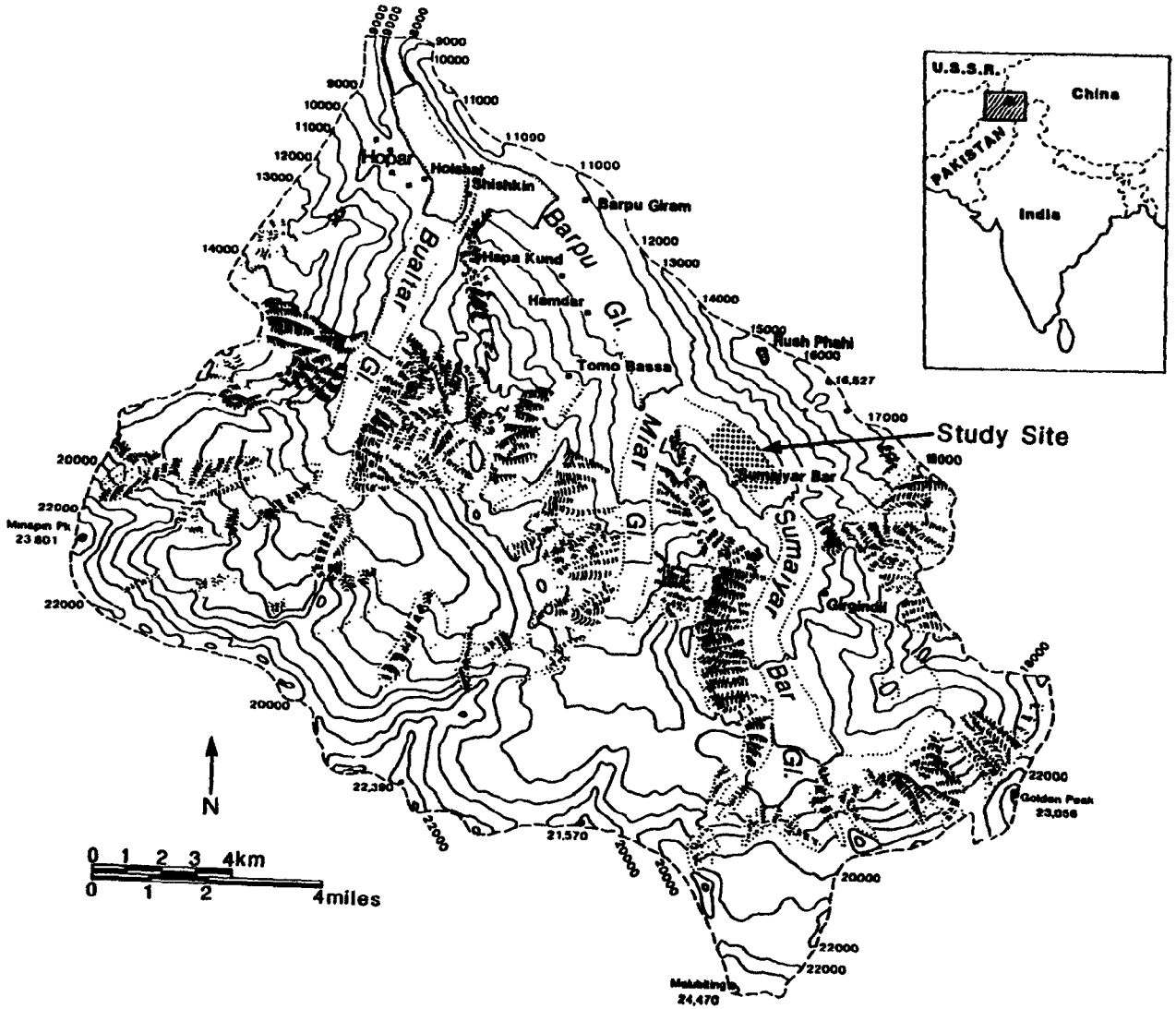

Figure 2.5
The Barpu-Bualtar Glacier System

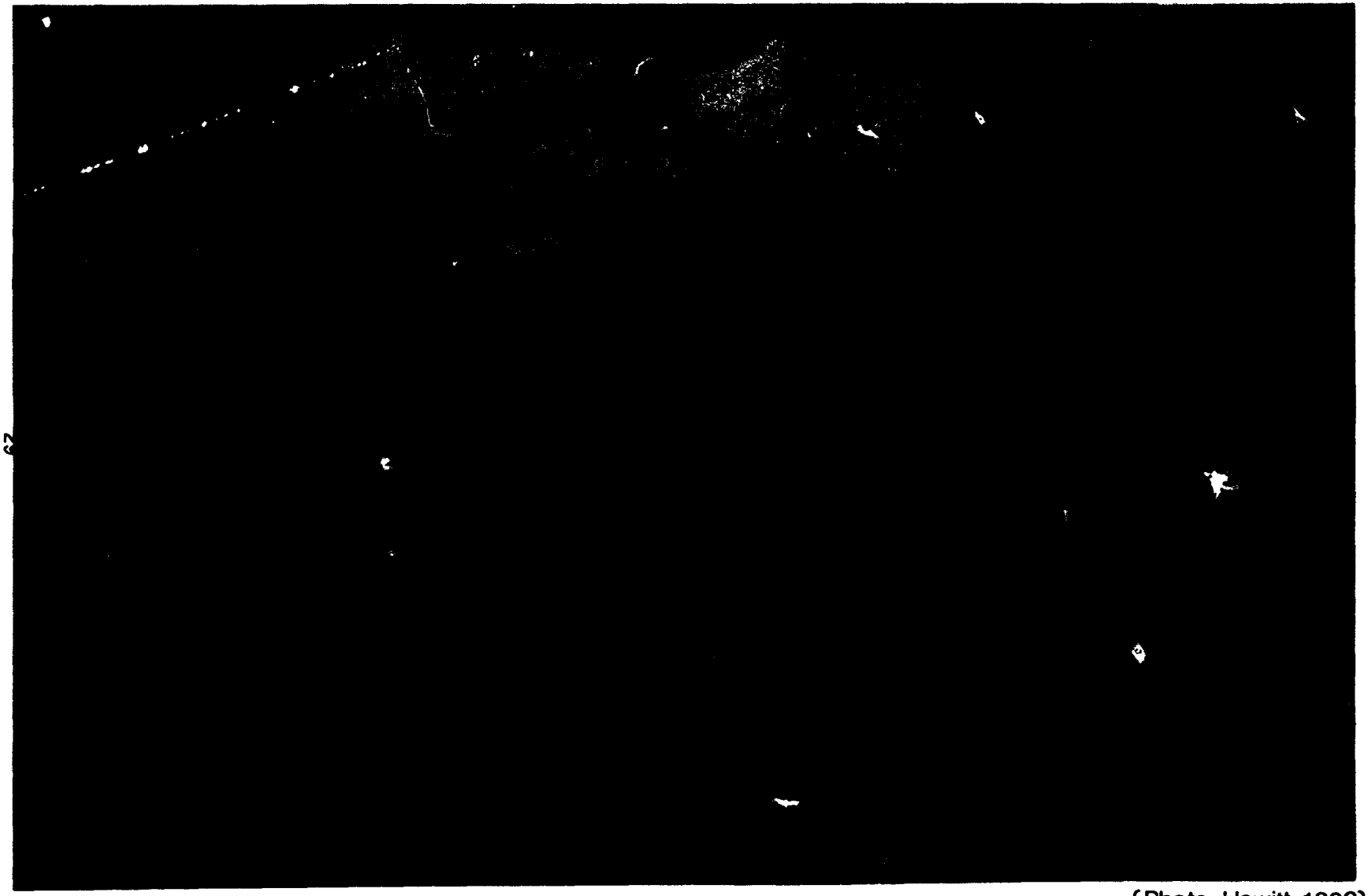

(Photo: Hewitt, 1986)

Plate 2.1

View of Upper B..pu Glacier Showing Study Area in Lower Foreground

Plate 2.2 (Photo: Hewitt, 1986)

View of Sumaiyar Bar Site (in foreground) at the Junction of Barpu and Miar Glaciers

The glacier is a debris-covered type (D-type), according to the Moribayashi and Higuchi (1977) classification of glaciers for Khumbu Region. The ablation zone is dominated by a rugged ice surface and heavy debris loads derived from the disintegration of metamorphic and some igneous rocks. The distribution of supraglacial moraine has a great influence on ablation, which in the study area does not vary with the elevation but with the thickness of the debris cover. The debris layer varies mostly 0 to 30 cm in middle of the glacier, and may exceed 100 cm along the margins. The debris consists of materials from clay size to occasional boulders as large as 4 m in diameter.

Ablation occurs predominantly during two or three months (mid-June to early September) of the year, the larger part in four to six weeks (August - September). Relatively high temperatures in mid-to-late summer over the ablation zone, and intense solar radiation are responsible.

The other big glacier of this region is the Bualtar, which stretches right down to the Hispar river and is flanked in its lower reaches by a large area of rain cultivation known as Hopar. Barpu glacier is divided from the Hispar Valley by a long ridge. It falls short of the Bualtar (Shipton, 1940).

Hillsides with unusually varied vegetation are found on the southern sides of the Barpu and Hispar. Water supply is provided either by seepage from the snowfields or by springs. The slope aspect protects them from excessive insolation.

2.4 CLIMATE

This discussion follows the summary of broad climatic control and local climate described by Barry (1981), Barry and Chorley (1976), Boucher (1975), Hewitt (1988a and 1988b), Lockwood (1974), and Young (1981).

2.4.1 Broad Climatic Controls

The climate of Pakistan is classified as arid or semi-arid. Dense natural forests are present only in some areas higher altitudes where rainfall is heavy or at a location in close proximity to rivers.

The monsoons of Asia are caused primarily by the differential response of land and sea to incoming solar radiation. In the winter months, the Asiatic land mass gets much colder than the adjoining seas and north-east Asia, and becomes the centre of an intense high-pressure system. This Sub Tropical High Pressure (STHP) over Asia extends from Siberia to the outer fringes of the Himalayan massif.

There are four distinct climatic seasons:

1. Winter Season (December - March),
2. Summer Season (April - June),
3. Monsoon Season (July - September), and
4. Post-Mosoon Season (October - November).

Precipitation in Pakistan falls during two distinct periods. The first of these seasons, is from July to September. Rain during this period is the major component and related mainly to the monsoon depressions. The second rainfall season, originating from winter cyclonic storms from the west, occur. from December to

March. The region is dominated by the influx of westerly air masses.

During the winter season, the westerly jet stream lies over southern Asia, with its core located at about 12 km altitude. According to the WMO, any speed exceeding 30 m/s may be called a jet stream (Lydelph, 1985). It splits into two currents in the region of the Tibetan Plateau around the high mountains, the stronger branch flowing east-southeastward down the Ganges Plain, and the other curving northward and eastward through north China and Mongolia. The two branches reunite again to the east of the plateau and form an immense upper convergence zone over China. These two branches have been attributed to the disruptive effect of the topographic barrier on the airflow, but the northern jet may be located far from the Tibetan Plateau.

This subtropical westerly jet stream steers depressions towards the Karakoram and Northern India. These lows, which are not usually frontal, appear to penetrate across the Middle East from the Mediterranean. On an average six to seven western disturbances move across the Himalayan region every month in winter and are an important source of precipitation for Karakoram and northern India. Over most of the northern mountains, snowfall produces extensive winter snowpacks. These occur above 2000 m, and the great bulk of the moisture is certainly found above 3000 m a.s.l.

During the summer season, the belt of Sub Tropical High Pressure (STHP) over Central Asia begins to weaken and temperatures begin to rise rapidly. The land mass of Asia becomes much hotter than the sea areas to the east and south. In March and April western disturbances still occur with a frequency of three or four per month and they are less severe. A strong low-pressure area forms over Pakistan,

Afghanistan, and Iran; while high pressure areas build up over the north Pacific and south Indian oceans. Pakistan lies outside of the tropics and is dominated by shallow incursions of moist monsoon air in summer. The moisture-laden winds from the oceanic areas move towards the heart of Asia from the south.

In May and June the subtropical jet stream over northern India slowly weakens and disintegrates, causing the main westerly flow to move north into Central Asia. Pakistan experiences its highest temperatures during these months and rainfall amounts are generally small.

From early July or so there may be a significant influx of Monsoonal rains, especially in the more southerly and westerly basins. The monsoon season is characterised by the occurence of general south-west monsoon current. The Himalaya mountains provide the necessary conditions for the deflection of the eastern branches of the monsoons in a north-western direction along the Ganges Valley. This can result in the incursion of monsoonal air masses into the Karakoram, resulting in heavy precipitation.

Floods are most severe during the monsoon period, when depressions move inland from the Bay of Bengal and occasionally from the Arabian Sea (Figure 2.6). These depressions move in a northwesterly direction until they reach Rajasthan where some of them recurve northwards and cause heavy rainfall in the catchment areas of the Indus Basin.

Figure 2.6 TRACKS OF MONSOON DEPRESSIONS

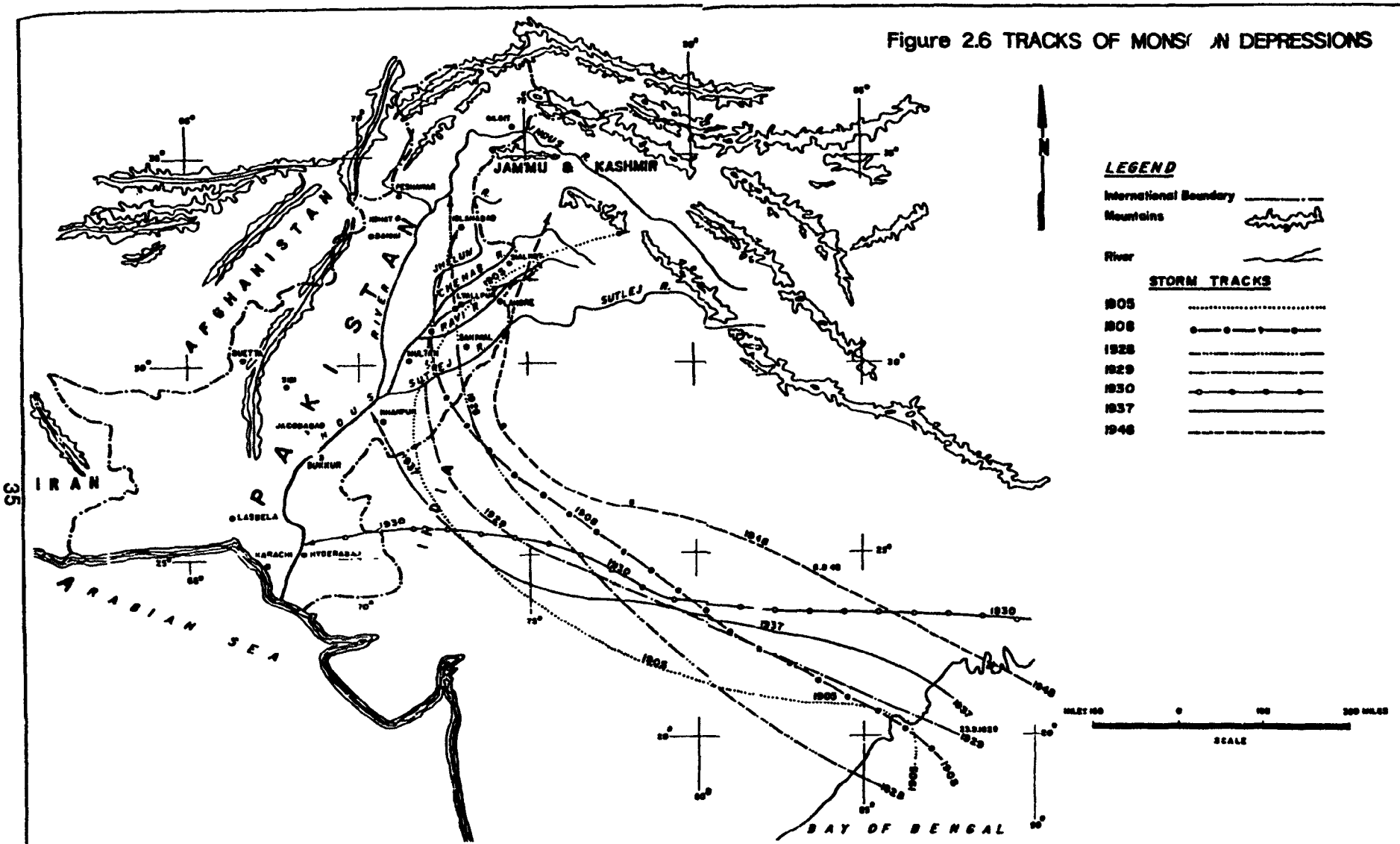

SOURCE: Flood Forecasting and Warning system for the Indus River Basin.
World meterological Organization, 1977.

In October and May the track of winds lies over the north of Afghanistan and the western Himalaya and Karakoram, but from December to April it shifts further south. The period from mid-September to mid-November is a transitory one during which monsoon conditions gradually change over to conditions characteristic of the winter season.

The northerly winds, which have crossed the great deserts of Central Asia, are free of moisture. October and November are the driest months of the year over the entire Indus Plains. To the south the high ranges act as a rain curtain, so that little rain reaches the main Karakoram chain.

2.4.2 Local Climate

The Karakoram Mountains have a climatic regime which is strongly modified by altitude, aspect, localised relief. Intense solar radiation, strong winds, and a great range of temperature are characteristic climatic features of the region. With clearer skies and the apparent northward movement of the sun, the mountain slopes receive greater amounts of solar radiation. There is a winter maximum rainfall in the northwest, but the Valleys are widely characterized by aridity.

The southern slopes are exposed to the humidifying influence of the monsoon even below 2000 m a.s.l., but the northern slopes are extremely dry. In the lower and central part of the slopes, rain and snow is precipitated in small quantities. The annual precipitation recorded at Bunji, Gilgit, Batura and Misgar in the Hunza valley is merely 100-300 mm (Miller, 1984 and Hewitt, 1988a). The valleys around Gilgit and Hunza are among the driest areas of Central Asia. These valleys have a moisture deficit of rainfall below potential evapotranspiration of more than 1000

mm per year. However, hydrological and glaciological estimates show that at least 2-3 m must fall annually over the surrounding mountains and glaciers; because 8-16 cm of precipitation cannot create such big glaciers as we find there (Batura Group, 1979). The high accumulation (snowfall) rate, rising to more than 8,000 mm/year in the upper regions (above about 4500 m) of the Nanga Parbat Range (Kick, 1978) and 1,000 to 2,000 mm in the high mountain ranges of Central Karakoram (Hewitt, 1988a), is the reason for a very active glacierization.

Nearly all the snowfall and thus most of the runoff to the Indus streams derives from Westerly air masses in the winter half of the year. However, the high altitude areas of the north and west receive some snowfall through the summer, which also derives from westerly sources. At Gilgit the westerly contribution to precipitation is about 63%, at Skardu it is 76%, while at the Kachura weather station it is found to be up to 84% (Butz and Hewitt, 1985).

From May through July, melting of seasonal snowcover in the mountain regions of U.I.B. (which involves almost 200,000 km^2 of the area) provides the bulk of the flow of the Indus Streams. The snow and icemelt from the Karakoram accounts for approximately 75% of the total runoff of the U.I.B. Figure 2.7 displays the runoff hydrographs for two gauging stations in the U.I.B. Some 80% of the total annual flow from the U.I.B. occurs between mid-June and mid-September. From May to Mid-July the runoff occurs primarily due to melting of seasonal snowpack in the foothills and at lower elevations within the glacierized basin. In June and July the transient snowline rises rapidly and from early July glacier ice becomes the larger contributor to runoff and subsequently dominates the runoff hydrograph from Mid-July to Mid-September.

Figure 2.7

INDUS RIVER
TOTAL MONTHLY DISCHARGE
1985

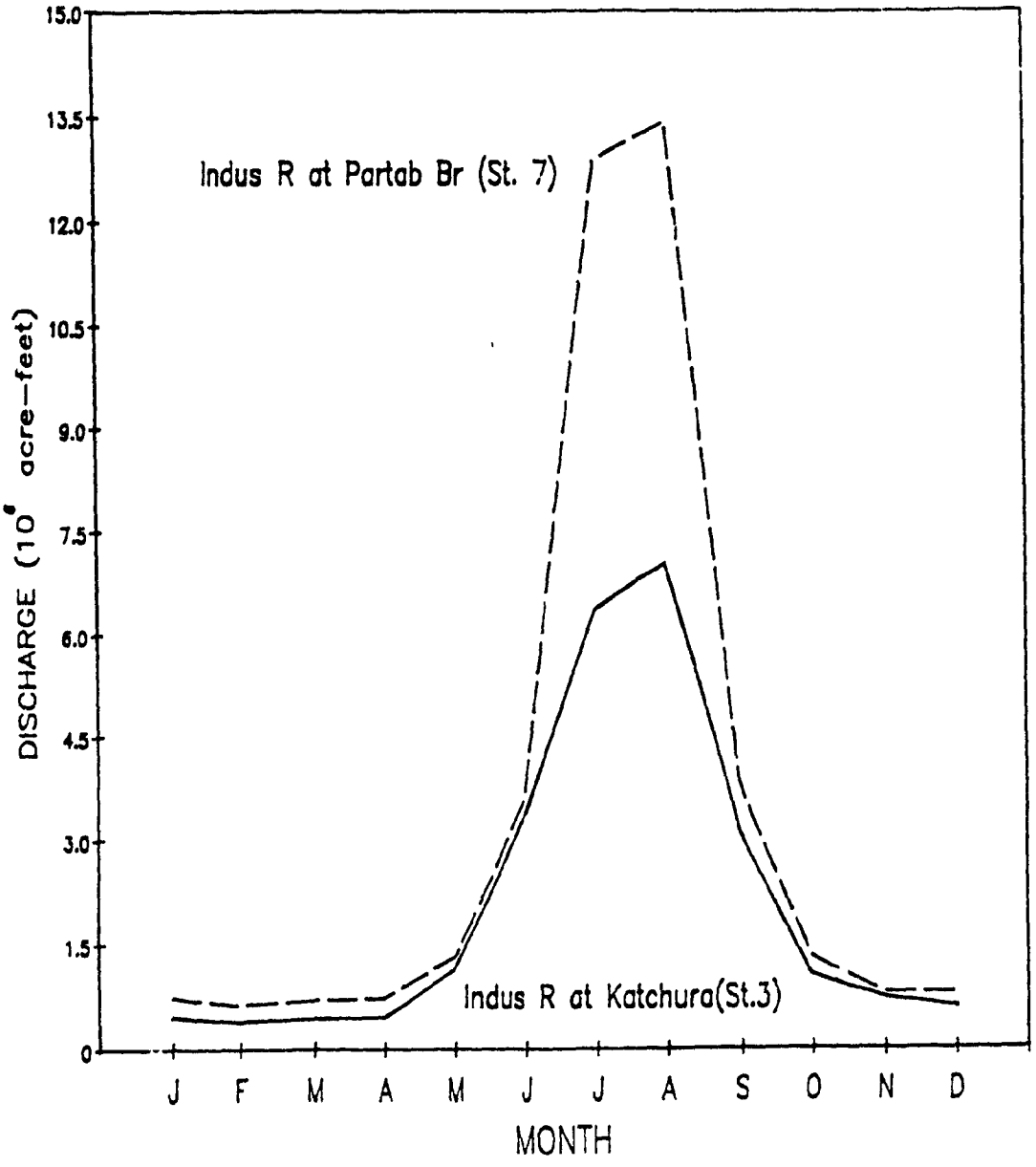

Source: Wake (1987)

There is also a Monsoonal rainfall contribution in late summer, which becomes the predominant moisture source in the southeasterly part of the region. Normally, the monsoon only affects the Karakoram to a small degree. At altitudes of more than 4800 m precipitation always occurs in a solid form.

Figure 2.8 illustrates the annual variation in monthly averaged minimum and maximum temperatures and precipitation for Gilgit and Skardu. The warm summer temperatures result in a strong seasonal variation in the hydrological response of the Karakoram due to melting snow and ice.

Figure 2.8

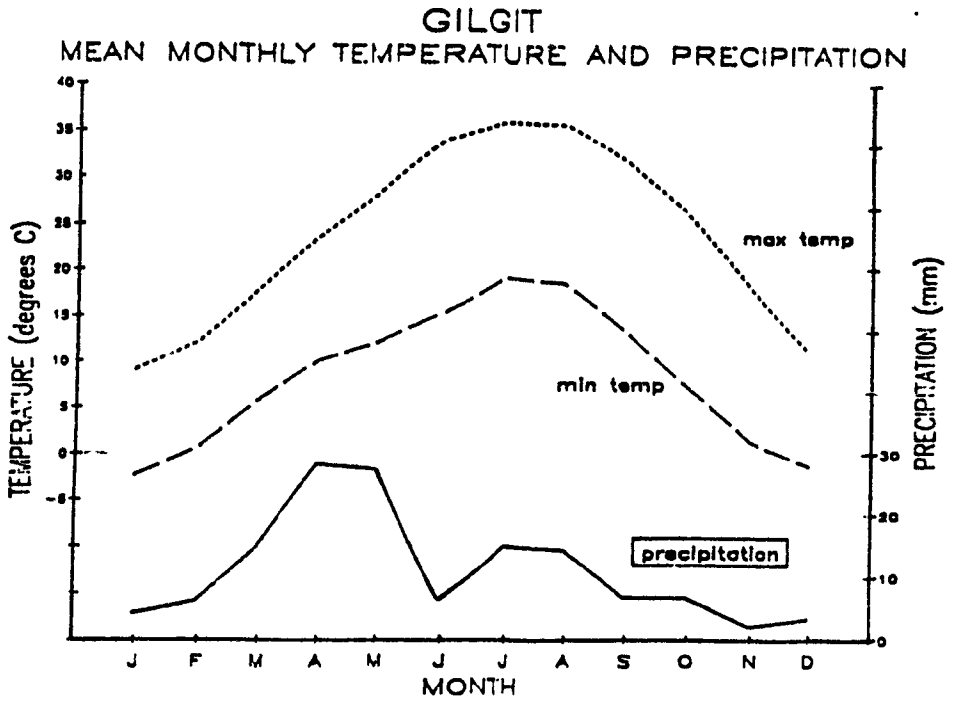

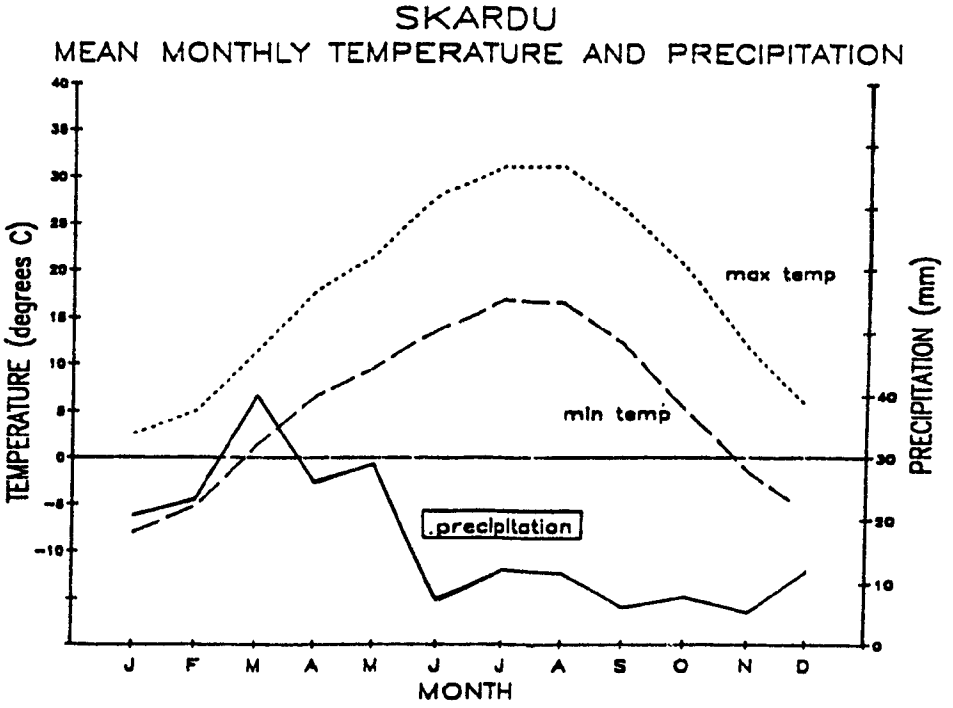

Source: Wake (1987)

At altitudes of 5700 m, the average temperature during the warmest month is lower than 0°C, and, at altitudes between 3900 and 5700 m, the temperature is lower than 10°C.

Altitude and topography play a significant role in controlling the local climate of the Karakoram range. Both of these factors are major controls on the amount of precipitation and insolation received. Altitude affects both the intensity and the mechanisms of melting of avialable snow and ice, and the rate of snow accumulation. Snow accumulation generally increases with altitude. Most of the actual yield of water to streams derives from a belt between those altitudes and 5000-5500 m a.s.l (Hewitt, 1988b). The snowline reaches its highest elevation in June and usually remains around 5,000 m until winter.

The effect of the orientation of surfaces is due to the differences in the solar radiation received by slopes. The north facing and south facing slopes commonly have quite different radiation regimes, producing marked differences in local hydrology (Young and Hewitt, 1988).

Altitudinal differences in precipitation are much more marked in the northern than in the southern slopes. There are also marked differences in the aridity on southerly as against northerly slopes. The transient snowlines are often 700-1000 m higher, and glacial coverage less, on south facing slopes of the same range.

On southerly slopes the surfaces are almost perpendicular to the sun for much of year, while direct sunshine is excluded from many northerly slopes to almost the same degree, therefore air temperature or sensible heat is decisive in melting on northerly slopes. The sublimation and evaporation losses are much larger

in southerly-oriented basins.

Chapter 3

Theoretical Background

3.1 GLACIER FLOW

Glaciers are rarely static for very long. As they respond sensitively to climate, and climate is not constant, so glaciers expand and shrink, extend and retreat (Grove, 1987).

A glacier flows because it deforms in response to stress set up in the ice mass by the force of gravity. Any point within the glacier is subjected to stress as a result of the weight of the overlying ice. This stress has two components; hydrostatic pressure and shear stresses. As hydrostatic pressure, related to the weight of the overlying ice, is the same in all directions; it is the shear stresses that cause particles to slip past one another (Chorley, Schumm, and Sugden, 1984).

Glaciers are formed of polycrystalline ice derived mainly from the original snow crystals. Experiments on single ice crystals show that they can deform plastically by gliding of one layer over another parallel to the basal plane. The deformation of polycrystalline ice depends markedly on the shape and orientation of the individual crystals. However, ice formed from consolidated snow is nearly random in orientation. This randomly oriented ice loses its random orientation

when deformed in simple shear (Rigsby, 1960) and favorably oriented for the flow that is proceeding.

Initially, glacier ice was considered a viscous solid with strain rate directly proportional to the stress, shown by "viscous flow curve" in figure 3.1. Glen (1952) did laboratory experiments on glacier ice and found that at low shear stresses (applied uniaxially) the rate of strain (deformation) is small; for high shear stresses, however, the rate increases very rapidly, so that a small increase of stress produces a large increase in strain rate, as shown by "flow law curve" in figure 3.1. According to Glen the glacier ice possesses properties in ermediate between those of an ideal viscous body and those of an ideal plastic body. Therefore, it is considered half way between plastic and viscous material.

Since the work of Glen, a considerable advance in the theory of ice flow has been made. In recent years, glacier ice is considered more appropriately, as perfect plastic material with a yield stress of 1 bar (100 K Pa or 10^6 dynes $cm^{-2} \simeq 1$ kg $cm^{-2} \simeq 1$ atmosphere) (Andrews, 1975; Paterson, 1980; and King, 1984).

According to Nye (1952), in a glacier the state of stress is not uniaxial but triaxial, and in particular, there is a hydrostatic pressure acting deep in the ice. It is assumed that the rate of strain is very small up to a certain shear stress (≤ 1 bar), and that a shear stress greater than 1 bar does not occur in nature ("perfect plasticity curve" in Figure 3.1). When the yield stress (at which the material starts to to deform) is reached, the strain rate becomes very large.

Figure 3.1 RELATIONSHIP BETWEEN STRESS AND STRAIN

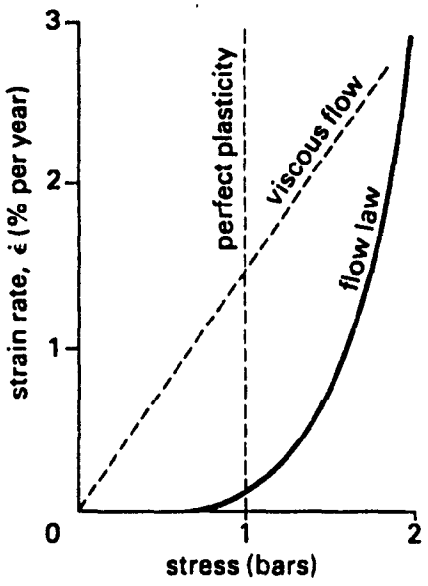

SOURCE: KING, 1984

According to Bentley (1987), Goudie (1984), and Raymond (1980), three basic kinds of motion can result. One is deformation (or creep) of ice itself through internal shear, that takes place under the action of gravity, depending on the stresses involved -- the weight of the overlying ice column and the slope of the ice surface. As a function of depth, strain rate is a maximum near the bed, because both the shear stress and the temperature are maximum there.

The second kind of motion is basal sliding across a rigid, presumably wet, bed; the rate of sliding should depend upon the amount of water present. Ice normally forms from water at 0 °C, but the temprature at which water freezes is reduced under pressure, and as a glacier moves it exerts pressure and therefore some melting may take place at its base. A thin film of water may exist between the glacier and the bedrock. This film reduces friction and hence allows the glacier to slide.

Finally, there is deformation of the bed beneath the glacier, that is produced by the compression and extension due to glacier bed configuration. Tensional fractures are examplified by crevasses in the upper layers of the glacier. Shear fractures occur where thrusting takes place along a slip plane or fault.

The shear stress at any point, acting parallel to the bottom of the glacier, is given by the relationship;

$$\tau = \rho g h \sin \alpha$$

where; ρ is the ice density, g is the acceleration due to gravity, h is the ice thickness, and α is the surface slope angle measured from the horizontal. This equation shows a direct relation of shear stress to the surface slope steepness and thickness of the glacier. Shear stress will reach a maximum at the base of the ice

and decline to zero at the surface. Calculations on many glaciers indicate that the basal shear stress varies within a small limit (0.5 to 1.5 bar) (King, 1984). This also suggests that ice behaves as a plastic material.

Now in the theory of perfect plasticity, the yield stress τ has a value of 1 bar. Referring to equation above, it can be seen that

$$\tau/\rho g = h \sin \alpha = a \text{ constant.}$$

In other words, any change in h must be compensated by a change in α, and we have a simple (but approximate) explanation of the readily observed fact in nature that glaciers become thinner on steeper slopes and thicker on gentler ones, assuming no longitudinal change in accumulation or ablation.

The deformation of ice crystals shows creep even at low stresses; but, unlike other materials, the creep rate shows an acceleration as time proceeds (Glen, 1963). This acceleration tends to attain a steady value as time proceeds, and this strain rate is related to the applied shear stress by a power law. Glen's flow law, adapted by Nye (1952) can be written as

$$\dot{\epsilon} = A \tau^n$$

where; $\dot{\epsilon}$ represents the strain rate, A is a constant related to the temperature of the ice (at 0 °C the value of A is 0.165, at -5 °C A is 0.054, and at -10 °C it is only 0.017, falling as low as 0.0015 at -20 °C; King, 1984), τ is the effective shear stress and n is an exponent with mean value of 3; which depends largely on the orientation of the ice crystals, being higher as the crystals become better oriented. The importance of Glen's law is that it demonstrates that the strain rate is highly sensitive to the shear stress.

The temperature of the ice mass plays a fundamental part in its movement and morphological activity (Embleton, 1979). Ice at or close to the melting point yields more readily to stress, so warm glaciers tend to deform more easily and flow more rapidly than cold glaciers (Rice, 1977). Paterson did laboratory experiments in 1977, and found that strain rate produced by a given stress at -10 °C is about 5 times that at -25 °C. Below the depth to which any winter cold wave penetrates temperatures will decrease because of the increasing pressure of ice overburden, at about 6×10^{-4} °C m^{-1} (Shreve and Sharp, 1970; cited by Embleton, 1979). Any heat generated by glacier movement is used in melting the lower surface of the glacier. Thus melt-water exists in varying quantities at the base of temperate glaciers and is vital in the basal sliding mechanism.

Experimentally, it has been shown that at moderate stress three main processes in glaciers occur, depending on temperature. Below -8 °C, the behavior is dominated by basal sliding; between -8 and -1 °C, creep is associated with a liquid phase at the grain boundaries and grain-boundary sliding; while near 0 °C, pressure melting and regelation are the chief processes if the pressure applied is high enough (Embleton and King, 1975). Pressure melting occurs when the melting point of ice is reduced under pressure; whereas, regelation is a reverse process by which the meltwater is frozen again by increasing the melting point of ice on release of the pressure.

The increased strain rate, produced by shear stresses, must affect both the velocity of glacier and its surface form (Rice, 1977). The surficial elements of the glacier, such as crevasses, folds, ogives, foliation, and facets, are mostly the result of these highly developed stresses.

3.2 FORMATION OF FACETS

Facets are usually plane or semi-circular inclined bare ice surfaces that form in the surficial part of a glacier. They generally form at a typical angle of 45° to the horizontal. These features are usually abundant in debris covered ablation areas.

Although facets play a significant role in ice ablation, they have been poorly documented in the literature. It seems that dynamic behaviour of the glacier and supraglacial debris are two of the most important factors in development of facets. Nye (1952, 1969), Sharp (1960), Paterson (1980), amongst others, have described the mode of glacier flow and stresses (discussed above) within the glacier which result in formation of crevasses. These factors may also have influence on the formation of facets.

Where gradient steepens, the glacier flows more rapidly and 'stretches' or extends, and thins. Where gradient becomes less steep, the glacier tends to be compressed, and thickens. The theory of compressive and extending flow was elaborated by Nye (1952). Compressive flow describes a situation where the longitudinal stress is compressive throughout the depth of the glacier. Extending flow describes a situation where the longitudinal stress is more tensile than the overburden pressure. Under such circumstances the velocity increases downglacier. Extending flow occurs where there is an addition of ice to the glacier surface, or where the bedrock slope beneath the glacier is convex. Both these conditions lead to an acceleration in glacier flow. Compressive flow occurs where there is a loss of ice at the glacier surface and where the glacier bed is concave. Such conditions favour a deceleration of glacier flow.

Nye (1952) has made theoretical investigations of the effects of accumulation and ablation on flow type using the simplified flow law of perfect plasticity. If R is the radius of bed curvature, α the surface slope of ice, ϕ the rate of ice discharge, $d\phi/dx$ the rate of addition of ice to the upper surface of the glacier (positive $d\phi/dx$ represents accumulation, negative $d\phi/dx$ represents ablation), then extending flow will occur when the expression

$$d\phi/dx + \phi/R \cot \alpha$$

is positive, and compressive flow when it is negative.

At the other extreme, if there is neither accumulation nor ablation it would then be the sign of R that decides the type of flow. A convex bed (R positive) would give extending flow, while a concave bed (R negative) would give compressive flow.

The trajectories of maximum shear stresses are defined by 'slip lines', (or planes of weakness) within the ice which are associated with them. Figure 3.2 shows the pattern of flow (i.e. the direction and surface expressions of the main slip lines). In extending flow these lines favour downward movement of ice, while in compressive flow they favour upward movement of ice. In both cases they are tangential to the bed but meet the surface at an angle of 45°.

The importance of the slip-lines is that they show the directions in which the ice has the greatest tendency to fracture by shear. Actually, the ice is not equally strong in all directions and the laminar structure of glacier probably provides surfaces of weakness.

The compression that occurs in a shortening of a unit of ice which is

balanced by its increase in thickness. Practically, all glaciers undergo at least a modest degree of extending and compressive flow because of differential acceleration and wastage of ice mass (Sharp, 1960).

Figure 3.2 (a) COMPRESSIVE AND EXTENDING FLOW AND ASSOCIATED SLIP LINES.
(b) THE DISTRIBUTION OF COMPRESSIVE AND EXTENDING FLOW IN A GLACIER
(Nye, 1952)

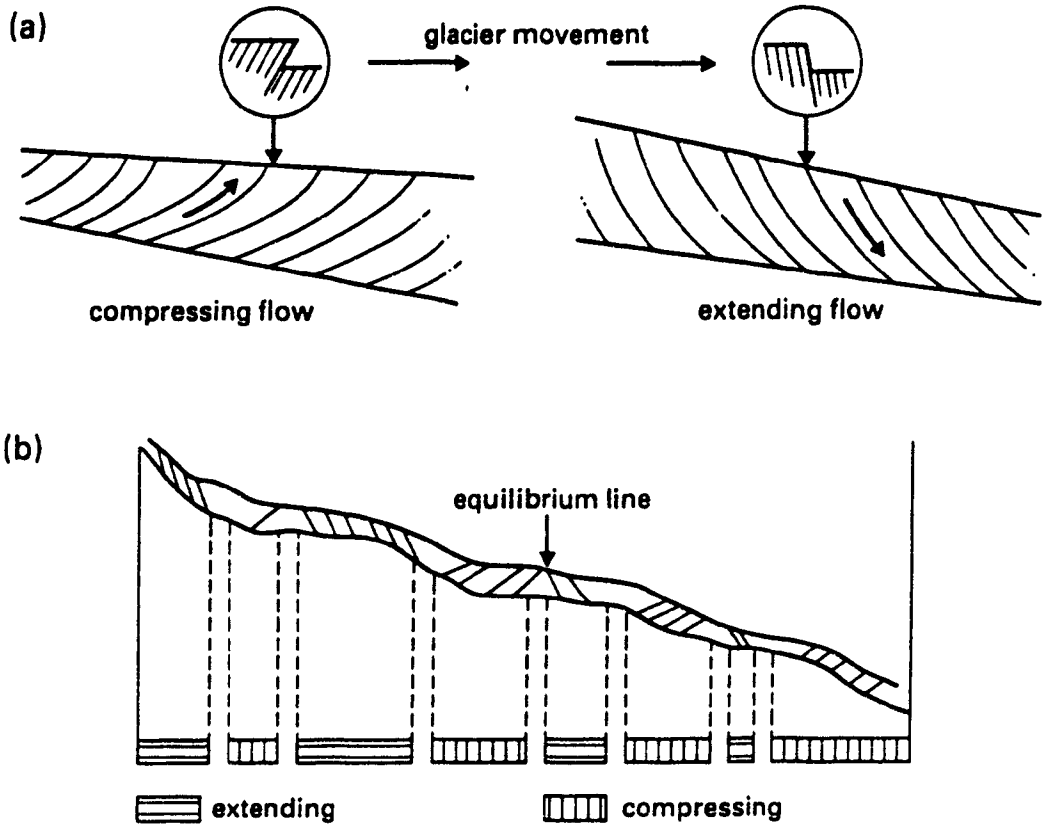

Glaciers are seldom straight along their entire length. Instead, their channels often take a curving path through the mountains, with bands ranging from gentle arcs to abrupt right-angle turns. This longitudinal curvature in a glacier valley would influence the distribution of stress and velocity (Echelmeyer and Kamb, 1987).

The velocities are also increased by surging of glacier ice by as much as 10-100 times the normal velocity. The surge frequently consists of (a) a wave of thickening ice subjected to compressive flow, (b) a zone of high velocity ice with intensely fractured ice behind the wave crest, and (c) a zone of tension or extension where the ice is thinning and slowing down once more (Sugden and John, 1976).

It is seen that the facets are mostly associated with debris covered ablation zones. Facet development may be sought in the effects of intense insolation on the two types of glacier surfaces - that which is mostly clear ice, and that which is covered with debris loads. The debris covers on the surfaces around the slopes, protect the underlying ice from direct insolation, whereas bare ice slope surfaces absorb large amounts of radiation income resulting in higher ablation. Both these factors help to modify the facets.

Although a horizontal surface received greater amounts of solar radiation than facets, its melting was retarded by thick debris cover and a large amount of radiation absorbed by debris went back to atmosphere. Whereas the intensification of the slope surface melting was achieved largely due to decreasing surface albedo by blackening material or dust.

If there were no debris cover at all on the horizontal surface, the ablation would have been higher or at least the same as facet ablation. Hence, it might be

difficult for facets to remain in their existing shape. It may be the differential rate of absorbed solar radiation that keeps the facet in its shape, and in this connection the role of debris cover is significant.

3.3 ABLATION PROCESSES

Ablation is the term used to denote all processes by which snow and ice are lost from a glacier including melting (surface, englacial, and subglacial), removal by wind or avalanches, the physical loss of ice at the glacier terminus and evaporation (Dean, 1974). Practically, all the ablation takes place at the surface due to melting. The amount of loss by englacial and subglacial ablation is usually negligible compared with surface ablation, except in the case of floating glacier tongues and ice shelves (Meier, 1962; Embleton and King, 1975; Paterson, 1981). Condensation and evaporation quantities are approximately equal (Collins, 1988) and the difference is relatively small and can be omitted from ablation studies.

Surface melting varies both spatially and temporally due to variations in incoming solar radiation and convective and turbulent heat transfers. On the average over the period 1930-39, in June on Karsa Glacier (Sweden) solar radiation caused 75% of the wastage of snow (Sharp, 1960). The relative effectiveness of solar radiation generally increases with altitude owing to clearer air and lower air temperature. Hoinkes (1955) in a study of the Eastern Alps found that 81 to 84 percent of the energy causing ablation is supplied by short-wave radiation from the sun and sky. Only 16 to 19 percent come from the air in the form of actual and latent heat. Generally up to 70% of surface melt is accounted for by solar radiation. The remaining 30% is termed non-radiational melt and arises from near-surface turbulent heat transfer, latent heat of condensation, net long-wave radiation, ar-

conduction of heat through moraine material (Ward, 1950). According to the Batura group (1979), 89.2% of the total heat was derived directly from solar radiation and 10.8% from heat conduction of air and condensation heat of vapour.

The heat transfer from air, through convection and condensation, is a function of air temperature (as well as of wind speed, humidity, etc.) (Schytt, 1967). Latent heat transfers result when moist air migrates across the glacier surface and is chilled by conduction from the underlying cold material. Air is very poor conductor of heat. Consequently, Conduction is the least significant mechanism of heat transfer in the atmosphere (Tarbuck and Lutgens, 1976). If the relative humidity is great enough so that the air reaches the dew point as it is cooled in contact with the ice, condensation occurs. Condensation of water vapour at 0 °C results in releasing 600 calories of heat and this is sufficient to melt 7.5 grams of glacial material which is close to the melting point (Sharp, 1960; Thompson, 1977).

Evaporation occurs when the relative humidity is so low that air in contact with ice does not reach the dew point as it is cooled to 0 °C. The amount of evaporated ice is negligibly small and is seldom more than 1% of total ablation (Janes, 1976). This is a very wasteful process requiring approximately 680 calories to evaporate one gram of ice (Ahlmann, 1935; Sharp, 1960; Thompson, 1977), and this amount of heat energy is not readily available in glaciated regions. Conversely the heat of fusion only requires 80 calories to melt one gram of ice and this is the main reason why melting is the dominant ablation process. The ablation is greatest in periods with warm and humid air; in periods with warm and dry air, ablation is much less. On the whole evaporation plays an unimportant role in ablation as compared with melting (Ahlmann, 1935).

The amount of heat given off as a result of rain on the ice is also very small (Hoinkes, 1955; Flint, 1957 and 1971). In part, this is due to the fact that the temperature of much rain water is not far above freezing so the supply of heat available is small. Ten millimeter of rain at 10 °C has a heat content sufficient to melt only 1 mm of ice (Sharp, 1960).

3.3.1 Short-Term Ablation

Density decrease near the surface due to internal ablation by transmitted radiation is an important consideration in short-term ablation measurements in the order of a few hours. The surface of a glacier experiencing ablation frequently consists of a layer of porous ice with loosely interlocking crystals, varying in thickness from a few to a few tens of centimeters. The development of fine, closely spaced, cryoconite holes in the bare ice surface on a day of relatively high radiation can be readily observed. The albedo of a melted surface, even in the absence of contaminating particles, is lower than the albedo of the same surface before melting. The lower albedo of the melting crust is largely due to the trapping of some of the incident total radiation inside the layer, due to multiple reflections at the walls of pores, channels, and cryoconite holes in the melting crust (Zotikov and Moisseeva, 1972; and Zotikov, 1986). Both the distribution of cryoconite and its continous changes in depth under varying meteorological conditions have an important influence on the short-term ablation.

During the period of formation of the weathering crust, more ice is being melted than would be apparent from surface lowering measurements. As the gross density of the weathering crust which has been melted away, during period of overcast and warm weather, is lower than that of normal glacier ice; the

measurements of surface lowering may give a misleading impression of high ablation rate (Muller & Keeler, 1969).

For long-term ablation measurements, where measured values of lowering the surface greatly exceed the depth to which sub-surface melting normally occurs (i.e. 15-20 cm), the local density can ordinarily be neglected (LaChapelle, 1959) and the mass loss from the surface layer may be expected to equal the product of surface wastage and the mean bulk density of glacier ice.

3.3.2 Debris Cover Effect on Ablation

The surface of a glacier is seldom a surface of pure ice or snow. Instead it is usually covered with a large or smaller layer of dust, fine particles of moraine, etc. (Zotikov, 1986). These superficial moraines on mountain glaciers form as a result of three processes: the deposition of colluvial material on the glacier surface, the melting-out of englacial moraine, and the widespread development of thrust moraine (transfer of debris from the glacier bed to the surface along shear planes) (Bozhinskiy and others, 1986). Material added to the glacier in the ablation zone tends to remain at the surface. A large quantity of rock debris is transferred onto a glacier surface by avalanching. Small to medium-scale av anches descending tens or hundreds of meters may carry 10^2- $10^5 m^3$ of mixed material (Drewry, 1972).

The supraglacial debris strongly affects the ablation processes. There are large differences in reflection, absorption, thermal conduction, and infrared re-radiation by debris covers according to their thickness, composition, and moisture-content (Hewitt, 1985b).

Acceleration of ablation under a thin layer occurs because of darkening of

the surface, decrease of its albedo and increasing absorption of solar radiation energy (Fujii, 1974), whereas a thick and continuous cover (say, > 2 cm) serves to protect underlying ice, greatly reducing ablation.

At high altitude or high latitude there are great contrasts in temperature between sun and shade (Ogilvie, 1904). The different rates of melting of glacier ice in association with debris cover presents a fascinating study in the exchange of heat between the surface and the atmosphere. The temperature of the melting ice surface is usually at 0 °C, whereas the temperature of the rock debris surface is often much higher than the air temperature. A debris cover protects a glacier from the direct sunlight, and may therefore keep its temperature below 0 °C, and so prevent melting

Whenever a temperature gradient exists within a system, energy is transferred. Heat transfer can be defined as the transmission of energy from one region to another as a result of temperature difference between them (Clayton, 1974). That is, heat flow through a debris cover is controlled by the thickness of the debris and by the difference between top and bottom surface temperatures. For example, where the distance between the two points is increased (the debris cover is thickened) and the top and bottom temperatures are constant, the thermal gradient is decreased. This causes a decrease in the amount of heat that can be transferred through the debris. The heat flow through debris can be given as $\lambda\ \Delta T/\Delta Z$, where; λ = coefficient of thermal conductivity (an intrinsic property of the material through which the heat is transferred), ΔT = temperature difference, and ΔZ = thickness of debris cover. Thermal resistance (Rk) is directly proportional to the debris cover thickness and inversely proportional to the thermal conductivity, i.e. $Rk = Z/\lambda$. A point below the surface is shielded from extremes and is colder during hot, and

warmer during cold, hours, than the surface.

The debris cover plays a major role in developing or changing the local topography of glacier. Even if the englacial sediment arrives uniformly at the surface of the glacier, it soon becomes nonuniformly distributed. As described earlier, any slight difference in the insulating ability of supraglacial debris will cause differential melting, which results in "topographic irregularities" on the ice. This promotes mass movement and a nonuniform distribution of the supraglacial sediment. The 'dirt cone' and 'glacier table' are the effects of debris on melting. In glacier table, the boulder protects ice beneath it from sun's rays, while in the case of dirt cones, the ice surface, where locally protected from the sun by a film of debris, forms a cone while the rest melts to lower level.

The major portion of absorbed solar radiation by debris is lost by radiation outwards when the sun is low and by conduction - convection to the air, before, it can be conducted to the underlying ice. The thicker the surface moraine, the more the amount of heat is spent therein, and the weaker the ablation becomes. Below a certain critical thickness, however, the insulating effect ceases to be evident and is in fact replaced by an opposite effect, by transmitting heat to ice (Wilson, 1953).

The efficiency of heat absorption by the debris at Sumaiyar Bar glacier is indicated by the fact that debris temperatures commonly rise 7-10 °C above air temperatures on sunny days.

3.3.3 Artificial Dusting of Glacier

For many years Chinese peasants in some of the western provinces reputedly have been "blackening" glaciers by spreading thin film of loess, the wind-blown silt so common in parts of China, over the ice in order to hasten melting (Dyson, 1972).

In Russia techniques had been tested for melting snow and ice in the lowlands of Europe and Siberia by spreading ashes, slag, soil, coal, and soot. One snow-dusting experiment on the north coast of Siberia showed that dusted snow melted eight times faster than undusted snow. More recently the Russians have found by experimenting on glaciers in the Tien Shan (a mountain chain reaching up to about 8,000 m) that a thin layer of coal dust, spread over the ice surface greatly accelerated melting by increasing the absorption of solar radiation, and that it is possible by such methods to increase the annual runoff in mountain rivers by more than 50% (Dyson, 1972; Kotlyakov and Dolgushin, 1972; and Schultz, 1974).

3.4 SOLAR RADIATION

Radiation from the sun is essentially the primary source of energy for terrestrial life (Becker, 1979). Practically all of the energy for all physical and biological processes occuring on earth arrives in the form of solar radiation (Yao, 1981). It is the single most important control of climate.

Climate is described in terms of several elements. Chief of these, as regards their effects on the earth's living things, are solar energy, temperature, precipitation-humidity, and winds. Each of these elements functions as a climatic control and influences each of the other elements. Other climatic controls include altitude, the distribution of land and water, terrain barriers, the vast

semipermanent cells of high and low pressure, ocean currents, and a great variety of atmospheric disturbances.

Solar radiation is both an element and a control of climate. Its influence is expressed most directly through air temperature distribution, but indirectly solar energy is the ultimate cause of nearly all changes and motions within the atmosphere.

The amount of solar energy that any latitude on the earth's surface receives depends mainly upon two factors: (i) the intensity of solar radiation , or the angle at which the rays of sunlight reach the various parts of the earth's spherical surface, and (ii) the duration of solar radiation, or length of day. These factors are varied by latitudes and seasonal changes in the path of the sun in the sky. The intensity of solar radiation varies (with geographical location, time of day, and season etc.) from zero to about 1.5 cal/cm^2/min.

Rays of sunlight are always parallel, but because of the earth's changing orbital positions, these rays reach different latitudes of the earth's curved surface at different angles in different seasons. The intensity of insolation is greatest where the sun's rays strike vertically, as they do at parallels within the belt lying between the tropic of cancer and the tropic of capricorn at certain times of the year. With diminishing angle, the same amount of solar energy spreads over a greater area of ground surface , so the polar regions receive the least insolation over a year's time on the average. Since an oblique solar ray is spread out over a larger segment of the earth's surface than a vertical one, it delivers less energy per unit area. On any given day the sunlight is much more intense at noon than in the early morning or late afternoon hours. This phenomenon significantly increases the importance of

slope aspect and angle of a surface.

The solar energy arriving at the earth's surface is composed of a direct component, a diffuse component, and a reflected one. Thus the total or global radiation income of any surface is the sum of all these components such that

$$R = Q + q + qr$$

where; Q is direct short-wave radiation from the Sun, q is diffuse short-wave radiation, that has been scattered or reflected from atmospheric constituents as well as radiation reflected from the underlying terrain, qr is short-wave radiation from neighboring surfaces. The diffuse sunlight does not come directly from the sun, but it is first reflected from dust particles, air, clouds, and water snow, landscapes, mirrors, and other earthbound surfaces.

For natural surfaces over the most of the world, it is global solar radiation (Q+q) which provides the greater part of the radiation income. The diffuse component constitues about 5 to 15 percent of the total (Wieder, 1982), depending on the cloudiness of the sky, but in some regions this proportion varies widely. The semi-arid regions of India, for example, receive about 20 to 25 percent of global radiation as diffuse radiation when the skies are clear (Mani, 1976). A theoretical determination of global radiation involves the assimilation of several independent variables, including declination of the sun, latitude, optical air mass and dust attenuation (Goodison, 1972).

The net income of radiant energy per unit area of the surface called net radiation, Rn, and can be directly measured with suitable instruments.

Net radiation can be written as;

$$Rn = Rs - Rs^* + Rl - Rl^*$$

Where; Rs is the downcoming flux of solar radiation, both as direct sunshine and as diffuse radiation, is called the incoming short-wave radiation or insolation, having wavelength from 0.3 to 4 microns (1 micron = .001 mm). The term Rs^* represents the shortwave radiation reflected from the surface and can be expressed as rRs, where r is the reflection factor (or albedo) for the surface in question. The third term, Rl, is the incoming longwave radiation. Clouds, dust, haze, and some of the gaseous constituents of the atmosphere emit radiation in accordance with their temperatures and emission spectra, ranging 3-100 microns wavelength. The upward flux of long-wave radiation, Rl^*, is the radiation emitted by the surface according to its temperature.

When solar energy is in transit through the atmosphere, it may be 'reflected', 'transmitted', or 'absorbed'. Only that part which is absorbed heats the air. The atmosphere weakens solar energy through (1) selective scattering, chiefly of the short waves of blue light, by very small obscuring particles, (2) diffuse reflection of all wavelengths by layer particles, such as cloud droplets, and (3) absorption of selected wavelengths, chiefly by water vapor concentrated in the lower strata of the atmosphere.

It is estimated that about 34% of solar radiation reaching the outer limits of the air layer is returned to space by scattering and reflection from clouds, small dust particles, and molecules of air, as well as by direct reflection from the earth's surface. This percentage lost is known as the earth's 'albedo', has no part in heating either the solid-liquid earth or its atmosphere. Another 19% of the total solar

radiation acts directly to heat the air, for it is absorbed by the atmosphere, most of it by water vapour. The remaining 47% is transmitted to the earth's surface either as direct sunlight or as diffuse daylight (Trewartha, 1968). Thus, only about two-thirds (66%) of the solar radiation is available for heating the atmosphere.

3.4.1 Slope Effects On Incoming Radiation

Solar radiation is a chief controlling factor for melting of snow and ice, and is much affected by surface geometery of the area. Slope and aspect have a great influence on the components of the energy balance. Some surfaces face the sun in such an orientation and slope angle that they can receive the greatest concentration of the radiative energy from the sun during the day.

The standard way of accounting for the solar heating of a glacier surface is to treat the surface as being smooth and having a fixed albedo (Pfeffer and Bretherton, 1987). Faceted ice surface has a large heat absorbing capacity, by expos.. ~ the ice surface at different angles of incidence, and can act as solar collector. Any slight change in the surface angle will change the angle of incidence of the sun (i.e. the angle between sun's ray and normal to the surface). Incoming direct radiation on any surface is thus controlled by its slope and azimuth. The additional amount of radiation received by slopes by reflection from neighbouring surfaces only becomes appreciable when the slopes are steep (Geiger,1969).

As said earlier, the amount of radiation is also dependent on latitude and time of the year. A slope at a particular latitude may not receive the same radiation amount throughout the year or even throughout the day, because of the moving of the earth around the sun (affects on sun's declination) and revolving on its orbit.

Both of these motions change the striking angle of sun's rays continuously. For example, at latitude about 36° N, in summer (when the sun is on northern hemisphere) gentle south-facing slopes (10°-15°) receive greatest radiation, whereas in winter (when the sun is on southern hemisphere), steep southern slopes (50°-60°) receive greatest radiation.

At latitudes 23.5°-90° N the southern slopes always receive greater radiation than other slope aspects. At latitudes between equator and 23.5° N the radiation is greater on south-facing, only when the sun is on southern hemisphere (i.e in the northern winter).

Observations were made of the incoming radiation on 40° slopes for direction 0° to 360° , in winter 1987 at latitude 43.47° N (Waterloo). The south-facing slope received almost 12 times the radiation received by north-facing slope. Whereas north-facing slope did not receive any amount of direct incoming radiation, it rather received only the diffuse radiation (8% to 10% of the radiation on that of southern slope) due to being under the shade Cloud covers decrease the influence of slope and aspect considerably, because incoming diffuse short wave radiation is almost independent of the orientation of slope surface (Kuusisto, 1984).

3.4.2 Significance of Slope Angle and Azimuth at Sumaiyar Bar

The example of radiation pattern at Sumaiyar Bar (36.15° N) for different south-facing slopes (for June 1) is shown in Figure 3.3. Slopes up to 15° received greater amount of radiation than that of horizontal surface (the sun' declination was 21.1° N that day). The radiation income on slope of 15° is as much as on horizontal surface, beyond this angle radiation goes on decreasing, and it is reduced by 20% on

45° slope. Since the typical facet angle was found to 45°, it is not beneficial as far as incoming radiation is concerned. These facets play a significant role in ablation in other ways. Due to steep angle, these slopes are almost free of debris loads or having only a thin film of dust layer which absorbs and traps far more of the sun's radiant energy. Whereas, the effect of radiation is much more reduced by heavy debris around these facets. In this sense, the angle of 45° is quite beneficial; although, it receives much less radiation as compared to debris covered surfaces.

As far as the slope aspect is concerned, the southern facets receive greatest radiation during the day (Figure 3.4). It will be seen in chapter 5 that facets are very commonly concentrated in SW direction. On SW facets some 80% radiation of that on horizontal surface was observed during the study. At Sumaiyar Bar the slope angle (45°) and slope aspect (SW) are both playing an entirely positive role in overall ablation.

Figure 3.3 INCOMING SHORT WAVE RADIATION ON SOUTH FACING SLOPES (JUNE 1, 1987)

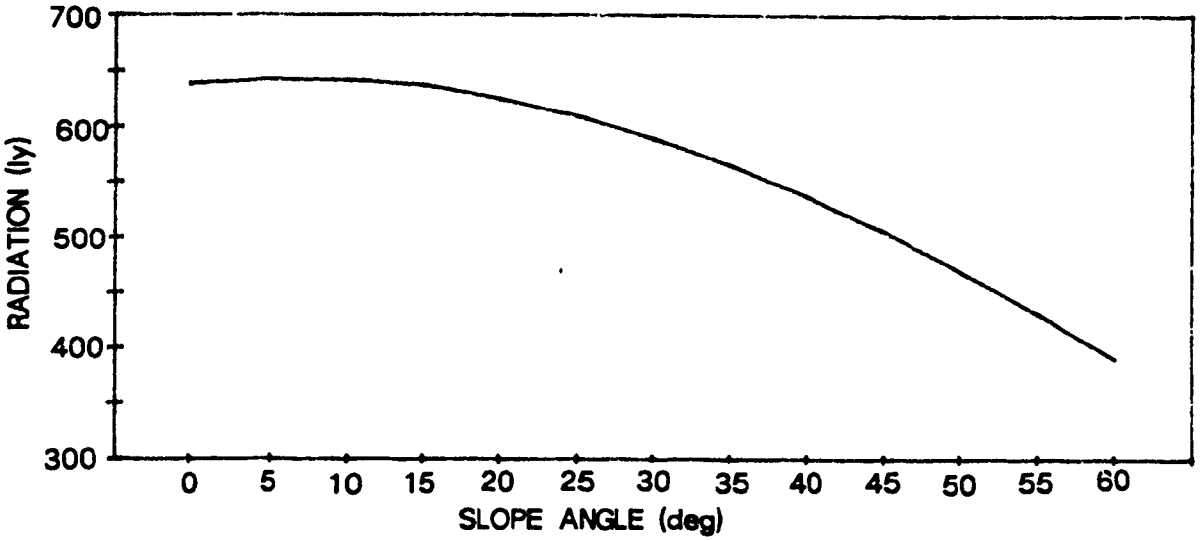

Figure 3.4 INCOMING SHORT WAVE RADIATION ON 45° SLOPE FOR DIFFERENT ASPECT (JUNE 1, 1987)

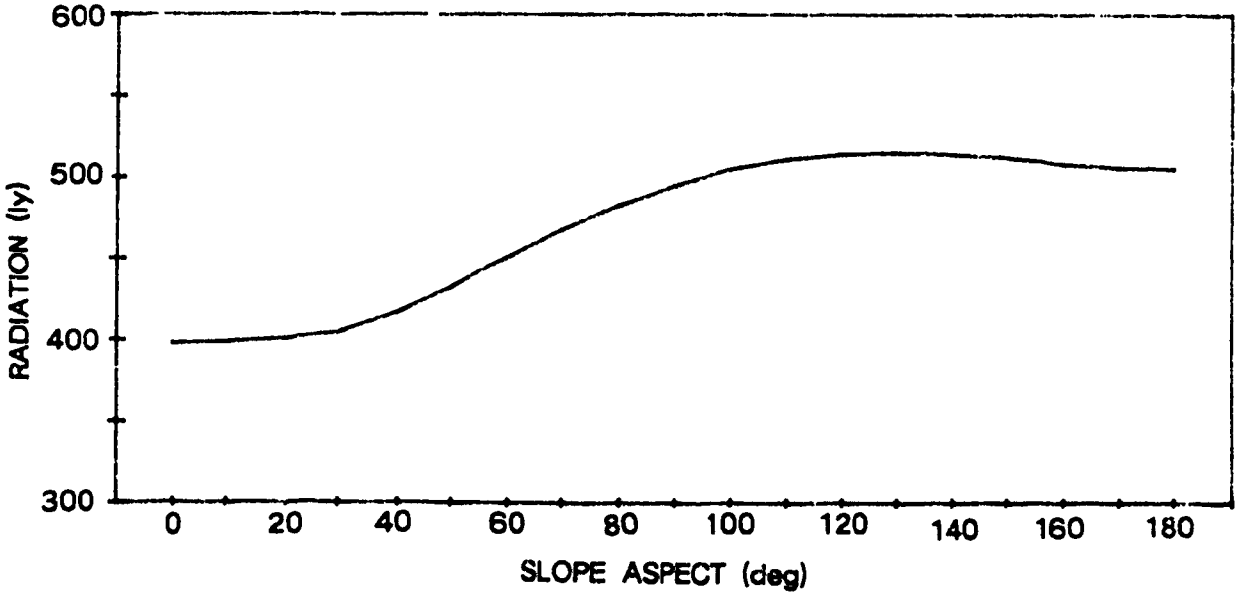

There is a seasonal influence on the azimuth. The lower the solar height and shorter the daily path of the sun, the greater the difference becomes, e.g. for a solar declination of -15° (Feb. 7, Nov. 4) a 45° S-facing slope receives 1.7 times as much energy as a horizontal surface, while a 45° N-facing slope does not receive any energy at all (see Table 3.1).

Table 3.1 DIRECT INCOMING RADIATION ON HORIZONTAL SURFACE AND 45° SLOPES AT SUMAIYAR BAR (LAT: 36.15° N)

Day	Sun's declination	Horizontal surface	S-Facing slope	N-Facing slope
May 22, Jul 22	+20	641	518 (.8)*	389 (.61)
May 02, Aug 11	+15	605	543 (.9)	311 (.51)
Apr 16, Aug 28	+10	560	558 (1.0)	232 (.41)
Apr 03, Sep 10	+5	506	558 (1.1)	155 (.31)
Mar 08, Oct 06	-5	401	541 (1.4)	36 (.09)
Feb 23, Oct 19	-10	340	510 (1.5)	10 (.03)
Feb 07, Nov 04	-15	282	473 (1.7)	0
Jan 19, Nov 24	-20	222	423 (1.9)	0

* energy expressed as the ratio of horizontal and slope surface radiations.

Chapter 4

Methodology and Procedure

Hydrological, glaciological, and meteorological investigations were carried out above 3000 m a.s.l. during the 1987 summer field season in the Barpu Glacier Basin. Ablation studies were carried out at Sumaiyar Bar from May 24 until July 24. The description of all field work and procedures are given as follows:

4.1 ABLATION MEASUREMENTS

The measurement of change in thickness of an ice layer is essentially a measure of the decrease in volume of the ice layer; whereas ablation, in its practical sense, is the decrease of mass within a layer (Hubley, 1954). Ablation values are in cm of water equivalent throughout in this paper, except where otherwise stated. The statement that ablation equals to 1 cm will generally mean that ablation removes a total of 1 cm^3 of water equivalent from the volume represented by a vertical prism having a horizontal cross-sectional area equal to 1 cm^2 and extending from the base to the surface of the glacier.

Measuring the vertical lowering of the surface level relative to a fixed point

is the common method of assessing mass wastage. The height difference is converted to mass figure by multiplying by the density of glacier ice which is assumed to remain constant with respect to time and space.

Seligman (1950) measured the density of ice at 0 °C giving a mean of 0.9059 gm/cm^3. Taking this in conjunction with several measurements of ice with air bubbles, yields values below 0.9; he prefers to use 0.9 as the density of glacier ice rather than the usual 0.91 for practical purposes. Glacier ice would tend to increase rather than decrease its density due to presence of salt solutions. Ward (1950), Butkovich (1955), Meier (1962), and Paterson (1981) measured the values of glacier ice densities as 0.91, 0.9171-0.9173, 0.917, and 0.8-0.91 gm/cm^3 respectively. Paterson suggested that it may be sufficiently accurate to assume a density of 900 kg/m^3, as also prefered by Seligman.

The entire surface (except facets) of the study area was covered with debris which protects ice surface from direct solar radiation and a surface, free of cryoconite holes and large air bubbles was found beneath the debris cover. Furthermore, no change in surface configuration was found during study. Hence, a uniform density of 0.9 gm/cm^3 was used in this study.

All the ablation measurements are based on surface wastage only. The glacier is generally assumed to be in a state of isothermal melting with no appreciable heat conducted to or from layers deep beneath the surface (Platt, 1966).

4.1.1 Ablation Stakes

Overall, 50 wooden stakes – 2 m long with 4 by 4 cm cross section – were established for facet and debris covered surface ablation measurement. The bottom

stakes of facets M & N were excluded from the analyses (not shown in Figure 4.1), since their measurements seemed to be unreliable. Similarly, the stakes J2, O1, and O2 were also excluded from 'flat surface ablation' study. A total of 37 and 45 stakes were, therefore, respectively used for facet and flat surface ablation study (later is given in Table 5.2, p. 85).

The stakes were placed in a narrow hole drilled with a hand-operated ice drill. The stakes were anchored firmly into the ice hole so that it remained in a fixed position relative to the glacier surface. The stake may float in the meltwater in the hole due to wet conditions in the ice as described by Ostrem and Stanley (1969). Care was taken to ensure that each stake was "frozen solidly" in the ice.

4.2 FACET ABLATION

Overall, fourteen facets were selected, in the study area described in section 2.3, for detailed study on the basis of aspect since a typical slope angle of 45° was found for all facets. While all other facets within the study area were studied for slope angle, aspect, their concentration based on orientation, and debris condition on surface, etc. The facet network is shown in figure 4.1.

To study the effects of orientation on ablation, the facets were grouped into eight categories, namely N-, NE-, NW-, E-, W-, SE-, SW-, and S-Facing. The dominant orientation of facets in the study area was SW and W. However, only a few facets were oriented in N, NE, and S direction. Therefore, only three facets not in predominant SW and W orientation were studied to compare ablation variation in aspects (see Table 5.8 and Figure 5.9 for details).

Figure 4.1 FACET AND ABLATION STAKE NET WORK

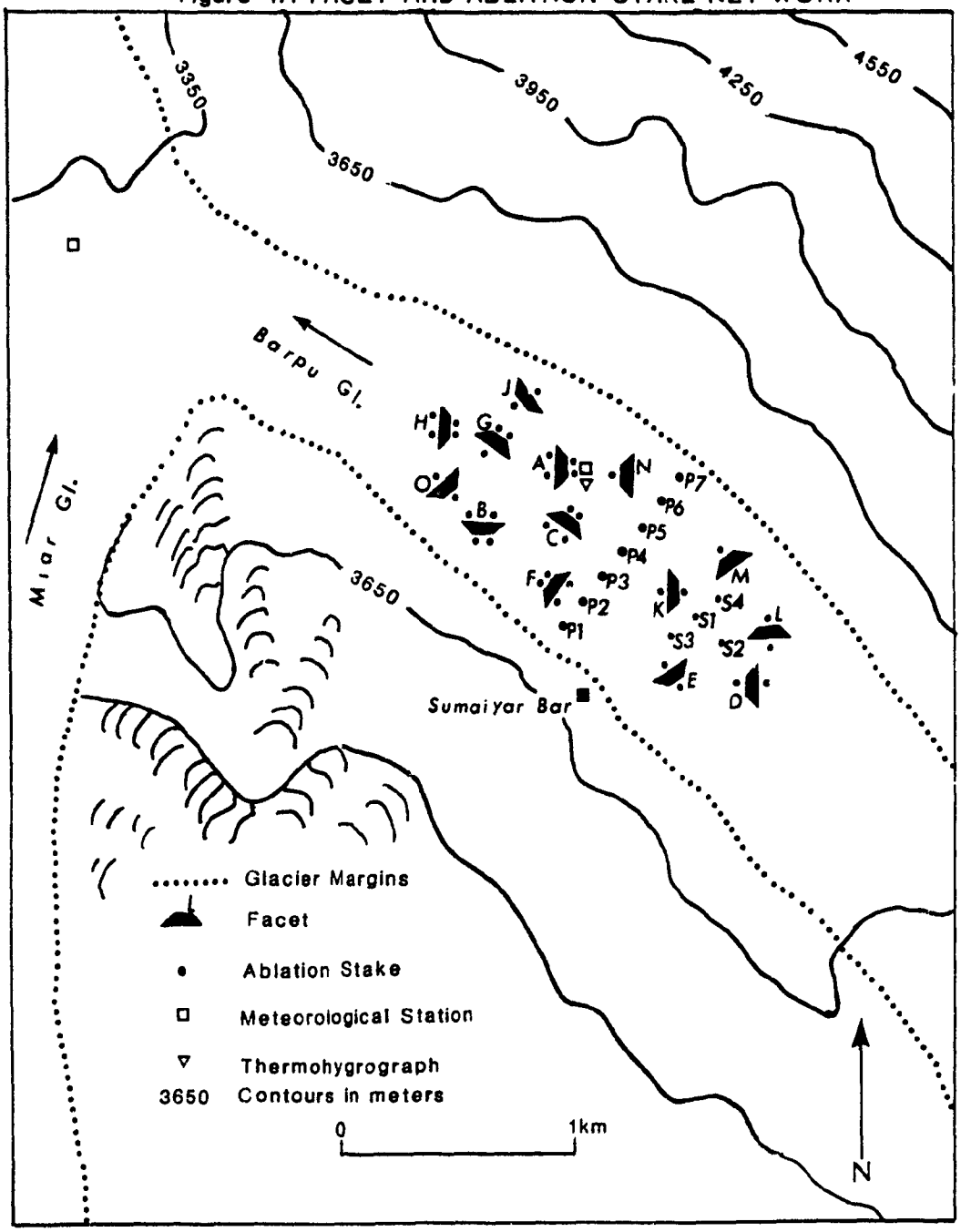

The arrangement of facets and stakes are shown approximately

All facets were surrounded by two to four stakes, depending on size of the facet. Two stakes were inserted near the top edge and two near the bottom edge of the facets. The horizontal distances from facet edge to inner side of the stakes (Figure 4.2) were measured usually over a three day interval. The difference between successive readings gave value of the recession of the slope surfaces. Ablation rate for a facet was calculated as the mean of all four or two stakes' measurements except facets M & N, where only one stake for each facet was used. No stakes were inserted on the face of the facet slope for the following two reasons. Firstly, due to steep angle and height (10 to 25 m) of slope it was dangerous and difficult to drill in the middle or near the top of the slope surface. Secondly, there was a danger due to continous fall of boulders. If stakes would have been placed on the surface, they could be crushed by speeding downslide of boulders due to 45° slope. Even some of the stakes near the bottom edge of facets were broken by boulder slidings. Besides, it was sometimes dangerous to measure horizontal distance between bottom edge of the facet and the stake. It would have been more dangerous to measure the stakes right on the slope surface of the facets.

The slope angle and azimuth were measured periodically and no changes were found in these two characters at all, therefore it is assumed that the facets melt uniformly throughout the surface area. A Brunton Compass was used to measure slope azimuth and angle. The compass was tied to a two meter long wooden stake which then used for measuring the slope angle by placing stake at several places on the slope surface. The average of these values represented slope angle for that facet.

Figure 4.2 FACET ABLATION MEASUREMENT

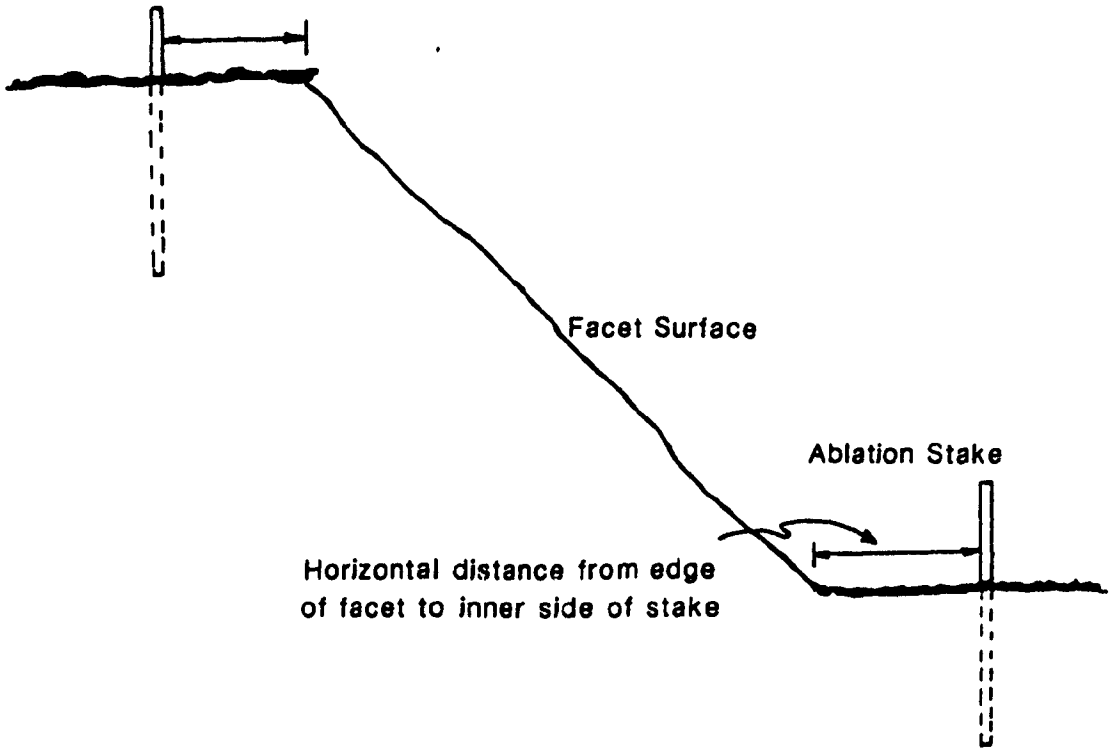

Because of the recession of facets, all sized debris (ranging from less than 1mm to more than 1 m) slips from top to bottom of the slope surface continuously due to steep angle (45° as typical). The debris, usually smaller than 1 cm deposited in the surface cavities, helps in transmitting the energy to the ice surface. The debris conditions were checked by the albedo measurements on each facet. The debris, especially the large size boulders sliding on the facet also keeps the surface smooth and free of spongy conditions due to this friction.

The amount of solar radiation received by different slope aspects varies largely and one cannot estimate the facet ablation without knowing it's concentration with respect to orientation. To estimate weighted ablation rate, the area of all facets within study area was measured with respect to their aspect. In addition, it was necessary to calculate the percentage area of debris covered surface for 1 km^2. Debris covered area can be calculated by subtracting total facet area from 1 km^2. But since the facets result in increasing the surface area, actually there will be more than 1 km^2 of area within 1 km^2.

In fact, the slope area when transformed on horizontal plane will be reduced by a factor, 0.7071, taking slope angle as 45° (cos 45° = 0.7071). Therefore the debris covered area is obtained by subtracting the facet area multiplied by 0.7071, while for other calculation the actual facet area is used. The total surface area is increased by about 24,000 m^2/km^2 when the account for facets is taken.

4.3 FLAT SURFACE ABLATION

The stakes established to measure the facet ablation were also used for flat surface ablation measurement under their existing debris conditions.

Ostrem and Stanley (1969) described the ideal condition for a stake network, to achieve a representative ablation rate, that "stakes should be scattered uniformly over the entire surface so that every part of the glacier is covered by an equally dense network". But since this distribution pattern is ideal and not practical, they suggested a long line up the centre with transverse lines at regular intervals. According to Arnold (1981), the accuracy of the mean value of ablation is a function of the number of ablation stakes and their distribution over the area. He used 18 to 22 stakes over an area of 1.7 km^2 on White Glacier study in 1969-70. Adams (1966) used the same pattern with 23 stakes per km^2.

In the present study, both of these conditions were met. All the stakes were scattered over the entire study area. Overall 45 ablation stakes were used within 1.5 km^2 area (see figure 4.1).

The stake measurement was normally considered as the difference of the distance from top of the stake to the ice surface. The stake-straight edge method was applied where a pond developed around the stake. This method, described by Adams (1966), states that the mean of the distance from a fixed mark on the stake to the underside of a 50 cm straight edge laid first parallel and then perpendicular to the direction of flow of the glacier. An ice-ax was used as a straight edge. Since, almost all the stakes were covered with debris layer, care was taken to replace the debris around stakes, removed while measuring the ablation.

Ablation with reference to the debris cover thickness was measured at all 45 stakes under their existing debris conditions. A tendency of debris cover to change its depth with respect to time due to the dynamic characteristic of the glacier and external climatic conditions was found. Three short periods were, therefore, selected

to study the debris cover effect on ablation, during which no changes occurred in debris cover thicknesses.

4.4 DEBRIS BUDGET SURVEY

A debris survey was conducted to study the debris concentration, size and thickness distribution over 1.1 km^2 of area. Over 110 grid points were marked within the area at 100 meters apart with help of a hip chain. The debris cover thickness at each point was then measured (the debris depths at five different places within approximately 5 m^2 area were measured, mean of which represented the debris depth at that grid point). A frequency curve for debris thickness is plotted, so that the weighted ablation can be estimated. Three regression equations were derived by which the ablation under each debris thickness for 110 grid points may be predicted for weighted ablation rate, in this manner both, area and thickness of debris cover, were taken into account to estimate ablation rate. For comparing the flat surface ablation with facet ablation, the mean of 45 stake ablation is taken.

4.4.1 Grain Size Measurements

Size distributions of debris coarser than 1 mm were measured at each grid point within 1 m^2. Twenty five randomly chosen debris particles from course sand to huge boulders (up to 100 cm) were measured along the B-axis (i.e the shortest axis of particle). The supraglacial debris was sampled at three locations across the glacier for size distribution analysis smaller than 1 mm debris size.

4.5 METEOROLOGICAL OBSERVATIONS

An electronic data logger (called 'Ecobug') was installed on facet A near stake A1, shown in figure 4.1 to collect temperature data. All three temparature sensors (thermilinear thermisters, YSI 44203, range -30° to +50°C; Wake and Limnoterra. 1987) were calibrated on site. The temperatures of the ice surface under a 10 cm debris cover, at the debris surface, and at 1 m above the ice surface were recorded hourly from May 24 to July 24. The data had been down loaded onto microcassettes with the help of a portable Epson microcomputer on each 7th or 10th day at the site, and then transferred to hard copies by giving the slope and Y intercept values, calculated by calibration. Care was taken to minimize the chances of data loss due to cassette damage etc. The ecobug worked very well through out the season.

Relative humidity and temperature were also recorded on weekly charts by Thermohygrograph, placed inside Stevenson screen near ecobug station. The screen was fixed on 1.2 m high ridge built by boulders. The cloud cover (in tenths) was recorded at 9:00 a.m., 12:00 noon, 3:00 p.m., and 9:00 p.m. each day. The type and condition were also recorded. The wind speed data from Miar station was used which was about 1 km from the study area. The Taylor wind anemometer height was 2 m above the ice surface.

To determine the debris property on facets, albedo measurements were taken with a Pyranometer by holding it parallel to the facet surface. The outgoing short-wave radiation was measured by putting the instrument upside down parallel to the surface. Albedo was then calculated in usual manner, i.e. by dividing the outgoing radiation by incoming radiation multiplied by 100. Due to a shortage of

instruments, the Pyranometer was used only for one day during the entire season when it was removed from the Phahi Phari main meteorological station. It is, therefore, not sufficiently accurate to use these values for the entire season, instead only incoming short wave radiation is used for correlation with the ablation. These albedo values, however, give an idea of facet surface property in respect to absorption of solar radiation.

The incoming direct short-wave radiation on different facets were computed by the computer programmes presented by Ohmura (1969) and later modified by Fuggle in 1970. These programmes are based on the method of calculating direct shortwave radiation income of slopes, described by Garnier and Ohmura (1968). These programmes are written in Fortran IV, by which the direct shortwave radiation income of slope, knowing slope angle and azimuth, can be computed on daily and hourly bases. Sun's declination was calculated for each day from 'sine curve' presented by Garnier and Ohmura (1970), while the transmissivities vary from 0.5 to 0.85 based on climatic conditions mainly on temperature and cloud cover in addition to radiation data at Phahi Pheri and Miar main meteorological stations.

The direct incoming shortwave radiation is used for correlation with the ablation. Slope angle in association with azimuth greatly affects the amount of incident incoming direct solar radiation (Young, 1976). The diffuse component constitues 5 to 15% of the total (Wieder, 1982) and is independent of the slope and aspect. Furthermore, the main objective in using the radiation estimates was to get relative values for the different slopes and aspects rather than absolute estimates.

Chapter 5

Results and Discussion

In this section the factors affecting ' ' ablation at Sumaiyar Bar are discussed. A final estimate of ablation; based on topographical, morphological, and meteorological conditions of the glacier; is presented. A statistical model based on meterological conditions under the existing lacier surface conditions is also presented.

The angle and aspect of facets were checked periodically during the season and no change in these two factors was observed. As mentioned earlier, the typical slope angle of 45° was observed. Therefore, keeping slope angle as constant, facet ablation is discussed on the basis of aspect only.

Although the debris covered area was not absolutely plane or horizontal, it was treated as a horizontal or flat surface for comparison with facet surfaces. The slope of debris covered surface was neglected since the heavy debris loads overcome the slope effect on ablation under cover. Since almost all the flat surface area was covered with debris load, the flat surface and the debris covered surface will mean the same. To differentiate the facet ablation from flat surface ablation, the facet ablation will be denoted by respective aspects (e.g. N ABL, SE ABL, E ABL, etc.).

Table 5.1 shows the mean daily ablation data of 45 stake maesurements for 62 days, and the ablation rate of 2.7 cm/day with a standard deviation of 0.38 cm/day.

Since the ablation was measured usually over a period of several days, the ablation rate is the mean of these days. The standard deviation, therefore, is not much meaningful but will give some idea of ablation variation.

The error in each ablation measurement for flat surface and facet was assumed at ∓0.2 and ∓1 cm respectively. This gives ∓0.03 to ∓0.07 cm/day for flat surface ablation rate and ∓0.1 to ∓0.3 cm/day for facet ablation rate.

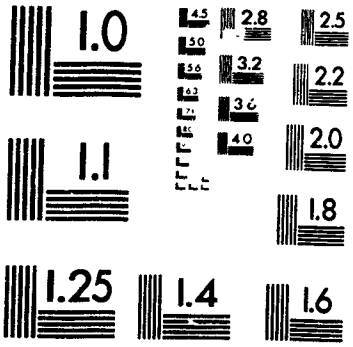

Table 5.1 MEAN ABLATION OF 45 STAKE MEASUREMENTS

Day	Ablation (cm)	Cumulative ablation (cm)
May-24	2.8	2.8
25	3	5.8
26	3.2	9
27	3.3	12.3
28	3.4	15.7
29	3.6	19.3
30	3.6	22.9
31	3.2	26.1
Jun-01	2.8	28.9
02	2.8	31.7
03	2.8	34.5
04	2.8	37.3
05	2.8	40.1
06	2.8	42.9
07	2.8	45.7
08	2.8	48.5
09	2.3	50.8
10	2.2	53
11	2.2	55.2
12	2.2	57.4
13	2.3	59.7
14	2.4	62.1
15	2.4	64.5
16	2.4	66.9
17	2.3	69.2
18	2.4	71.6
19	2.2	73.8
20	2.1	75.9
21	2.1	78
22	2.1	80.1
23	2.1	82.2
24	2.3	84.5
25	2.4	86.9
26	2.4	89.3
27	2.4	91.7
28	2.9	94.6

continued . . . .

Table 5.1 (continued)

Day	Ablation (cm)	Cumulative ablation (cm)
29	3.1	97.7
30	3	100.7
Jul-01	2.8	103.5
02	2.8	106.3
03	2.9	109.2
04	2.8	112
05	2.9	114.9
06	2.9	117.8
07	2.9	120.7
08	2.9	123.6
09	2.9	126.5
10	2.9	129.4
11	2.6	132
12	2.4	134.4
13	2.7	137.1
14	2.8	139.9
15	2.7	142.6
16	2.8	145.4
17	2.8	148.2
18	2.8	151
19	2.9	153.9
20	3.2	157.1
21	3.2	160.3
22	3.2	163.5
23	3.2	166.7
24	3.2	169.9

Average Ablation F[illegible]or 62 Days = 2.7 cm/day

σ = 0.38 cm

The mean ablation for the 45 stakes is given in Table 5.2, in which ablation at each stake location is the mean of 62 days. This shows the ablation pattern of the glacier surface under study with a standard deviation of 0.96 cm between stakes. The rates of ablation were mostly uneven over the glacier and were related mainly to the differential debris deposition, which affected the absorption of insolation. The flat surface ablation rates changed within a short distance. Stake series A, for example, shows ablation pattern around facet A. The ablation rate at stake A1 and A2, which were fixed on top of the facet, was approximately 3.5 cm/day. At the bottom of the facet, at stakes A3 and A4, the measured ablation rate was, on average, approximately 2.7 cm/day. Stake series D, E, F, H, and L displayed a similar pattern. The P series of stakes, starting from the left margin of the glacier, also show that ablation rates were affected primarily by debris deposition. The ablation rate gradually increased from the left margin (1.1 cm/day at stake P1) to the right (5.4 cm/day at stake P6) suggesting that the debris cover thickness was greatest on the left side of the glacier (see debris cover thickness at P series in Table 5.4). The greatest debris cover thickness (30 cm) was measured at stake P1, whereas at P6 it was only 1.5 cm. This would suggest that under the same atmospheric conditions the flat surface ablation is mainly controlled by the debris cover.

Table 5.2 MEAN ABLATION RATE AT EACH STAKE LOCATION FOR THE PERIOD May 24 - July 24 (62 days)

Stake #	Ablation (cm/day)	Stake #	Ablation (cm/day)
A1	3.5	H1	3.1
A2	3.4	H2	2.3
A3	2.6	H3	2.6
A4	2.8	H4	1.6
B1	2.2	J1	1.9
B2	2.1	K1	2.8
B3	2.3	K2	2.7
B4	2.2	L1	3.8
C1	2.1	L2	2.1
C2	2.3	M	3.4
C3	2.0	N	2.6
C4	2.3	P1	1.1
D1	3.3	P2	1.4
D2	2.3	P3	4.6
E1	0.7	P4	3.2
E2	1.4	P5	4.5
F1	3.7	P6	5.4
F2	3.0	P7	4.3
F3	2.9	S1	3.2
F4	2.4	S2	3.3
G1	2.3	S3	3.9
G2	1.9	S4	3.9
G3	1.9		

Average Ablation Rate of 45 Stakes = 2.7 cm/day

σ = 0.96

Total ablation = 2.7 × 62 = 170 cm

5.1 FACTORS AFFECTING ABLATION

Factors affecting ablation at Sumaiyar Bar can be grouped into three classes, (1) *debris cover*, (2) *facets*, and (3) *meteorological conditions*. Of course the *elevation* is another important controlling factor for ablation but, the study was performed at about 3500 m elevation which is the mean elevation of the ablation area of Barpu glacier. The study area is, therefore, a representative one regarding elevation.

5.1.1 ABLATION AFFECTED BY DEBRIS

Almost all the study area of Sumaiyar Bar is covered by heavy debris loads except for the slope surfaces and ice pinnicles. Because flat surface ablation was mostly affected by debris cover, it will be useful to consider the debris conditions on the study area first.

The frequency distribution of debris cover thickness is given in Figure 5.1. Within a 1.1 km^2 area, each depth measurement was taken at 100 m intervals. The higher values of debris thickness were observed near the margin of the glacier while in the middle the depths were mostly concentrated between 1 and 12 cm, 12.4 cm being the average debris depth for whole area with a standard deviation of 12.6 cm.

About 20% of area was covered by debris layer under 3 cm thick (Table Table 5.3 and Figure 5.2) which accelerated the ablation rate. Almost 55% of area was occupied by debris 3 to 15 cm thick. The remaining 25% of the area was covered with debris layer from 16 to 70 cm thick. this means that the ablation was decelerated under 80% of the debris covered area.

Table 5.3 FREQUENCY DISTRIBUTION AND CUMULATIVE PERCENTAGE OF DEBRIS THICKNESS.

Debris Depth (cm)	Frequency (f)	% of total number	Cumulative %
0 - 5	35	31.82	31.82
5.5 - 10	28	25.45	57.82
10.5 - 15	19	17.27	74.54
15.5 - 20	11	10	84.54
20.5 - 25	6	5.45	89.99
25.5 - 30	2	1.82	91.81
30.5 - 35	3	2.73	94.54
35.5 - 40	1	0.91	95.45
40.5 - 45	2	1.82	97.27
45.5 - 50	0	0	97.27
50.5 - 55	1	0.91	98.18
55.5 - 60	0	0	98.18
60.5 - 65	1	0.91	99.09
65.5 - 70	1	0.91	100
Total	110	100	

Figure 5.1 FREQUENCY DISTRIBUTION OF DEBRIS COVER THICKNESS

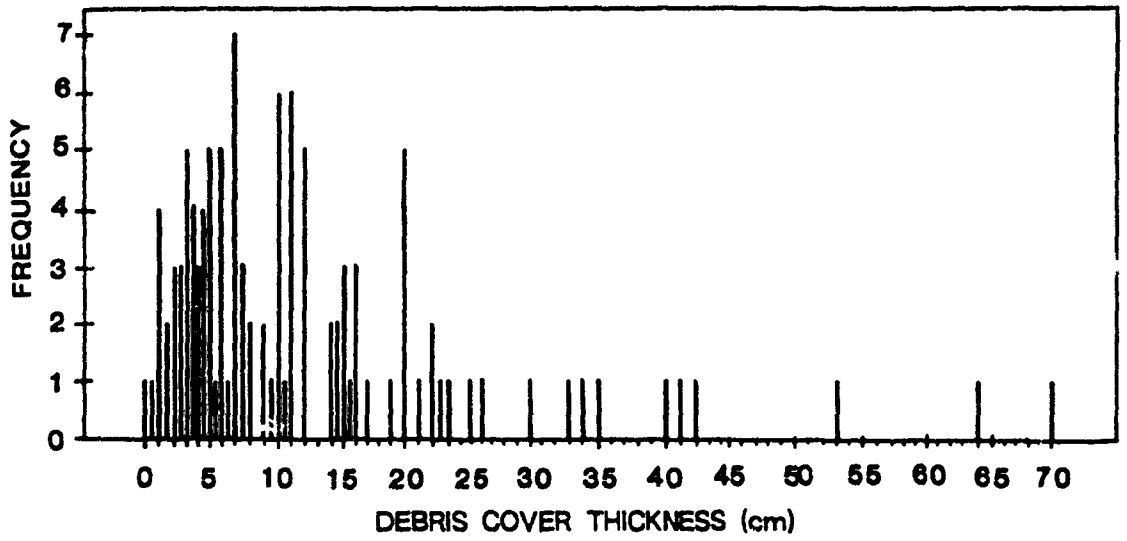

Figure 5.2 CUMULATIVE PERCENTAGE CURVE FOR DEBRIS COVER BY THICKNESS

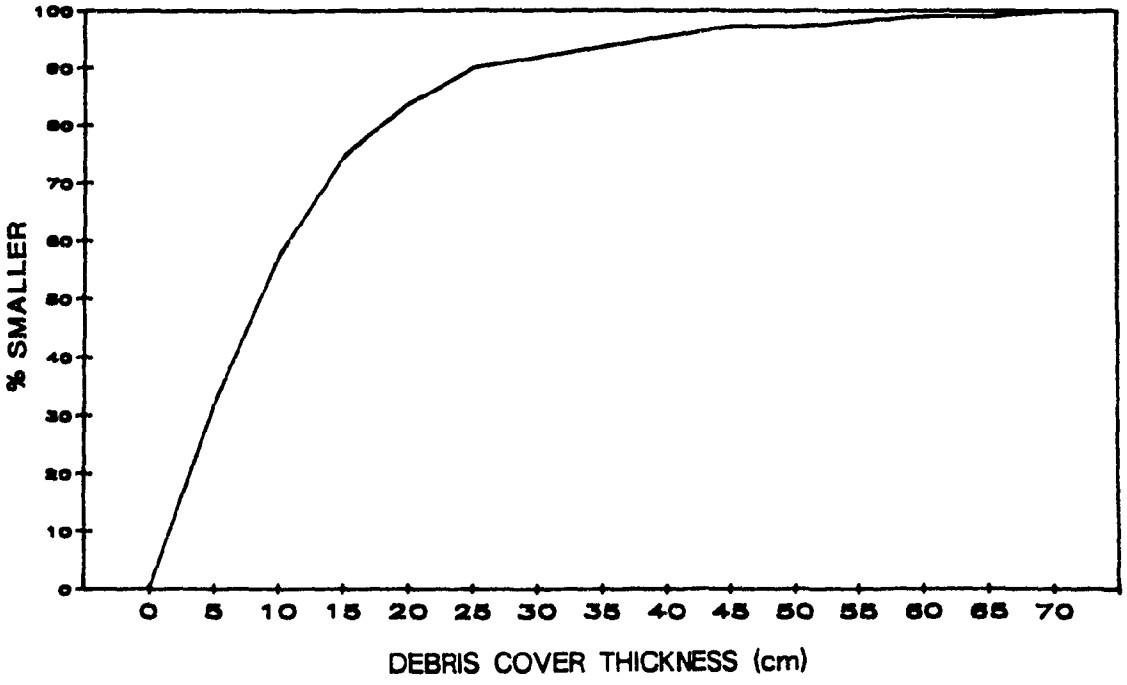

During study, it was found that debris cover depth changes with respect to time due to dynamic behavior and differential rate of glacier ice melting. Therefore, to study the effect of debris cover on ablation, three different periods were selected (see Table 5.4) during which the debris cover was found at constant depth. From this table it can be seen that the changing of debris depth was not asymmetric, i.e., at some locations it increased with the time and at another it decreased; while at some locations it was almost at the same depth. Similarly, the rate of change of depth was also not steady. At stake C4, for example, the debris depth was 4.3 cm during the Period-1 (May 26 - June 1) and 11 cm during the Period-2 (June 25 - July 1), which decreased again during Period-3 (July 13 - July 19). In fact these changes in depth were not abrupt, since these selected periods are not continuous; the intermediate periods (i.e. June 1 - June 25, and July 1 - July 13) might be the transition periods. The measurement error of debris cover thickness was ∓0.3 cm.

Table 5.4 EFFECT OF DEBRIS COVER THICKNESS (D) ON ABLATION (ABL)

Stake #	Length of Survey					
	Period-1		Period-2		Period-3	
	May 26 - Jun 1		Jun 25 - Jul 1		Jul 13 - Jul 19	
	D (cm)	ABL (cm/day)	D (cm)	ABL (cm/day)	D (cm)	ABL (cm/day)
A1	5.5	4	4.6	4.4	4.5	4.2
A2	4	4.9	4.5	2.7	3.5	4.9
A3	7	3.9	7.5	2.7	7.5	2.3
A4	5.6	4	6	2.8	6.5	3.2
B1	4.7	3.7	8	1.9	10	3.1
B2	5.9	2.9	7.5	1.8	9	3.6
B3	5.9	2.6	10	2.7	10	2.8
B4	6.3	2.7	10	2.4	4	3.2
C1	7.6	2.8	8	2.2	7	3.5
C2	6.6	3.6	9	3.2	11	1.9
C3	5.3	3.1	14	2.4	11	1.9
C4	4.3	4.1	11	2.4	9	2.2
D1	6.2	3.6	-	-	9.7	3.8
D2	6	3.5	-	-	13.7	1.3
E1	43.6	.8	35.5	.6	-	-
E2	8.6	2	13	1.5	15	1.5
F1	5.6	3.5	-	-	3.5	5.4
F2	7.9	2.9	-	-	-	-
F3	4.7	6.2	6	2.4	14.9	1.9
F4	7.8	2.9	8	.7	-	-
G1	4.1	3.3	-	-	-	-
G2	7.6	2.6	-	-	-	-
G3	3.3	5.5	-	-	20	1.7
H1	9.2	2.3	-	-	-	-
H2	8.1	3	-	-	-	-
H3	3.9	7.4	-	-	9	2.3
H4	5.3	2.6	-	-	15	1.8
P1	30	1.1	27	1.5	27.3	1.6
P2	28	1.1	26	2.9	26.4	1.9

continued . . . .

Table 5.4 (continued)

Stake #	Length of Survey					
	Period-1		Period-2		Period-3	
	May 26 - Jun 1		Jun 25 - Jul 1		Jul 13 - Jul 19	
	D (cm)	ABL (cm/day)	D (cm)	ABL (cm/day)	D (cm)	ABL (cm/day)
P3	2.9	4.4	2.5	5.4	2.7	5.2
P4	7	4.4	7	3.3	8	3.5
P5	4	5	3	5.4	4.5	5.1
P6	1.5	6	0	6.5	0	6
P7	5	4.9	-	-	4.3	4.1
S1	7	3.3	7	3.5	-	-
S2	4	4.2	4	3.4	-	-
S3	6	4.3	6	4.5	-	-
S4	2	5.6	2	3.7	-	-
J	.5	7	.6	8	1	5
K1	-	-	6	4.4	4	3.5
K2	-	-	-	-	7	3.7
L1	-	-	2	5.4	3	4.6
L2	-	-	5	3.7	6	3
M	.5	7	1	9.3	1.2	9
N	-	-	9	3	12.5	3.2

Ablation under 45 different debris cover depths are plotted for these three time periods (see Figure 5.3), which show typical pattern. The critical thickness of debris cover for acceleration and retardation of ablation was found around 3 cm and the most effective thickness for ablation was around 1 cm. The ablation was almost doubled under 1 cm debris depth as compared to ablation on bare ice surface (Figure 5.3a). It shows clearly that debris depth under 3 cm enhances ablation of the Sumaiyar Bar site. Since the average depth was found to be about 12.4 cm, this negatively affects the ablation by protecting almost 80% of ablation area. The ablation under debris cover 12.4 cm thick is reduced by 68% on average. Recent observations have demonstrated that a debris cover of the order of 15 cm thick is capable of reducing the underlying ice surface ablation rate by about 75% (Gordon et. al., 1978). The mean ablation rate of bare ice surface was estimated at 6 cm/day, while ice beneath a debris layer of 1 cm thick, ablated at the rate of approximately 9.5 cm/day. This shows 63% increase in ablation rate under 1 cm thick debris cover.

Figure 5.3 RELATION OF MEAN DAILY ABLATION TO DEBRIS COVER THICKNESS

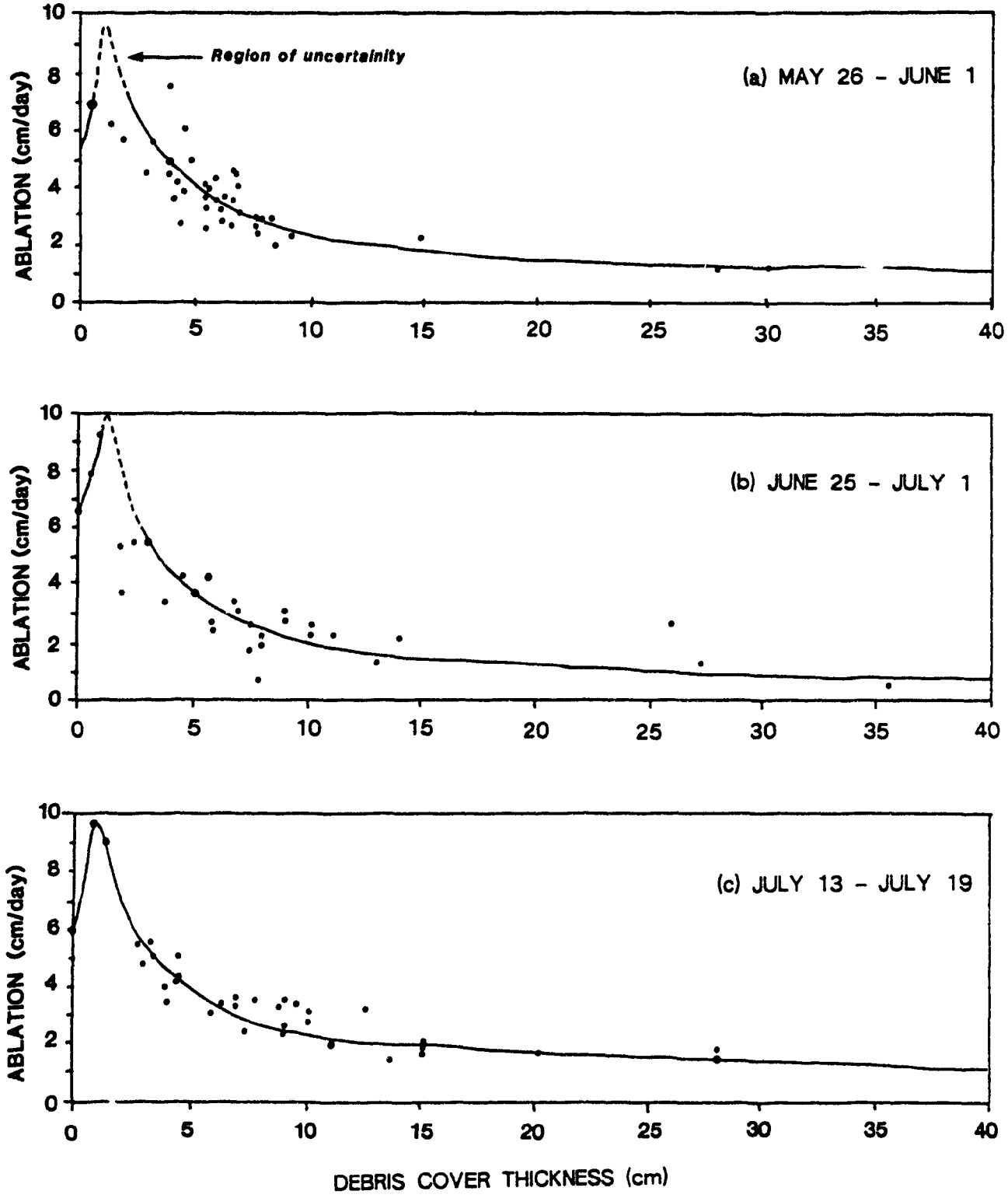

The significance of the debris cover on the ablation was also tested statistically. Although the ablation is not a linear function of debris cover thickness perfectly but when transformed on log log scale, the ablation of glacier ice may be calculated by assuming that ablation rate is a linear function of debris cover thickness. The average ablation for 45 stakes underlying debris cover thicknesses for three periods are calculated, and linear regression of ablation against debris cover thickness obtained for all three periods. The results are shown in Table 5.5. In all three cases a more than 70% variation in ablation is explained by debris cover. The third equation with highest correlation coefficient (R = -.91) between ablation and debris depth is then used to estimate the ablation over entire 1 km^2 area, or weighted ablation, in other words. This equation explains 82% variation in ablation by debris cover.

Table 5.5 SIMPLE REGRESSION AND CORRELATION: Ablation (ABL) vs. Debris Depth (D)

Period	Equations	S.E. of estimate	r	$r^2 \times 100$
1	Log ABL = 0.903 - 0.498 Log D where $1 \leq D \leq 40$	0.110	-.854	73
2	ABL = 6.69 - 4.17 Log D where $1 \leq D \leq 35$	1.030	-.842	71
3	Log ABL = 0.98 - 0.572 Log D where $1 \leq D \leq 27$	0.095	-.905	82

The summary of weighted debris covered ablation is given in Table 5.18, which will be discussed in section 5.2. The weighted flat surface ablation rate was estimated at 2.3 cm/day, which is reduced by 15% from unweighted ablation rate.

The ablation rate 2.3 cm/day is more representative because this is achieved by considering 110 points over almost 1.1 km^2 of area, in which all 110 points spread equally with 100 m apart. Hence, all the area under study was covered, whereas 2.7 cm/day was based on 45 points. In this connection, it is very helpful to know the debris budget for the ablation zone, because the debris depth, especially in the present case, changes within very small distances presenting very high differential melting rates.

Equation 3 in Table 5.5 may be valid only for predicting ablation under debris layer 1-27 cm to avoid extrapolation, because the actual ablation measurements were taken under 0-27 cm debris thickness for this period. From figure 5.3 it can be seen that ablation increases under debris cover 0-1 cm thickness, while decreasing after 1 cm depth. There are actually two curves instead of one, and two separate regression equations should be established for each curve. If we use all the values in one regression analysis, the equation will give only decrease in the ablation; while actually there is an increase in ablation for debris depth 0-1 cm. To avoid this problem, the ablation values equal to and more than 1 cm were used in analyses, so it may be used for depth greater than 1 cm. Each equation is valid for debris thickness greater than 1 cm and less than the actual maximum debris depth under which the ablation was measured. The separate equation for the first part of the curve can be established if we have sufficient values of ablation measurements under debris cover of this range (0-1 cm). Since the average debris cover depth is found as 12.4 cm, the equation achieved is sufficient to estimate weighted ablation.

However, these equations are valid only under the measured external meteorological conditions during study (i.e. May 24 - July 24), since under the particular debris depth the ablation was also affected by these atmospheric conditions at the same time. Furthermore, these equations were derived only to know the variation in ablation by debris and to estimate weighted debris covered ablation rate and not to predict ablation.

5.1.2 ABLATION AFFECTED BY FACETS

Facet ablation, as described in chapter 4, was measured on the basis of aspects. Since it is only the incoming solar radiation which is affected by slope angle and aspect, the facet ablation will be compared on the basis of their aspect and incoming radiation. Other meteorological factors will be dicussed later.

The mean daily ablation for all facets are given in Table 5.6a - 5.6c.

Table 5.6a FACET ABLATION

Day	N-Facing Facet: B		NE-Facing Facet: J		NW-Facing Facet: E,O	
	cm/day	Σ cm	cm/day	Σ cm	cm/day	Σ cm
May-24	3.5	3.5	4.4	4.4	5.1	5.1
25	3.5	7	4.4	8.8	5.1	10.2
26	3.5	10.5	4.4	13.2	5.1	15.3
27	3.5	14	4.4	17.6	5.1	20.4
28	3.6	18.1	4.4	22	5.3	25.7
29	3.6	23.7	5	27	5.4	31.1
30	3.6	29.3	5	32	4.9	36
31	3.4	33.4	3.9	35.9	4.9	40.9
Jun-01	3.3	36.7	3.7	39.6	4.2	45.1
02	3.3	40	3.7	43.3	4.2	49.3
03	3.3	43.3	3.7	47	4.2	53.5
04	3.3	46.6	3.7	50.7	4.2	57.7
05	3.3	49.9	3.7	54.4	4.2	61.9
06	3.3	53.2	3.7	58.1	4.2	66.1
07	3.3	56.5	3.7	61.8	4.2	70.3
08	3.3	59.8	3.7	65.5	4.2	74.5
09	3.3	63.1	3.7	69.2	4.2	78.7
10	3.6	66.7	3.7	72.9	4.2	82.9
11	3.6	70.3	3.7	76.6	4.2	87.1
12	3.6	73.9	2.9	79.5	4.2	91.3
13	2.7	76.6	2.1	81.6	3.5	94.8
14	2.4	79	2.1	83.7	2.8	97.6
15	2.4	81.4	2.1	85.8	2.8	100.4
16	2.4	83.8	2.1	87.9	2.8	103.2
17	2.4	86.2	2.1	90	2.8	106
18	2.4	88.6	2.1	92.1	2.8	108.8
19	3.2	91.8	2.3	94.4	3.2	112
20	3.5	95.3	2.3	96.7	3.8	115.8
21	3.5	98.8	2.3	99	3.8	119.6
22	3.5	102.3	2.3	101.3	3.8	123.4
23	3.5	105.8	2.4	103.7	3.8	127.2
24	3.8	109.6	2.5	106.2	4.1	131.3
25	4.1	113.7	4	110.2	4.6	135.9
26	4.1	117.8	5.3	115.5	4.6	140.5
27	4.1	121.9	5.3	120.8	4.6	145.1
28	4.1	126	5.3	126.1	4.7	149.8

continued . . . .

Table 5.6a (continued)

Day	N-Facing Facet: B		NE-Facing Facet: J		NW-Facing Facet: E,O	
	cm/day	Σ cm	cm/day	Σ cm	cm/day	Σ cm
29	4.1	130.1	5.3	131.4	4.7	154.5
30	4.1	134.2	5.3	136.7	4.7	159.2
Jul-01	4.3	138.5	5.9	142.6	5.9	165.1
02	4.5	143	6.6	149.2	6.9	172
03	4.5	147.5	6.6	155.8	6.9	178.9
04	4.5	152	6	161.8	6.6	185.5
05	4.5	156.5	5.4	167.2	5.9	191.4
06	4.5	161	5.4	172.6	5.9	197.3
07	4.5	165.5	5.4	178	5.9	203.2
08	4.5	170	5.4	183.4	5.9	209.1
09	4.5	174.5	5.4	188.8	5.9	215
10	4.5	179	5.4	194.2	5.9	220.9
11	3.7	182.7	4.9	199.1	3.8	224.7
12	2.8	185.5	4.3	203.4	2.5	227.2
13	2.8	188.3	4.3	207.7	2.9	230.1
14	2.8	191.1	4.3	212	3.2	233.3
15	2.9	194	4.3	216.3	3.2	236.5
16	3.1	197.1	4.3	220.6	3.2	239.7
17	3.1	200.2	4.3	224.9	3.2	242.9
18	3.1	203.3	4.3	229.2	3.2	246.1
19	2.9	206.2	4.4	233.6	5.4	251.5
20	2.6	208.8	4.4	238	7.7	259.2
21	2.6	211.4	4.4	242.4	7.7	266.9
22	2.6	214	4.4	246.8	7.7	247.6
23	2.6	216.6	4.4	251.2	7.7	282.3
24	2.6	219.2	4.4	255.6	7.7	290
Average Ablation Rate :	3.5		4.1		4.7	
σ :	0.8		1.2		1.4	

Table 5.6b FACET ABLATION

Day	SE-Facing Facet: F,M		SW-Facing Facet: C,G		S-Facing Facet: L	
	cm/day	Σ cm	cm/day	Σ cm	cm/day	Σ cm
May 24	5.5	5.5	5.9	5.9	5.6	5.6
25	5.6	11.1	5.9	11.8	5.6	11.2
26	5.6	16.7	5.9	17.7	5.6	16.8
27	5.9	22.6	5.9	23.6	5.6	22.4
28	5.9	28.5	6.8	30.4	6.4	28.8
29	5.9	34.4	8.6	39	7	35.8
30	5.4	39.8	8.6	47.6	7	42.8
31	4.8	44.6	7.7	55.3	6.5	49.3
Jun 01	4.8	49.4	7	62.3	6.2	55.5
02	4.8	54.2	7	69.3	6.2	61.7
03	4.8	59	7	79.3	6.2	67.9
04	4.8	63.8	7	83.3	6.2	74.1
05	4.8	68.6	7	90.3	6.2	80.3
06	4.8	73.4	7	97.3	6.2	86.5
07	4.6	78	7	104.3	6.2	92.7
08	4.6	82.6	7	111.3	6.2	98.9
09	4.6	87.2	6	117.3	5.5	104.4
10	4.6	91.8	5.1	122.4	5.1	109.5
11	4.6	96.4	5.1	127.5	5.1	114.6
12	4.6	101	5.1	132.6	5.1	119.7
13	3.8	104.8	5.3	137.9	5.1	124.8
14	3.5	108.3	5.5	143.4	5.5	130.3
15	3.5	111.8	5.5	148.9	5.5	135.8
16	3.5	115.3	5.5	154.4	5.5	141.3
17	3.5	118.8	5.5	159.9	4.4	145.7
18	3.5	122.3	5.5	165.4	3.2	148.9
19	3.5	125.8	4.7	170.1	3.2	152.1
20	3.4	129.2	3.3	173.4	3.2	155.3
21	3.4	132.6	3.3	176.7	3.2	158.5
22	3.4	136	3.3	180	3.2	161.7
23	3.4	139.4	3.3	183.3	3.2	164.9
24	5.8	145.2	5.5	188.8	5.3	170.2
25	6.5	151.7	6.8	195.6	6.2	176.4
26	6.5	158.2	6.8	202.4	6.2	182.6
27	6.5	164.7	6.8	209.2	6.2	188.8
28	6.6	171.3	8.4	217.6	8.2	197

continued . . . .

Table 5.6b (continued)

Day	SE-Facing Facet: F,M		SW-Facing Facet: C,G		S-Facing Facet: L	
	cm/day	Σ cm	cm/day	Σ cm	cm/day	Σ cm
29	6.8	178.1	9.6	227.2	8.2	205.2
30	6.8	184.9	9.6	236.8	8.2	213.4
Jul 01	7.6	192.5	8.1	244.9	7.8	221.2
02	8.5	201	6.5	251.4	8.5	229.7
03	8.7	209.7	6.5	257.9	8.5	238.2
04	8.2	217.9	8.2	266.1	7.4	245.6
05	7.6	225.5	8.1	274.2	6	251.6
06	7.6	233.1	8.1	282.3	6	257.6
07	7.6	240.7	8.1	290.4	6	263.6
08	7.6	248.3	8.1	298.5	6	269.6
09	7.6	255.9	8.1	306.6	6	275.6
10	7.6	263.5	8.1	314.7	6	281.6
11	6.8	270.3	6.3	321	4.9	286.5
12	5.4	275.7	4.5	325.5	4.6	291.1
13	5.4	281.1	4.5	330	5.4	296.5
14	5.4	286.5	4.5	334.5	7.4	303.9
15	5.4	291.9	5.5	340	7	310.9
16	5.4	297.3	6.5	346.5	6.1	317
17	5.9	303.2	6.5	353	6.1	323.1
18	5.9	309.1	6.5	359.5	6.1	329.2
19	5.9	315	7.8	367.3	6.5	335.7
20	5.9	320.9	9.2	376.5	6.9	342.6
21	5.9	326.8	9.2	385.7	6.9	349.5
22	5.9	332.7	9.2	394.9	6.9	356.4
23	5.9	338.6	9.2	404.1	6.9	363.3
24	5.9	344.5	9.2	413.3	6.9	370.2
Average Ablation Rate :	5.6		6.7		6	
σ :	1.4		1.6		1.3	

Table 5.6c FACET ABLATION

Day	E-Facing Facet: D,N		W-Facing Facet: A,H,K	
	cm/day	Σ cm	cm/day	Σ cm
May 24	6.2	6.2	5.7	5.7
25	6.2	12.4	5.7	11.4
26	6.3	18.7	5.9	17.3
27	5.2	23.9	5.2	22.5
28	5	28.9	4.1	26.6
29	5	33.9	4	30.6
30	5.6	39.5	4	34.6
31	6.1	45.6	4.7	39.9
Jun 01	6.1	51.7	5.4	44.7
02	6.1	57.8	5.4	50.1
03	6.1	63.9	5.4	55.5
04	6.1	70	5.4	60.9
05	6.1	76.1	5.4	66.3
06	6.1	82.2	5.4	71.7
07	6.1	88.3	5.4	77.1
08	6.1	94.4	5.4	82.5
09	4.8	99.2	3.9	86.4
10	3.5	102.7	2.9	89.3
11	3.5	106.2	2.9	92.2
12	3.5	109.7	2.9	95.1
13	4	113.7	4	99.1
14	4.5	118.2	4.2	103.3
15	4.5	122.7	4.2	107.5
16	4.5	127.2	4.2	111.7
17	4.5	131.7	4.2	115.9
18	4.5	136.2	4.2	120.1
19	4.5	140.7	3.3	123.4
20	2.3	143	3.1	126.5
21	2.3	145.3	3.1	129.6
22	2.3	147.6	3.1	132.7
23	2.3	149.9	3.1	135.8
24	3.5	153.4	5	140.8
25	4.8	158.2	5.7	146.5
26	4.8	163	5.7	152.2
27	4.8	167.8	5.7	157.9
28	5.2	173	5.3	163.2

continued . . . .

Table 5.6c (continued)

Day	E-Facing Facet: D,N		W-Facing Facet: A,H,K	
	cm/day	Σ cm	cm/day	Σ cm
29	5.7	178.7	5.2	168.4
30	5.7	184.4	5.2	173.6
Jul 01	5.7	190.1	5.3	178.9
02	5.7	195.8	5.8	184.7
03	5.7	201.5	5.8	190.5
04	5.3	206.8	5.3	195.8
05	4.9	211.7	5.3	201.1
06	4.9	216.6	5.4	206.5
07	4.9	221.5	5.4	211.9
08	4.9	226.4	5.4	217.3
09	4.9	231.3	5.4	222.7
10	4.9	236.2	5.4	228.1
11	4.5	240.7	5	233.1
12	4.1	244.8	3.6	236.7
13	4	248.8	4.1	240.8
14	3.9	252.7	4.5	245.3
15	4.1	256.8	5.1	250.4
16	4.1	260.9	5.8	456.2
17	4.1	265	5.8	262
18	4.1	269.1	5.8	267.8
19	5.9	275	5.8	273.6
20	7.7	282.7	5.9	279.5
21	7.7	290.4	5.9	285.4
22	7.7	298.1	5.9	291.3
23	7.7	305.8	5.9	297.2
24	7.7	313.5	5.9	303.1

Average Ablation Rate :

	5.1	4.9
σ :	1.3	0.9

The total ablation of different facets is compared in Figure 5.4, and the cumulative ablation pattern is shown in Figure 5.5, while the Figure 5.6 shows the mean ablation rate based on 62 days along with the mean daily radiation income on each slope. This clearly shows that the facet ablation is a function of radiation income. The expected results were achieved here, i.e. the southern slopes ablated at higher rate mainly because of radiation, as dicussed earlier. The SW facet ablation (6.7 cm/day) was about twice that of N facet ablation (3.5 cm/day) and 2.5 times of that of flat surface ablation, whereas the incoming radiation on SW facets was only 80% of that of a horizontal surface. The highest radiation rate (479 ly/day) was received by SW and SE facets, among all facets. While radiation rate at debris covered surface was 599 ly/day (the highest among all surfaces). This comparison clearly shows the significance of slope (especially the SW facing) and debris covers in ablation rate of Barpu Glacier.

Some slopes received the same amount of radiation during the day but a slight irregularity was found in ablation rate because of different values of surface reflectivity. For example, NW and NE facets (Figure 5.6) received same amount of radiation but a higher value of ablation for NW facet is due to the lower albedo. The case SW and SE slopes is similar. The highest ablation rate on SW facets is due to the highest rate of incoming radiation and to the lower value of albedo. The standard deviation of ablation for SW facets was highest (i.e. 1.6 cm) and correlates well with the radiation, whereas N facet ablations deviated around 0.8 cm.

The incoming radiation and ablation for different surfaces are also compared in the same diagram. Actually, two types of comparisons are made here

simultaneously. One comparison is between flat surface ablation and slope surface ablation; while other comparison is between the ablations of debris covered surface and bare ice surface, since all the facets represented almost bare ice surface.

Figure 5.4 COMPARISON OF TOTAL ABLATION OF FACETS
(MAY 24 - JULY 24)

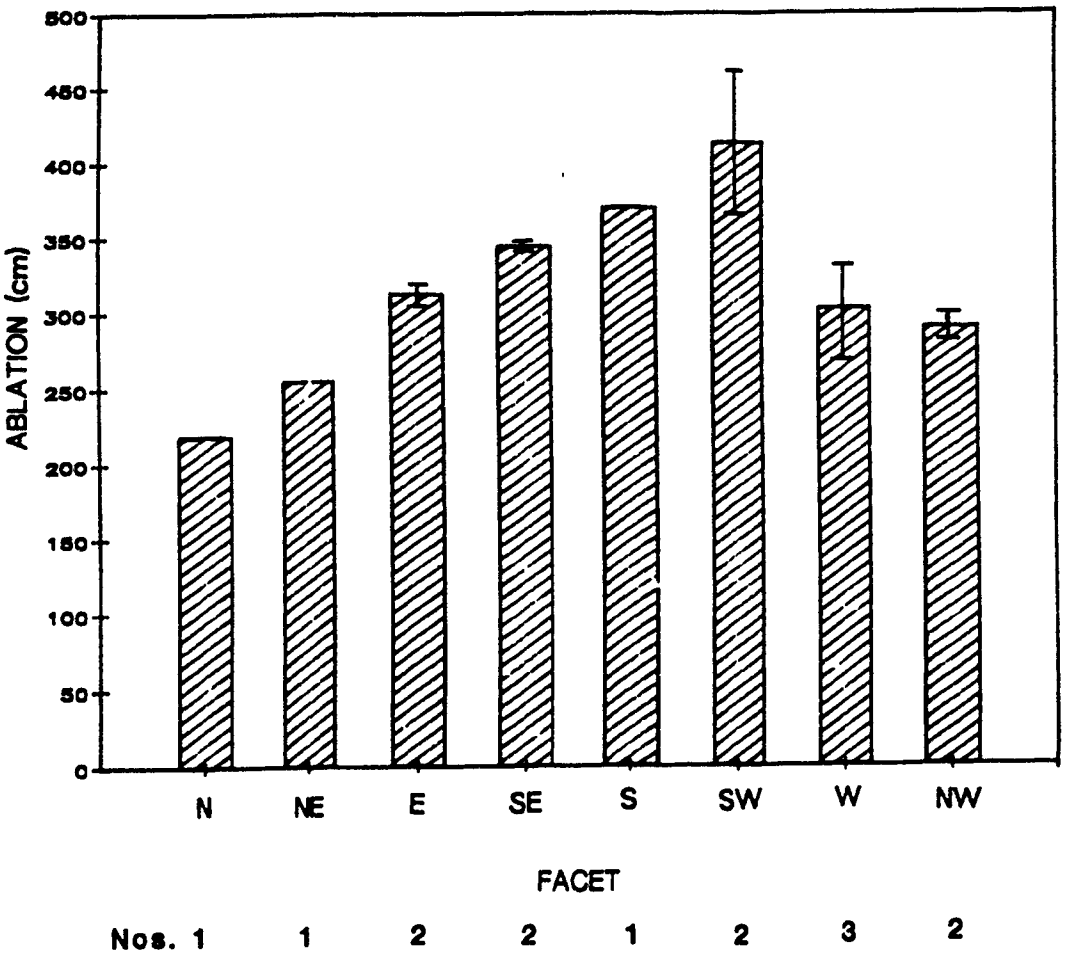

Figure 5.5 COMPARISON OF CUMULATIVE ABLATION PATTERN OF DIFFERENT FACETS AND DEBRIS COVERED ICE SURFACE

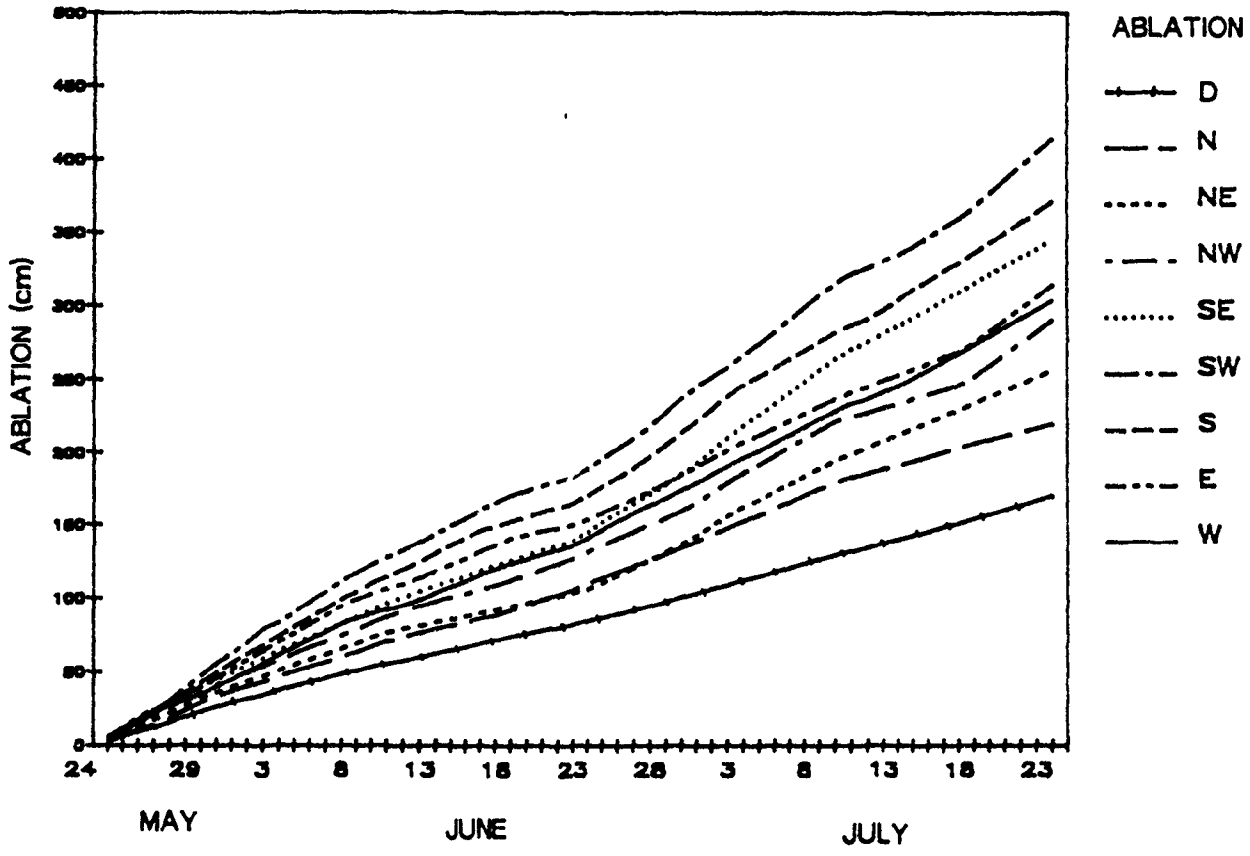

D denotes debris covered surface.

Figure 5.6 COMPARISON OF INCOMING SHORT WAVE RADIATION AND ABLATION FOR DIFFERENT SLOPE ASPECTS

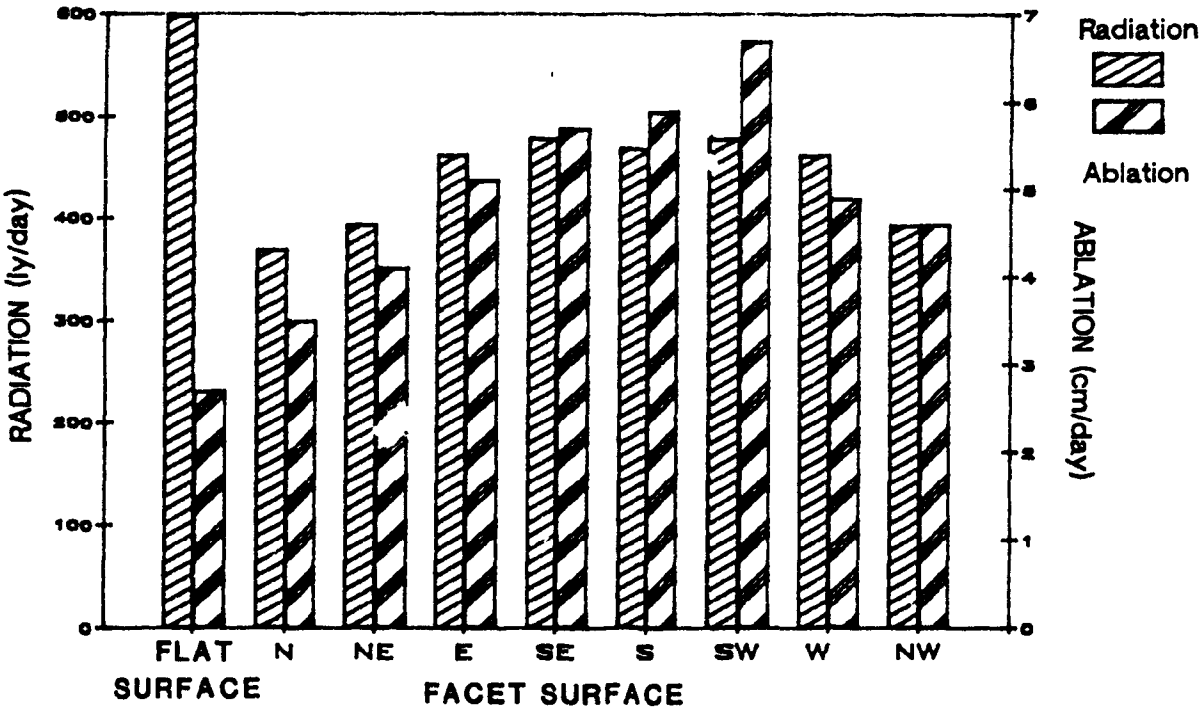

Albedo (%)	13.8	15.5	15	14.2	14	12.6	15.8	13

The mean daily short wave radiation income on different slopes is given in Table 5.11. Although the greatest amount of radiation was received by horizontal surface, it gave lowest ablation rate due to heavy debris loads. Even on N facing facets, where the radiation rate was lowest, the ablation rate was higher, i.e. 3.5 cm/day as compared to 2.7 cm/day under debris covers. While the N facing slope is receiving only 62% of radiation of that on a horizontal surface (see Table 5.7).

Table 5.7 SUMMARY OF RADIATION AND ABLATION ON/OF FACETS AND HORIZONTAL DEBRIS COVERED SURFACE.

		Facet surface							
	Flat surface	N	NE	E	SE	S	SW	W	NW
RAD rate (ly/day)	599	369	394	463	479	469	479	463	394
RAD expressed as % of that on horizontal surface	100	62	66	77	80	78	80	77	66
ABL rate (cm/day)	2.7	3.5	4.1	5.1	5.6	6.0	6.7	4.9	4.7
Increase in facet ablation expressed as % of that of flat surface ablation		30	52	90	107	122	148	81	74

Generally, the N facing slopes, especially the steeper ones (as in present study), are the most insignificant as far as the radiation income and its effects are concerned. But here even these slopes play a significant role in increasing the overall ablation rate mainly due to exposed ice surface to the atmosphere.

The pattern of ablation affected by radiation on different surfaces are shown in Figures 5.7a through 5.7p. Although the incoming short-wave radiation has different intensities on different slope aspects, the pattern is almost the same for all facets because all other external atmospheric conditions were same except the direct component of solar radiation, which is affected by slope aspect. Ablation also shows a similar behaviour which is a function of radiation.

The high ablation period may be classified into three groups. The most extensive ablation occurred during late May and early June. The second extensive ablation period was late June to early July. Period between the Mid July to onward was the third high ablation period.

Figure 5.7 INCOMING RADIATION AND ABLATION PATTERN OF DIFFERENT SURFACES

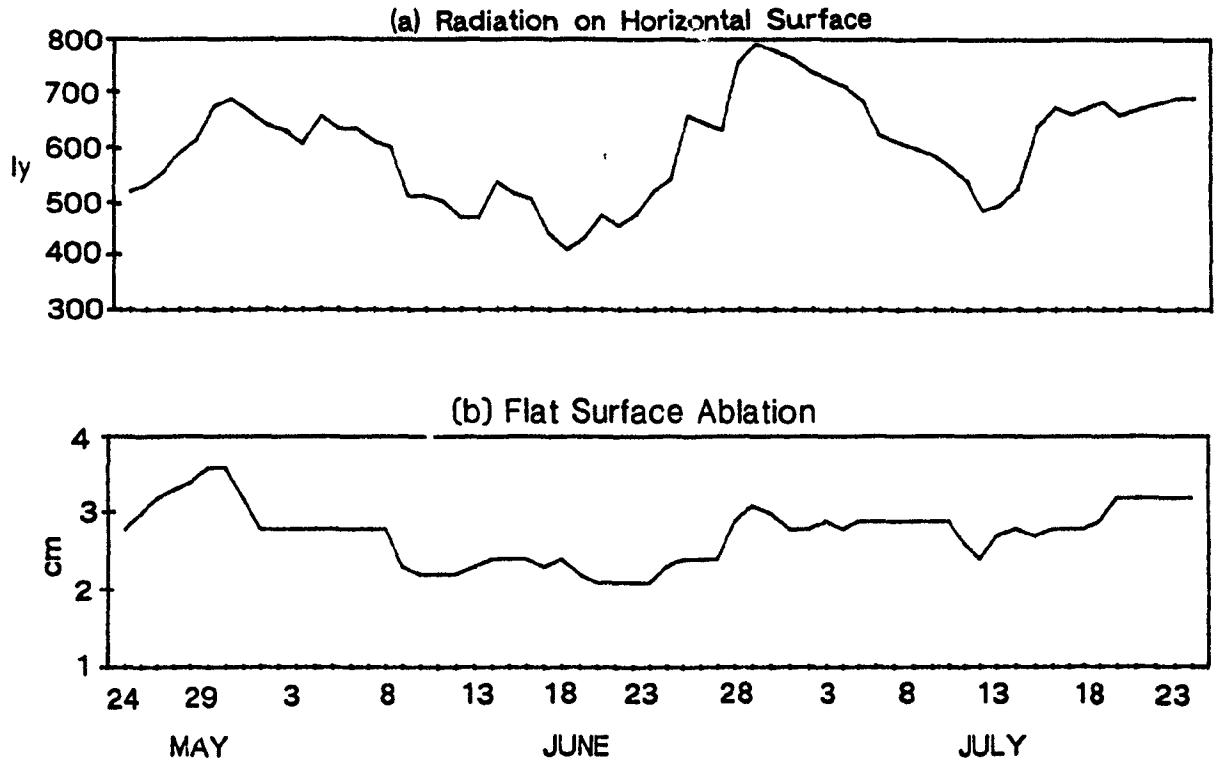

Figure 5.7

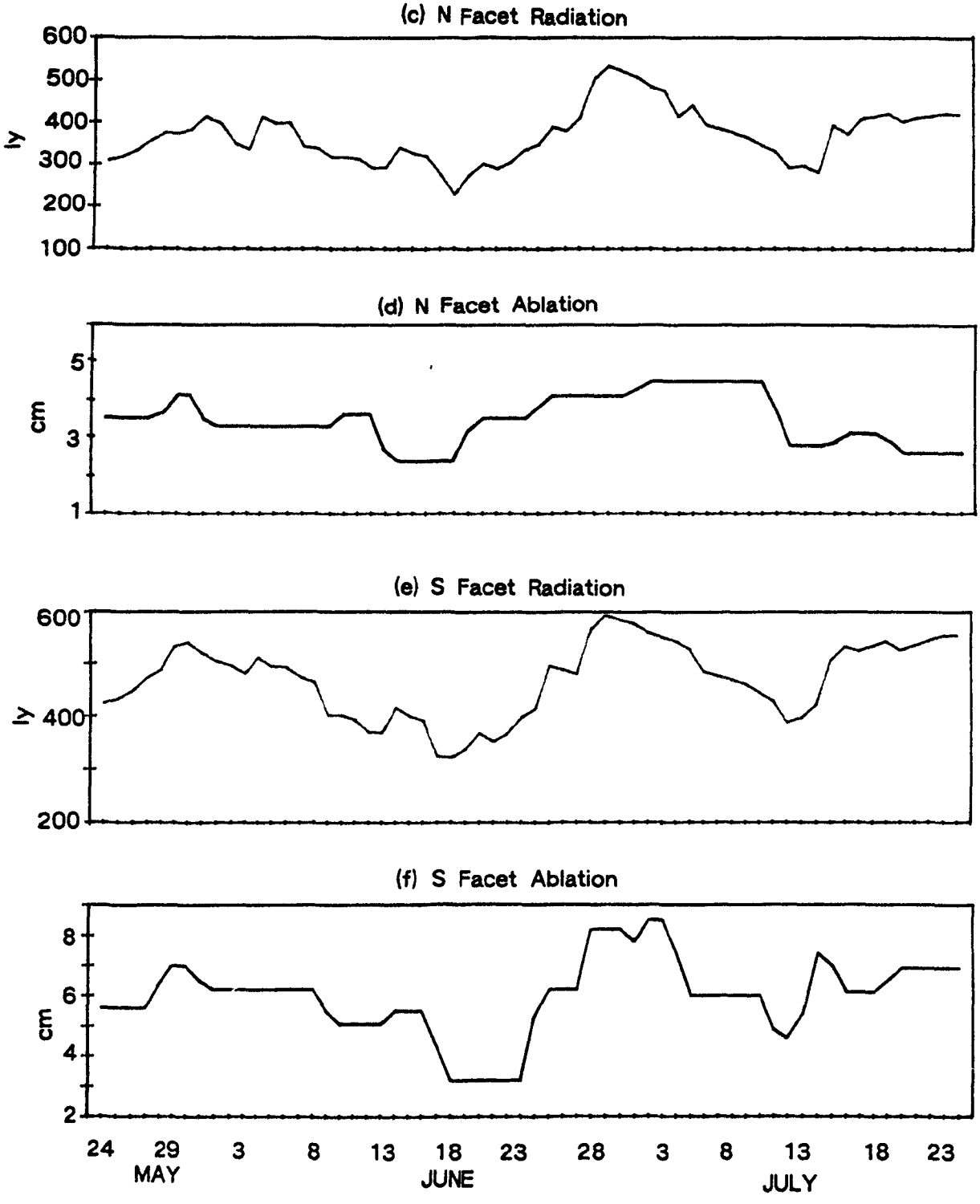
(c) N Facet Radiation
600
500
400
300
200
100
ly
(d) N Facet Ablation
5
3
1
cm
(e) S Facet Radiation
600
400
200
ly
(f) S Facet Ablation
8
6
4
2
cm
24
29
3
8
13
18
23
28
3
8
13
18
23
MAY
JUNE
JULY

Figure 5.7

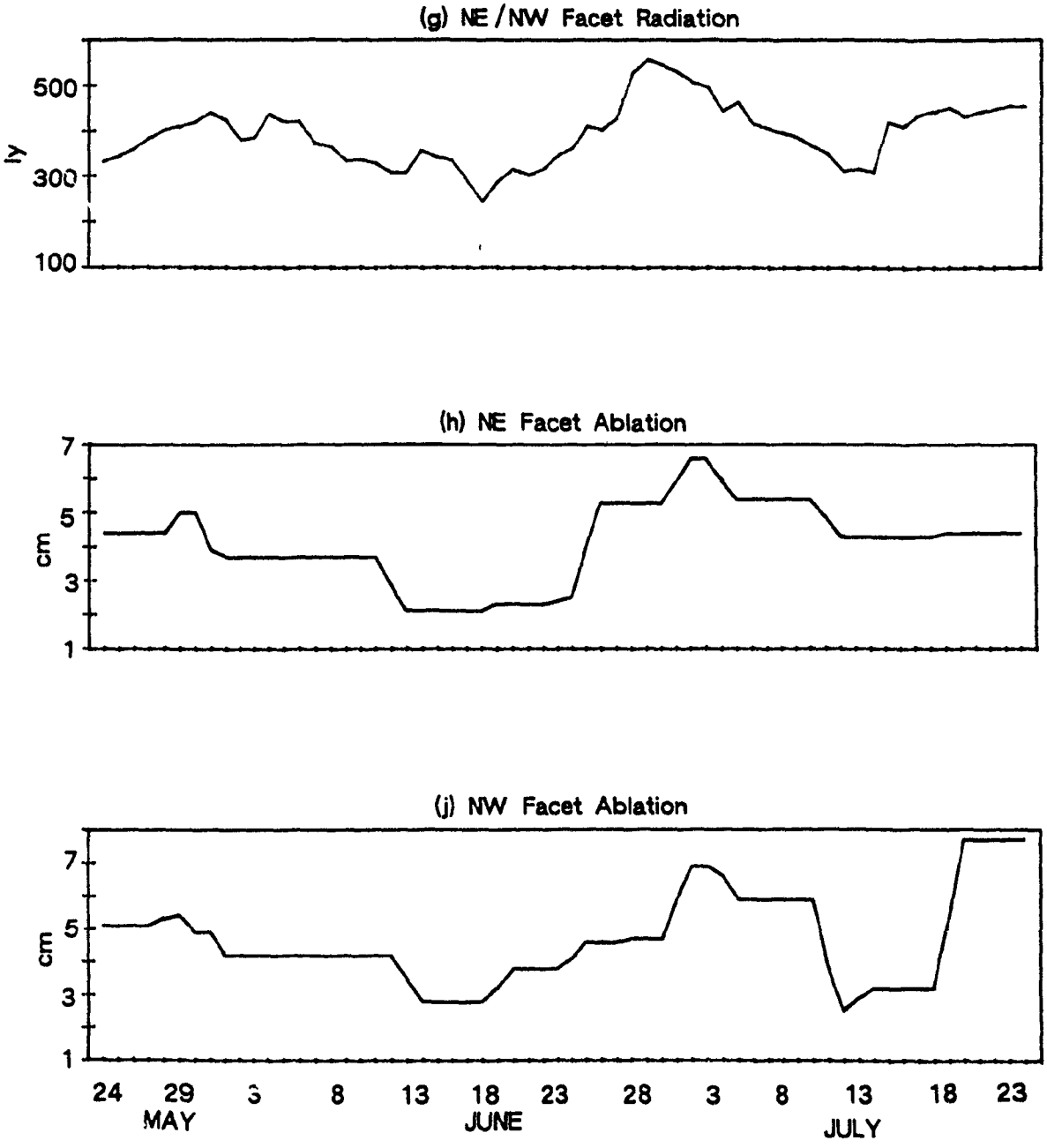
(g) NE / NW Facet Radiation
500
300
100
ly
(h) NE Facet Ablation
7
5
3
1
cm
(j) NW Facet Ablation
7
5
3
1
cm
24
29
MAY
3
8
13
18
JUNE
23
28
3
8
13
JULY
18
23

Figure 5.7

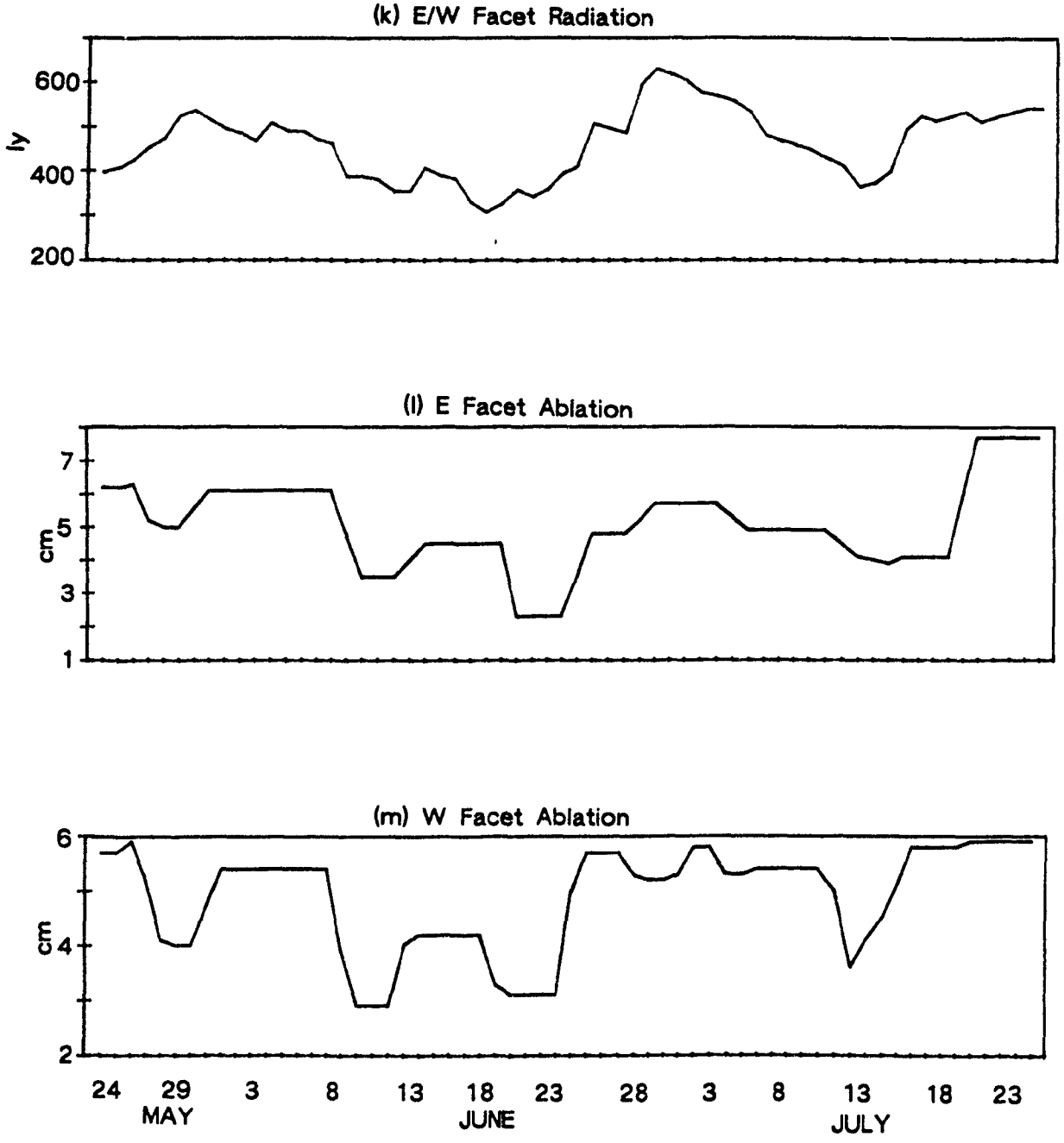
(k) E/W Facet Radiation
600
400
200
ly
(l) E Facet Ablation
7
5
3
1
cm
(m) W Facet Ablation
6
4
2
cm
24
29
3
8
13
18
23
28
3
8
13
18
23
MAY
JUNE
JULY

Figure 5.7

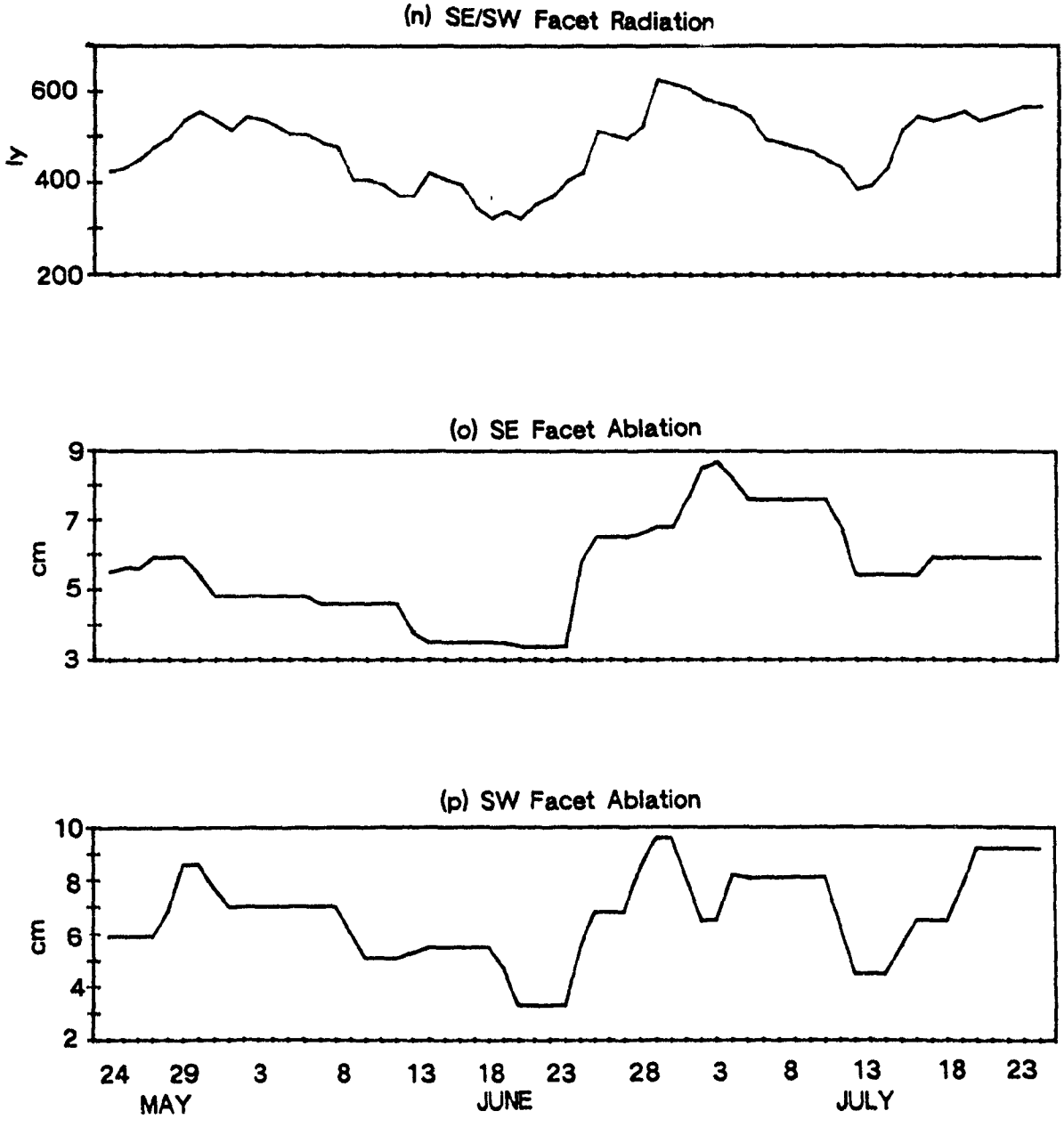
(n) SE/SW Facet Radiation
600
400
200
ly
(o) SE Facet Ablation
9
7
5
3
cm
(p) SW Facet Ablation
10
8
6
4
2
cm
24
29
3
8
13
18
23
28
3
8
13
18
23
MAY
JUNE
JULY

To see the effect of slope aspect on ablation, a regression equation;

$$ABL = 3.588 + .017\ Aspect \mp .58$$

was derived, which is significant up to level .0002 and shows a high correlation between ablation and slope aspect. The aspects were designated by degrees to each side of north (see Table 5.8). This equation explains almost 70% variation in ablation by aspect, but as in the case of debris covered ablation, this equation is also valid only under the measured meteorological conditions during study period.

Table 5.8 MEAN ABLATION RATE OF DIFFERENT FACETS

Facet	Aspect	Degrees from North	Ablation (cm/day)
B	N	0	3.5
J	NE	45	4.1
O	NW	45	4.4
E	NW	45	4.7
D	E	90	5.1
N	E	90	4.8
A	W	90	4.4
H	W	90	5.4
K	W	90	5.3
M	SE	135	5.8
F	SE	135	5.7
C	SW	135	5.9
G	SW	135	7.5
L	S	180	6.0

5.1.3 ABLATION AFFECTED BY METEOROLOGICAL CONDITIONS

Glaciers are a progeny of climate. They are utterly dependent upon elements of the climatic environment for birth and sustaining life (Sharp, 1960). The hypothesis that glaciers are closely related to variations of weather conditions has been subscribed to for over two hundred years (Walcher, 1773; cited Posamentier, 1977).

It is known that glaciers are natural moderators of streamflow and that runoff from glaciers can be greater during warm, dry years than during the cool wet ones (Krimmel and Tangborn, 1974). According to Flint (1957), glaciers are much more sensitive to variations in ablation than to variations in accumulation. Hence, temperature rather than precipitation, although not always, is the climatic factor primarily responsible for the fluctuations observed in the glaciers. It has often been assumed that air temperature, especially during the summer, is of great importance, not directly however, as this explains variations in ablation and mass balance. Finsterwalder and Schunk (1887) already assumed a relation between ablation and temperature for their study of the variation of the Suldenferner in the Eastern Alps (cited Braithwaite, 1981). The temperature mainly reflects change in heat supply from the air. While, Hoinkes (1955) and Ostrem (1972) suggest that temperature should be mainly regarded as an index of radiation and of the probability that summer precipitation will fall as snow which increases the surface albedo.

The simple cross correlations between the independent variables shown in Table 5.9 indicate that the air temperature is most correlated to incoming radiation. This suggest that temperature is a fairly good index for radiation. Relative

humidity is better correlated with wind speed and cloud cover than temperature, while the wind speed has good correlation with all the meteorological variables but best with the relative humidity and cloud cover.

Table 5.9 MATRIX OF CROSS CORRELATION COEFFICIENTS BETWEEN THE INDEPENDENT VARIABLES: Radiation (RAD), Temperature (T), Wind speed (WS), Relative humidity (RH), and Cloud cover (CLD).

	RAD	T	WS	RH	CLD
RAD	1	.977	.496	-.160	-.319
T	.977	1	.443	-.175	-.352
WS	.496	.443	1	-.797	-.721
RH	-.160	-.175	-.797	1	.872
CLD	-.319	-.352	-.721	.872	1

The meteorological data is presented in Tables 5.10 and 5.11. Figure 5.8 is the graphical presentation of this data. The calculated radiation income of slope are plotted with each facet ablation (Figures 5.7a through 5.7p), since both the ablation and radiation are more directly related to each other. From Figure 5.8 it can be seen that the ablation is mainly a function of air temperature which is the index of radiation.

Table 5.10 METEOROLOGICAL OBSERVATIONS: Altitude; 3,530 m

Day	Temperatures (°C)					R.H. (%)	Cloud (tenths)	W.S. (m/s)
	Ice surface	Debris surface	At 1 m height mean	min	max			
May 24	-1	7	-3	-10	6	–	1	–
25	0	11	-1	-7	6	–	0	–
26	0	11	3	-7	14	21	0	–
27	0	12	6	2	15	26	0	–
28	0	13	8	2	15	30	4	–
29	0	14	9	-5	17	33	2	–
30	1	15	10	5	17	37	3	–
31	2	14	10	3	17	39	0	–
Jun 01	2	13	9	5	15	42	4	–
02	0	5	6	2	10	59	10	–
03	0	4	4	2	9	54	10	–
04	0	11	8	1	15	31	1	–
05	0	11	8	-3	18	23	0	4
06	0	11	8	2	16	24	0	3.3
07	0	11	4	-9	12	22	0	3
08	0	8	2	-5	7	39	6	2.2
09	0	4	-7	-13	3	55	9	.8
10	0	5	-6	-14	9	38	4	1.7
11	0	4	-4	-13	11	29	7	1.6
12	0	5	-12	-14	-8	25	3	2.3
13	0	5	-10	-13	-7	25	3	2.2
14	0	5	-10	-13	-8	34	4	2.2
15	0	3	-12	-13	-11	54	10	1.1
16	0	2	-13	-14	-11	57	10	1
17	0	3	-12	-14	-10	45	6	1.3
18	0	3	-11	-13	-8	39	5	1.6
19	0	8	0	-13	13	34	5	1.8
20	0	5	5	9	2	56	9	1.7
21	0	0	1	-2	4	60	10	1
22	0	4	3	-5	13	42	3	1.1
23	0	7	5	-1	11	43	6	1.7
24	0	10	7	2	15	33	2	2.4
25	0	10	7	3	13	43	5	1.4
26	0	10	6	-5	14	40	7	2.5
27	0	12	2	-5	15	–	4	2.4
28	0	12	7	-6	18	–	3	2.6

continued . . . .

Table 5.10 (continued)

Day	Temperatures (°C)					R.H. (%)	Cloud (tenths)	W.S. (m/s)
	Ice surface	Debris surface	At 1 m height mean	min	max			
29	0	10	7	-5	16	–	4	2
30	0	10	5	-5	13	–	3	2
Jul 01	0	9	8	4	13	–	6	1.9
02	0	11	3	5	16	–	4	–
03	0	12	10	4	14	–	7	-
04	1	13	11	5	19	–	0	–
05	0	13	11	6	19	–	5	–
06	1	14	1	-7	13	–	0	–
07	1	11	-3	-7	1	–	5	–
08	1	12	2	-6	15	–	5	–
09	2	13	0	-9	11	–	5	–
10	4	16	-8	-10	-6	–	3	–
11	5	13	-8	-10	-7	–	5	2.6
12	2	4	-10	-10	-9	–	10	1.4
13	3	7	-9	-12	8	–	10	1.1
14	2	8	-8	-12	14	–	3	1.8
15	2	8	8	4	15	–	5	1.8
16	2	10	9	4	16	–	5	2.5
17	3	10	-6	-6	16	–	6	3.1
18	3	9	8	-8	16	–	–	2.3
19	3	9	9	5	15	–	–	2.2
20	1	8	8	4	13	–	–	2.1
21	2	12	11	5	20	–	–	2.9
22	2	14	14	8	21	–	–	–
23	1	15	15	8	22	–	–	–
24	1	15	15	8	22	–	–	–

Table 5.11 CALCULATED DIRECT INCOMING SHORT WAVE RADIATION ON DIFFERENT SURFACES

Day	H*	N	NE,NW	E,W	SE,SW	S
May 24	518	308	333	396	423	424
25	530	317	342	405	431	432
26	553	333	359	424	450	448
27	588	357	384	453	477	473
28	611	375	402	473	496	489
29	672	372	410	525	535	533
30	685	383	420	536	555	541
31	662	414	442	516	535	522
Jun 01	638	398	425	495	514	505
02	628	349	381	486	545	496
03	605	335	386	467	536	481
04	653	413	438	508	524	512
05	631	398	422	489	505	495
06	631	399	423	489	505	494
07	609	343	373	470	486	475
08	598	337	366	462	476	464
09	509	317	336	387	405	402
10	510	318	337	387	405	402
11	500	313	330	379	396	393
12	469	292	308	354	371	369
13	469	293	309	354	371	369
14	535	340	357	407	422	416
15	514	326	342	389	405	400
16	504	319	335	381	396	392
17	441	277	290	330	346	324
18	431	229	245	307	322	322
19	432	273	285	324	338	337
20	474	302	316	357	322	367
21	454	290	302	341	354	351
22	476	305	318	358	370	366
23	518	335	349	393	405	398
24	540	348	363	410	422	414
25	655	389	413	507	513	496
26	642	379	403	496	504	488
27	629	410	429	485	494	480
28	753	504	526	594	523	566
29	791	534	558	630	626	593
30	777	521	545	618	616	584

continued . . . .

Table 5.11 (continued)

Day	H*	N	NE,NW	E,W	SE,SW	S
Jul 01	762	507	531	604	605	576
02	736	484	509	576	584	559
03	722	473	497	568	574	551
04	708	414	446	556	564	544
05	683	440	465	533	544	527
06	621	394	417	480	495	485
07	608	384	406	469	486	477
08	596	374	397	459	477	469
09	583	363	386	448	467	461
10	560	346	368	429	449	445
11	537	330	351	410	431	429
12	482	291	311	364	387	388
13	492	297	318	373	396	397
14	523	281	309	399	430	421
15	636	393	421	494	515	506
16	671	371	410	525	545	533
17	658	407	437	514	535	525
18	669	414	444	524	545	534
19	681	420	453	534	555	543
20	656	401	433	512	535	526
21	667	410	442	523	545	535
22	677	414	449	532	555	544
23	688	420	456	542	566	554
24	687	418	455	541	566	555
Mean	599	369	394	463	479	469

* Horizontal Surface

Figure 5.8 METEOROLOGICAL OBSERVATIONS

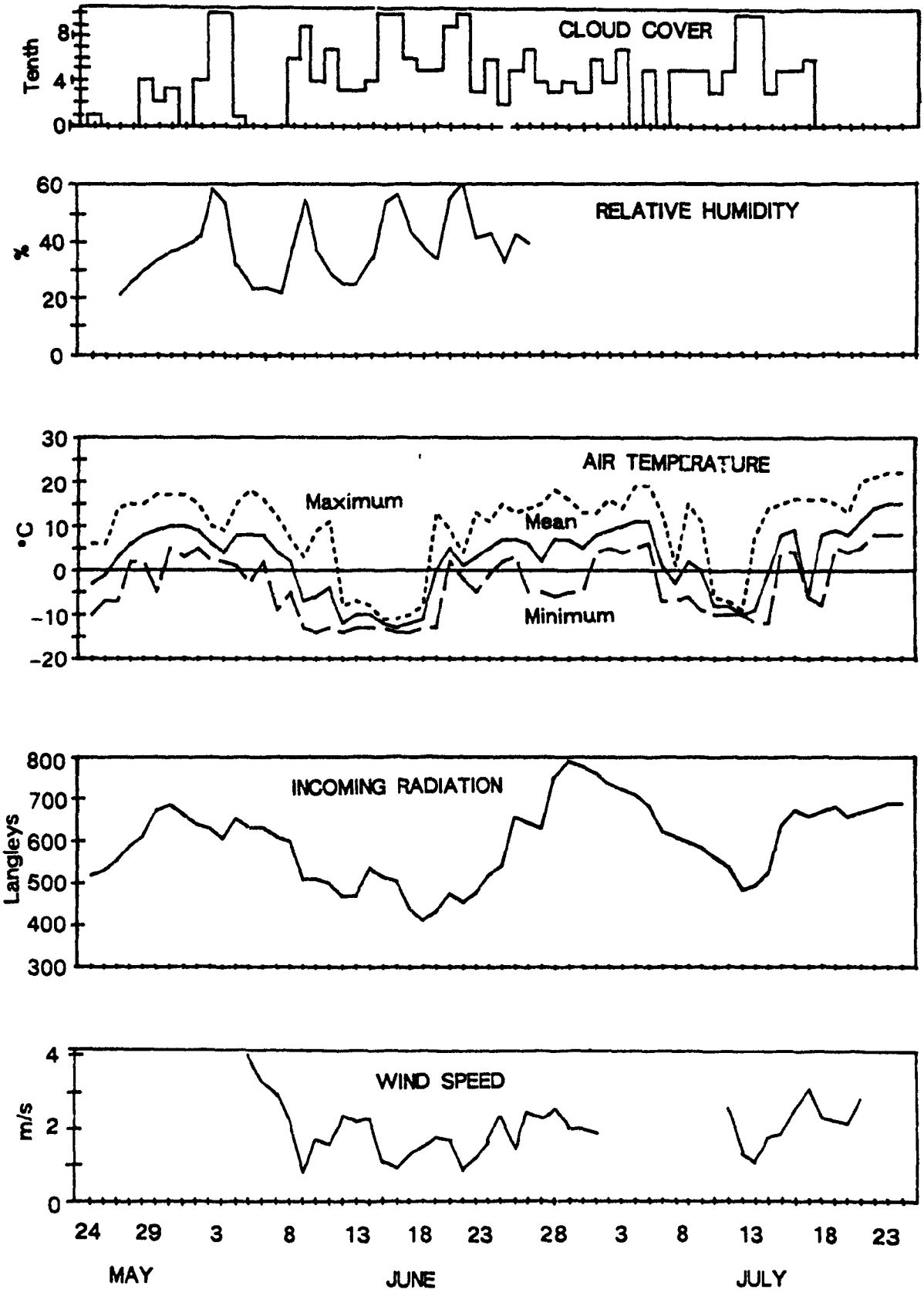

Although the purpose of this study was not entirely to analyse the meteorological factors effect on ablation, the regression analyses were performed only to investigate which of the various climatic parameters is best correlated with the daily ablation. It has been assumed that there exists a linear relationship between glacier fluctuation and meteorological factors. A curvilinear or much more complex relationship might be nearer the truth. Young (1976), and Power and Young (1979) correlated snow depth with elevation, and glacier melt rate with temperature respectively.

The ablation rates are representated by simple regression equations in terms of the daily mean temperature (Tmn), daily maximum temperature (Tmx), daily minimum temperature (Tmi), relative humidity (RH), cloud cover (CLD), radiation (RAD), and wind speed (WS) separately. The equations are presented in a general form;

$$ABL = a + bX \mp e$$

where; the intercept a is the mean ablation rate at external variable X of 0 value, the slope b is the variable response for ablation, and e is the standard error of the regression equation. The results are shown in Tables 5.12 and 5.13, $r^2 \times 100$ denotes the coefficient of determination and FS stands for flat surface ablation. The probable explaination for low values of r is that these variables are mathematically related in a curvilinear fashion whereas the correlation coefficient is only a measure of their linear association.

Although it does not represent good correlation between ablation and variables, it is clear that ablation is mostly explained by radiation and temperature.

Table 5.12 SIMPLE CORRELATION COEFFICIENTS (r): Ablation vs. Meteorological variables.

	RAD†	Tmn	Tmi	Tmx	RH	CLD	WS
FS* ABL	.534 (.0000)‡	.561 (.0000)	.450 (.0002)	.536 (.0000)	-.34 (.0567)	-.443 (.0007)	.510 (.0011)
N ABL	.332 (.0085)	.303 (.0165)	.178 (.1662)	.32) (.0111)	-.177 (.332)	-.306 (.0231)	.170 (.2892)
NE ABL	.407 (.0010)	.446 (.0003)	.327 (.0094	.501 (.0000)	-.308 (.0862)	-.230 (.0912)	.354 (.0291)
NW ABL	.557 (.0000)	.611 (.0000)	.572 (.0000)	.533 (.0000)	-.359 (.0436)	-.384 (.0038)	.310 (.0580)
E ABL	.473 (.0001)	.488 (.0001)	.419 (.0007)	.408 (.0010)	-.282 (.1183)	-.383 (.0039)	.477 (.0025)
W ABL	.514 (.0000)	.499 (.0000)	.441 (.0003)	.466 (.0001)	-.198 (.2779)	-.328 (.0146)	.591 (.0001)
SE ABL	.373 (.0029)	.387 (.0019)	.315 (.0126)	.419 (.0007)	-.364 (.0407)	-.234 (.0860	.371 (.0218)
SW ABL	.535 (.0000)	.525 (.0000)	.405 (.0011)	.477 (.0001)	-.266 (.1412)	-.347 (.0094)	.486 (.0020)
S ABL	.530 (.0000)	.517 (.0000)	.388 (.0018)	.515 (.0000)	-.268 (.1380)	-.257 (.0583)	.397 (.0135)

† Incoming short-wave radiation on surfaces relative to the slope aspects.

‡ Significance level

* Flat surface

Table 5.13 SIMPLE REGRESSION AND CORRELATION: Ablation vs. Meteorological Factors.

Eq. no.	Dependent variable	Independent variable	Constant	Regression coefficient	S.E. of estimate	$r^2 \times 100$
1	FS ABL	HR	1.59	.002	.32	28.5
2	FS ABL	Tmn	2.67	.027	.32	31.5
3	FS ABL	Tmi	2.82	.024	.34	20.3
4	FS ABL	Tmx	2.52	.022	.32	28.7
5	FS ABL	RH	3.12	-.013	.44	11.6
6	FS ABL	CLD	2.93	-.053	.34	19.7
7	FS ABL	WS	2.08	.236	.28	26
8	N ABL	NR	2.22	.004	.72	11
9	N ABL	Tmn	3.46	.030	.73	09.2
10	N ABL	Tmi	3.60	.019	.76	03.2
11	N ABL	Tmx	3.28	.026	.73	10.3
12	N ABL	RH	3.90	-.011	.75	03.1
13	N ABL	CLD	3.97	-.073	.71	09.4
14	N ABL	WS	2.98	.144	.57	03.1
15	NE ABL	NER	1.63	.007	1.09	16.6
16	NE ABL	Tmn	3.95	.068	1.07	19.9
17	NE ABL	Tmi	4.31	.054	1.1	10.7
18	NE ABL	Tmx	3.49	.064	1.04	25.1
19	NE ABL	RH	4.33	-.026	.96	09.5
20	NE ABL	CLD	4.51	-.093	1.24	05.3
21	NE ABL	WS	2.51	.585	1.10	12.6
22	NW ABL	NWR	.67	.011	1.17	31.1
23	NW ABL	Tmn	4.41	.11	1.12	37.3
24	NW ABL	Tmi	5.06	.11	1.16	32.7
25	NW ABL	Tmx	3.88	.08	1.19	28.5
26	NW ABL	RH	4.94	-.023	.70	12.9
27	NW ABL	CLD	5.03	-.137	1.04	14.7
28	NW ABL	WS	3	.515	1.13	10
29	E ABL	ER	1.85	.007	1.15	22.4
30	E ABL	Tmn	4.86	.082	1.14	23.8
31	E ABL	Tmi	5.32	.075	1.19	17.6
32	E ABL	Tmx	4.49	.057	1.20	16.7
33	E ABL	RH	5.89	-.031	1.25	07.9
34	E ABL	CLD	5.42	-.133	1.01	14.7
35	E ABL	WS	2.81	.88	1.16	22.8

Continued. . . .

Table 5.13 (Continued)

Eq. no.	Dependent variable	Independent variable	Constant	Regression coefficient	S.E. of estimate	$r^2 \times 100$
36	W ABL	WR	2.35	.006	.82	26.5
37	W ABL	Tmn	4.74	.061	.83	24.9
38	W ABL	Tmi	5.09	.058	.86	19.5
39	W ABL	Tmx	4.42	.048	.85	21.8
40	W ABL	RH	5.04	-.017	.99	03.9
41	W ABL	CLD	5.21	-.098	.89	10.7
42	W ABL	WS	2.86	.87	.85	34.9
43	SE ABL	SER	2.67	.006	1.32	13.9
44	SE ABL	Tmn	5.38	.070	1.31	15
45	SE ABL	Tmi	5.77	.061	1.35	09.9
46	SE ABL	Tmx	4.93	.064	1.29	17.5
47	SE ABL	RH	5.76	-.03	.92	13.2
48	SE ABL	CLD	6.02	-.112	1.47	05.5
49	SE ABL	WS	3.73	.656	1.17	13.8
50	SW ABL	SWR	1.84	.01	1.40	28.6
51	SW ABL	Tmn	6.39	.111	1.41	27.6
52	SW ABL	Tmi	6.99	.092	1.52	16.4
53	SW ABL	Tmx	5.83	.085	1.46	22.7
54	SW ABL	RH	7.19	-.032	1.38	07.1
55	SW ABL	CLD	7.19	-.172	1.46	12
56	SW ABL	WS	3.75	1.178	1.52	23.6
57	S ABL	SR	2	.009	1.10	28.1
58	S ABL	Tmn	5.76	.086	1.11	26.7
59	S ABL	Tmi	6.21	.069	1.20	15.1
60	S ABL	Tmx	5.27	.071	1.11	26.5
61	S ABL	RH	6.41	-.027	1.17	07.2
62	S ABL	CLD	6.37	-.110	1.30	06.6
63	S ABL	WS	4.03	.809	1.34	15.8

5.1.3.1 Multiple Regression Analyses

Step-wise multiple regression analyses were performed for ablation of different surfaces. In these analyses, the daily ablation values were regarded as the dependent variable, and meteorological parameters as independent variables. Posamentier (1977) used meteorological parameters in his 'climatic model' for glacier behavior (i.e. % of glacier advance). The procedure in the following regression analyses was adopted from his model. The computer programme SPSS-X was used for all statistical analyses.

It was assumed that there exists a linear correlation between the daily ablation and the independent meteorological parameters calculated as daily mean values, as also assumed by Lewkowicz (1986) in his short-term ablation model. A linear model of the conventional form was used, i.e.;

$$ABL = a + bX + cY + dZ \mp e$$

where; ABL is the dependent variable; X, Y, Z are the independent variables; b, c, d are the regression coefficients.

The normal procedure is to find the values of the coefficients a, b, c, etc. and their level of significance. Five climatic variables were employed; daily mean temperature, radiation, relative humidity, cloud cover, and wind speed. Of all the different equations possible there is one which affords the greatest significant reduction in the variance of the ablation. In the step-wise procedure this equation is determined by taking one variable into the equation at a time. The variable chosen is that which will result in the greatest reduction in the variance of the dependent variable. This step-wise operation continues until such time as the continuous addition of variables to the equation does not significantly reduce the variance of

the independent variable.

It was found that the ablation could be well explained with the use of only one or two meteorological parameters. When more variables were included, the residuals did not decrease significantly. In order to determine what combination of variables accounted for most of the variation in the ablation, the following equation for flat surface ablation was yielded;

$$ABL = .955 + .002\ RAD - .012\ T + .139\ WS \mp .14$$

The equations for other surface ablations are shown in Table 5.14. Only for the N facing facet was ablation not found to be correlated with radiation, while for other facets ablation was strongly correlated with radiation. The highest variation in ablation explained by radiation and temperature was for southern facets.

The cloud cover and relative humidity were insignificant for ablation. While wind speed affected flat surface ablation only.

Table 5.14 MULTIPLE REGRESSION COEFFICIENTS: Ablation vs Meteorological Factors

Eq. no	Ablation	Regression Coefficients RAD	T	W.S	Constant	S.E. of estimate	r	$r^2 \times 100$
1	FS*	.002	-.012	.139	0.955	.14	.842	70.9
2	N	–	.051	–	3.331	.38	.73	53.2
3	NE	.017	–	–	-3.111	.31	.94	88.4
4	E	.022	-.094	–	-4.764	.82	.776	60.3
5	SE	.011	–	–	-0.315	.69	.731	53.4
6	S	.023	-.069	–	-4.56	.46	.928	86.2
7	SW	.021	-.079	–	-3.513	.53	.915	83.7
8	W	.015	–	–	-1.782	.57	.839	70.4
9	NW	.007	.031	–	1.456	.38	.817	66.7

All coefficients are significant at better than the .0002 level.

* Flat surface.

Although this model for ablation is by no means the ideal model, almost 71% of the variation in the Flat surface ablation is neverthless accounted for. More than 80% variation was explained by meteorological factors for southern facets. The north facing facets were not better correlated with radiation, rather 53% of variation was accounted by temperature only.

Radiation, in general, is seemingly an excellent indication of the ablation pattern of Barpu Glacier, since the short-wave radiation reaches a maximum during this period (i.e. May - September).

5.2 STATISTICAL MODEL

Since the physical conditions (i.e. facets, and debris covers) of the glacier remain constant for a long period, the ablation rate can be predicted on the basis of meteorological conditions which vary even minute by minute. Once we know the debris conditions (i.e. areal and depth distribution) and facet conditions (i.e. areal and slope aspect distribution) and the ablation affected by these two conditions, the net ablation then can be predicted on the basis of external meteorological variables under the existing physical conditions of the glacier surface, providing that an allowance should be taken for facet contribution. In present study, for example, the overall ablation was increased by 13% when facet contribution was taken into account (Table 5.18).

It is almost impossible to use all physical and meteorological variables in one equation, because all the meteorological variables are changing with respect to time but facets and debris cover depths remain constant. The ablation can be compared for different facets and debris cover depth and a regression equation of ablation for different aspect or debris depth can be developed, as it was already done. The 45 stakes will represent 45 different measurements of debris depth at each stake location for which the external climatic conditions will be constant. But when the meteorological variables will be used in regression analysis, one ablation value (mean of 45 ablation measurements) for that day will be used, for which the debris conditions will be constant. In other words, the relationship between ablation and atmospheric conditions can be established even by one stake measurement, but it will require several days to have a good correlation between these two variables. In this case the debris depth will be the same and no correlation can be established

between ablation and debris depth by one stake. On the other hand, to establish a correlation between debris depth and meteorological conditions, several stakes with different debris depth are required. In this case each stake will represent one ablation measurement and relationship can be established even for one day. But, since the external atmospheric conditions will be the same for ablation measurement under each stake, no correlation can be established between ablation and meteorological factors. In fact these are extremely different cases, and we have to use separate equations for each of these three variables (i.e. meteorological conditions, slope aspect, and debris depth), which are independent of each other.

Because the ablation under debris layer or ablation of facets, is highly responsive to the climatic conditions, the net ablation can be predicted on the basis of these climatic conditions under existing surficial form. Of course debris depth changes due to dynamic behavior of glacier and differential melting rates but it takes a long time. Moreover, the decrease in debris depth at one location is compensated by the increase in depth at other location. The facets and debris covers may have the same distribution and concentration on the glacier, therefore, these two factors may affect the ablation in the same pattern for years. Since, the values of flat surface ablation used in statistical analyses, for correlating with the meteorological factors, were already affected by the debris, therefore the ablation for Barpu glacier may be predicted by the equation no.1 in Table 5.14, providing an allowance for facet contribution i.e.;

$$ABL = [0.955 + 0.002\ RAD - 0.012\ T \mp 0.139]\ 1.13$$

The flat surface ablation based on the meteorological conditions is multiplied by a factor 1.13 for allowance of facets. Now this equation will give the ablation

affected by facets, debris cover, and meterological conditions.

5.3 ESTIMATE OF ABLATION

5.3.1 Facet Ablation Rate

The facet ablation is estimated on the basis of areal distribution and ablation rate of facets with respect to aspect. Figures 5.9 and 5.10 show the facet contribution by their aspect per km^2 of area. These present quite interesting results, i.e. the faceted ablation zone is highly dominated by SW and W facing slopes. Almost 50% of area was occupied by SW facets, while the W facing facets area (over 30%) was the second largest. The other facets had an area under 10%, with the least contribution (1%) by SE facets.

Figure 5.9 FACET DISTRIBUTION BY AREA PER Km^2

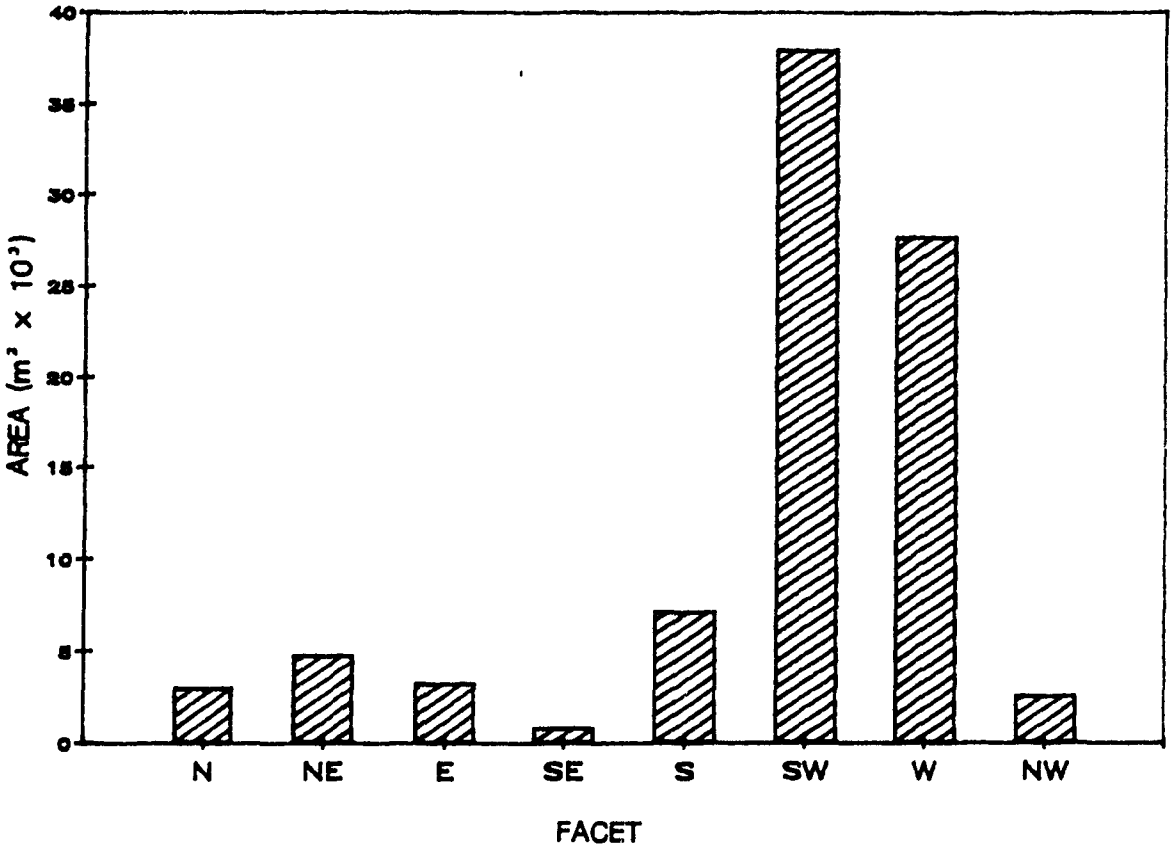

Figure 5.10

FACET AREA DISTRIBUTION FOR THEIR ASPECTS

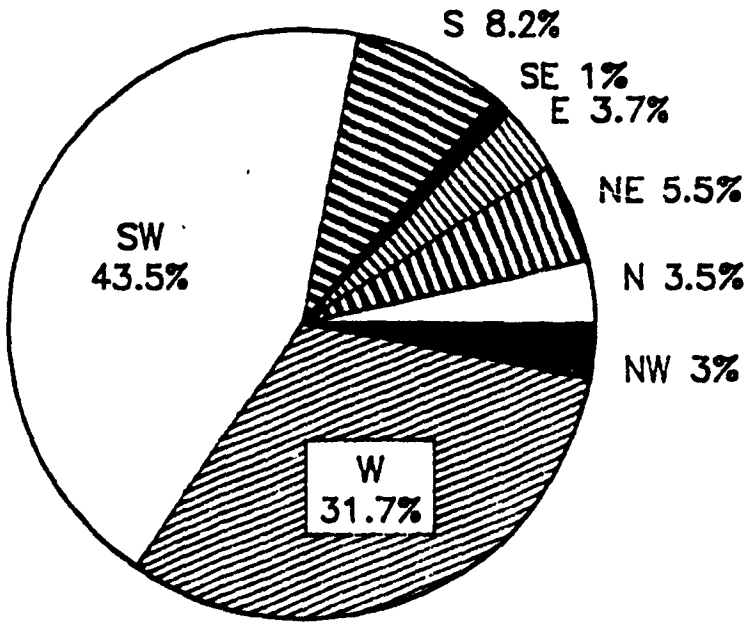

AREA

By comparing columns 3 and 4 in Table 5.15, it is noticed that fortunately the highest facet area (SW facing) gave the highest ablation rate (6.7 cm/day). While the second highest ablation (6 cm/day) was measured on S facing facets but their areal contribution is much less (i.e. 8.2%). The W facets which had over 30% of total facet area gave only 4.9 cm/day of ablation, but still this ablation rate was much higher than the flat surface ablation (i.e. ablation under debris covers). Therefore the overall ablation will be much affected by the SW and W facets, with all other facets also contributing positive role in net ablation, no matter how small in area it was, because all the ablation of facets (see column 4 in Table 5.15) are much greater than flat surface ablation (i.e. 2.7 cm/day).

Table 5.15 explains the method of estimating the weighted ablation rate of facets. The ablation of each facet aspect is first multiplied by its respective area, the total runoff is then divided by the total facet area (i.e. 87,318 m^2) giving facet ablation rate as 5.7 cm/day. In this ablation rate, all the facets have contributed according to their area and related ablation rate.

Table 5.15 SUMMARY OF ESTIMATION FOR WEIGHTED FACET ABLATION RATE

Aspect	Area m^2/km^2	% of total facet area	Ablation† (cm/day)	Runoff (Area x Ablation) (m^3/day)
N	3,026	3.5	3.5	105.91
NE	4,810	5.5	4.1	197.21
E	3,262	3.7	5.1	166.36
SE	860	1.0	5.6	48.16
S	7,132	8.2	6	427.92
SW	37,970	43.5	6.7	2543.99
W	27,678	31.7	4.9	1356.22
NW	2,580	3.0	4.7	121.26
Total	87,318	100		4967.03

∴ Weighted ablation rate = 4967.03 / 87,318 = .0569 m or 5.7 cm/day

†Average ablation rate of facets having same aspect.

5.3.2 Net Ablation Rate

The net weighted ablation rate was estimated in the same manner as applied for estimating the mean facet ablation rate. The facet and debris area per km^2 are shown in Figures 5.11 and 5.12. It was measured that over 91% of ablation zone of Sumaiyar Bar was under debris cover. The facet contribution was found to be only 8.7%.

Figure 5.11 AREAL DISTRIBUTION OF FACET AND DEBRIS COVERED SURFACE

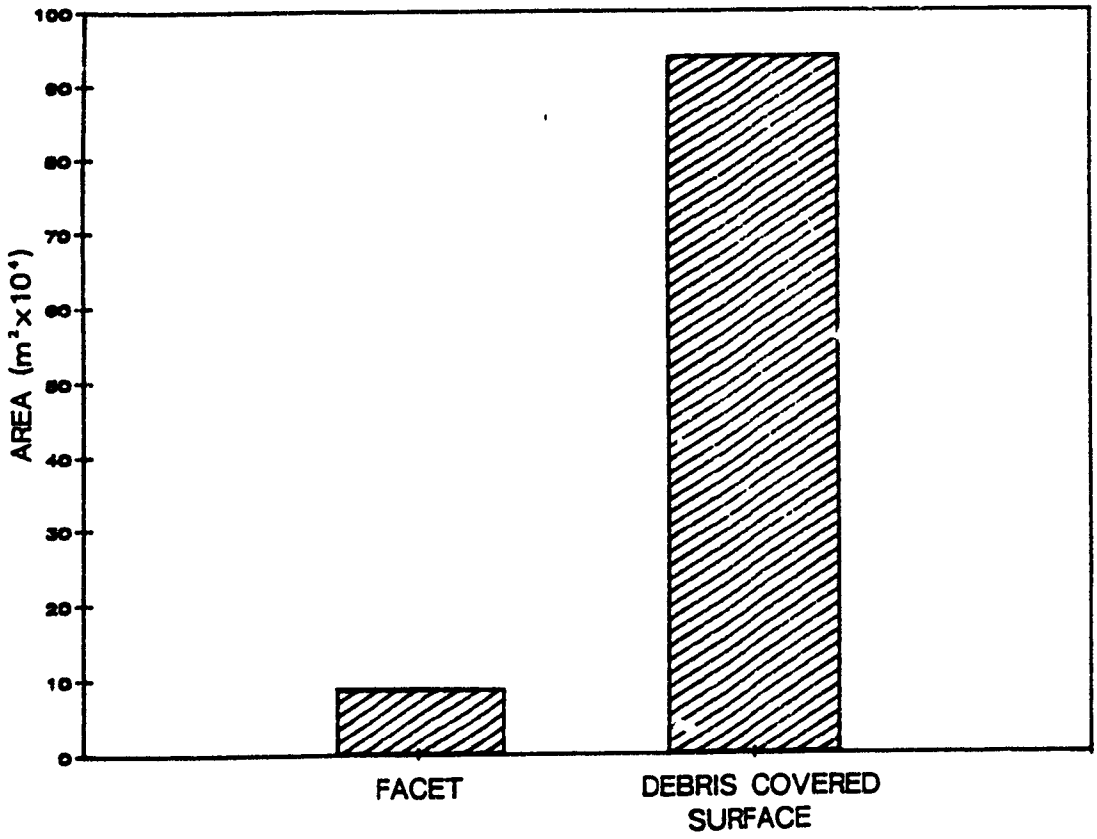

Figure 5.12 FACET AND DEBRIS COVERED SURFACE PERCENTAGE BY AREA

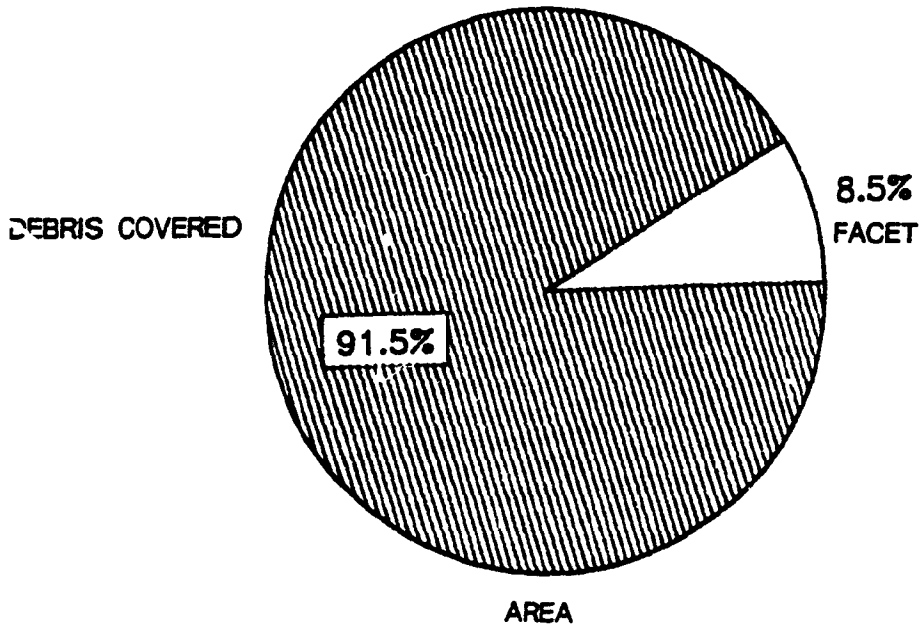

It is hypothesised that surface area increases with surface irregularity (Hobson, 1972). Facets, therefore, result in increasing the ablation area, giving more runoff, which is another positive role of facets.

Since the typical slope angle was 45°, the total facet area will be reduced by a factor 0.7071 when transformed on horizontal plane, and the debris covered area is estimated by subtracting this reduced area from 1 km^2. This will result in increasing the debris covered area and there will actually be more than one square kilometer within 1 km^2 of area It is estimated that the ablation area is increased about 2.5% due to faceted ice surface, which means that there will be actually 2.5% more surface area for melt available as compared to plane ice surface, hence the ablation rate will be further increased.

Table 5.16 SLOPE EFFECT ON SURFACE AREA

	Area (m^2/km^2)
Facet	87.318
Debris covered	1000.000 - 87.318 x 0.7071
or flat surface	=938.257.44
Total	1025.575.4

Area increased due to facets	= 25.575.4 m^2 (2.5%)
Now actual facet area	= 8.51%
and actual debris covered area	= 91.49%

The net ablation rate is estimated by actual debris and facet area, the summary of which is given in Table 5.17. The situation is very interesting and important here, that although the facet ablation rate is much higher, more than twice the flat surface ablation; but on the other hand, its areal concentration is very small as compared to debris covered or flat area. The net ablation rate is about 3 cm/day, which is 0.3 cm/day higher than flat surface ablation alone. In other words, if the facet contribution was not taken in account, the ablation rate would be 2.7 cm/day. The ablation rate, therefore, is increased about 11% due to facets.

The net ablation rate 3.0 cm/day is based on the ablation measurements under 45 stakes. If the flat surface ablation rate is calculated on the basis of debris cover concentration, it reduces from 2.7 to 2.3 cm/day (Table 5.18). The regression equation with highest correlation coefficient (R = -.905) is used to estimate weighted debris covered ablation, taking 12.4 cm average debris cover depth (see Figure 5.1).

If the ablation rate 2.3 cm/day is used in place of 2.7 cm/day in Table 5.17, the net weighted ablation becomes 2.6 cm/day. The facet contribution is further increased to 13%.

Table 5.17 SUMMARY OF ESTIMATION OF NET ABLATION RATE

Surface	Area (m^2/km^2)	% of total area	Ablation (cm/day)	Runoff (Area x Ablation) (m^3/day)
Facet	87,318	8.5	5.7	4,977
Debris Covered	938,257.4	91.5	2.7	25,333
Total	1025,575.4	100		30,310

∴ Net Ablation Rate = 30,310 / 1025,575.4 = .03 m or 3.0 cm/day

Ablation Increased due to Facets = .3 cm/day , (11.1%)

Table 5.18 SUMMARY OF NET WEIGHTED ABLATION RATE

Mean Debris Cover Thickness	= 12.4 cm
Regression Equation; Log ABL = 0.98 - .572 Log D , (R = -.905)	
Weighted Debris Covered Surface Ablation	= 2.3 cm/day
Net Weighted Ablation	= 2.6 cm/day
Ablation Increased due to Facets	= 0.3 cm/day , (13%)

5.4 CONCLUSIONS AND RECOMMENDATIONS

The various factors affecting ablation rate of Barpu Glacier have been discussed and the ablation rate has been estimated on the basis of these factors.

The ablation at Sumaiyar Bar was mainly controlled by debris cover under the same meteorological conditions. Since, the mean debris depth was measured at about 12.4 cm, it negatively affected the ablation rate. Almost 68% of the reduction in ablation was estimated as due to debris loads. The debris occupied more than 90% of the ablation zone within the study area, in which 80% debris cover protected the ice beneath, resulting in deceleration in ablation rate.

Facets positively affected overall ablation. Almost 13% ablation was increased due to faceted ice, which was dependent on the areal distribution of aspect. The incoming solar radiation, the main source of ice melting, was greatly affected and controlled by these differently oriented facets. The highest ablation rate was measured on SW facing facets which received the largest amount of incoming solar radiation.

Although the mean facet ablation rate was about twice the flat surface ablation, its effect on net ablation was 13%. This was mainly due to low areal concentration.

This study indicates the significance of debris and facets in ablation rate. Until we have sufficient results from similar studies at different elevations and on different glaciers, it is difficult to say at what percentage or degree these two factors do affect overall ablation rate in general.

The knowledge of areal and thickness distribution of debris cover and facet

configuration is essential to estimate an authentic ablation rate at different locations even on the same glaciers, since the distributions of facets and debris cover may be related to the elevation.

It was observed that debris cover thickness varied within a very small distance. Therefore, a large number of ablation stakes (say at least 30 stakes per km^2) should be established to get a representative abaltion rate. This large number of stakes can be avoided if we already have the knowledg about debris conditions (i.e. mean debris cover thickness and areal coverage). In this case the ablation can be measured under a few stakes having different debris cover thicknesses and a regression equation can be achieved. The ablation rate then can be estimated by this equation for mean debris depth for that area.

For this purpose a detailed survey should be conducted to measure these two factors (i.e. debris and facet distribution) for all major glaciers in the Karakoram range at least for three melting seasons. According to Inoue and Yoshida (1980) the facet area would be as high as 15% of total ablation area. In this case the ablation rate might be increased to more than 20%.

APPENDIX A
PAKISTAN GLACIER INVENTORY+

MOUNTAIN AREA Karakoram GLACIER Barpu

SOURCES:

Map Title and Number Hispar-Biafo Glacial Regions (The Geographical Journal: July-September 1950)

Compiled by E.E. Shipton Date 1950 (Surveyed 1939)

Scale 1:253,440 Contour Interval 250 feet

Map Title and Number India and Pakistan (Jammu and Kashmir) Topographic Series; Map NJ 43-14

Compiled by U.S. Army Map Service Date 1953 (Compiled from Survey of India;1945)

Scale 1:250,000 Contour Interval 500 feet

TERMINUS CO-ORDINATES:

Longitude 74°47' E

Latitude 36°13' N

MID-BASIN CO-ORDINATES:

Longitude 74°48' E (Barpu/Bualtar Basin)

Latitude 36°07' N (")

ORIENTATION:

Basin Long Axis 325° (NNW) Ablation Area 320° (NNW)

Accumulation Area 330° (NNW)

ELEVATIONS:

Maximum Basin Elevation	7,460 m	Glacier Terminus Elevation	2,835 m
Basin Elevation Range	4,625 m	Ablation Line Elevation	4,116 m

Mean Accumulation Area Elevation (a) 5,788 m* (b) 5,428 m*

Mean Ablation Area Elevation (a) 3,475 m* (b) 3,500 m*

LENGTH AND AREA:**

Maximum Glacier Length	29 km	Mean Main Stream Width	1.5 km
Maximum Length Ablation Area	18.5 km	Maximum Length Accumulation Area	10.5 km
Total Basin Area	414.98 km²	Glaciated Area	125.56 km²
Connected Glacier Area	117.53 km²		
Ablation Area	22 % 27.69 km²	Accumulation Area	78 % 97.87 km²

SLOPE-ASPECT DATA: TOTAL BASIN (Barpu/Bualtar Basin)

North facing	34.89 % 144.77 km²	South facing	8.81 % 36.55 km²
East facing	32.77 % 36.55 km²	West facing	23.53 % 97.65 km²

SLOPE-ASPECT DATA: GLACIATED SLOPES (Barpu/Bualtar System)

Average Glacier Slope Barpu 1:6.72 Miar 1:4.59

North facing	58.07 % 122.01 km²	South facing	3.67 % 7.71 km²
East facing	20.17 % 42.38 km²	West facing	18.09 % 38.01 km²

+ Prepared by David Butz.

* Ablation and accumulation area elevations are calculated in two ways: (a) average of highest and lowest elevations; and (b) mean of area-altitude calculations above and below ablation line.

** All area data refers to plan area.

Condensed From
PAKISTAN GLACIER INVENTORY

AREA-ALTITUDE RELATIONSHIP

MOUNTAIN AREA Karakoram

GLACIER Barpu

Total Basin:				Glaciated Area:			
2,440-2,743m	6.88	km²	1.65 %	2,440-2,743m		km²	%
2,743-3,048m	15.52	km²	3.74 %	2,743-3,048m	3.08	km²	2.45 %
3,048-3,353m	26.41	km²	6.36 %	3,048-3,353m	8.63	km²	6.87 %
3,353-3,658m	31.24	km²	7.53 %	3,353-3,658m	8.22	km²	6.55 %
3,658-3,962m	35.97	km²	8.67 %	3,658-3,962m	8.22	km²	6.55 %
3,962-4,267m	40.29	km²	9.71 %	3,962-4,267m	6.89	km²	5.49 %
4,267-4,572m	42.44	km²	10.23 %	4,267-4,572m	7.91	km²	6.30 %
4,572-4,877m	47.89	km²	11.54 %	4,572-4,877m	10.79	km²	8.59 %
4,877-5,181m	48.20	km²	11.62 %	4,877-5,181m	16.11	km²	12.83 %
5,181-5,486m	42.35	km²	10.21 %	5,181-5,486m	17.48	km²	13.92 %
5,486-5,791m	26.61	km²	6.41 %	5,486-5,791m	12.03	km²	9.58 %
5,791-6,096m	21.58	km²	5.20 %	5,791-6,096m	12.34	km²	9.83 %
6,096-6,401m	14.39	km²	3.47 %	6,096-6,401m	7.39	km²	5.89 %
6,401-6,706m	10.81	km²	2.60 %	6,401-6,706m	7.90	km²	6.29 %
6,706-7,010m	3.38	km²	0.81 %	6,706-7,010m	1.34	km²	1.07 %
7,010-7,315m	0.71	km²	0.17 %	7,010-7,315m	1.03	km²	0.82 %
7,315-7,620m	0.31	km²	0.08 %	7,315-7,620m	0.10	km²	0.08 %
7,620-7,925m		km²	%	7,620-7,925m		km²	%
7,925-8,230m		km²	%	7,925-8,230m		km²	%
8,230-8,535m		km²	%	8,230-8,535m		km²	%

APPENDIX B

Photographs of the Study Area

Appendix B.1

A Panoramic View of Barpu Glacier at Sumaiyar Bar Site From Northeast

photo by INAM, 1987

Appendix B.2

A View of Barpu Glacier at Sumaiyar Bar From Southwest

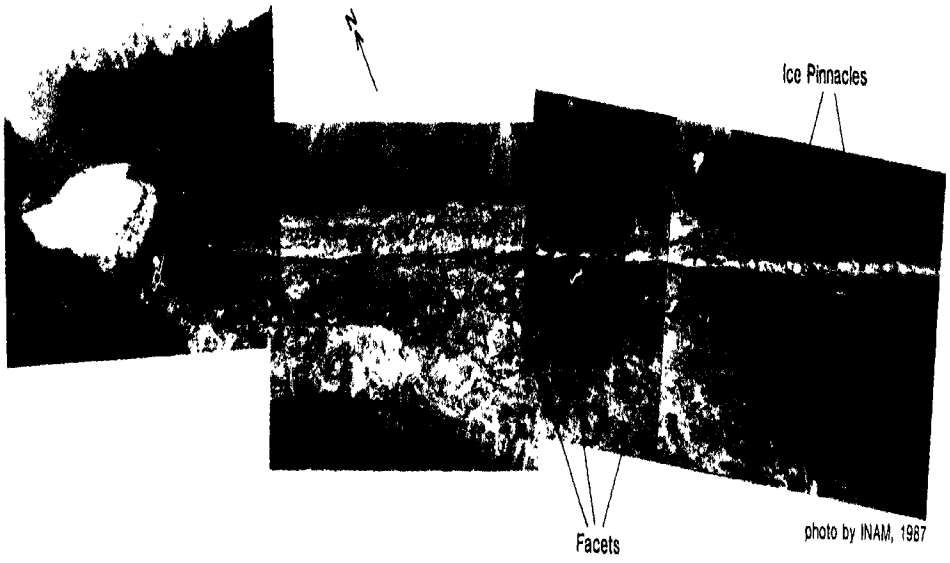

References

Abbas, B.M. (1967) Planning Water Development In Pakistan. INDUS Vol.10, No.9, October 1967. Wapda Printing Press Pakistan.

Adams, W. Peter (1966) ABLATION AND RUN-OFF ON THE WHITE GLACIER. Axel Heiberg Island Research Reports. McGill University Montreal, Glaciology, No.1. 77 p.

Ahlmann, Hans Wilhelmsson (1935) Contribution to the physics of glaciers. GEOGRAPHICAL JOURNAL. V-86, No.2, 97-113. The Royal Geographical Society Kensinton Gore London.

Andrews, J. T. (1975) GLACIAL SYSTEMS. An approach to glaciers and their environments. Institute of Arctic and Alpine Research and Department of Geological Sciences, University of Colorado. Duxbury Press, North Scituate, Massachusetts. 191 p.

Arnold, K. C. (1981) ICE ABLATION MEASURED BY STAKES AND TERRESTRIAL PHOTOGRAMMETRY - A COMPARISON OF LOWER PART OF THE WHITE GLACIER. Axel Heiberg Island Research Reports. McGill University, Montreal. Glaciology No.2, 98 p.

Barry, Roger G. (1981) MOUNTAIN WEATHER AND CLIMATE. Methuen London and New York. 313 p.

Barry, Roger G. and Chorley R. J. (1976) ATMOSPHERE, WEATHER AND CLIMATE. Methuen & Co. Ltd. 432 p.

Batura Glacier Investigation Group (1977) The Batura Glacier in the Karakoram Mountains and its Variations. SCIENTIA SINICA. Vol.XXII, No.8, April 4, 1977, pp. 958-978.

Becker, Clarence Frederick (1979) SOLAR RADIATION AVAILABILITY ON SURFACES IN THE UNITED STATES. Arno Press, New York.

Bentley, Charles R. (1987) Constraints on models in the Ross Embayment, Antarctica. THE PHYSICAL BASIS OF ICE SHEET MODELLING. Proceedings of the Vancouver Symposium, August, 1987. International Association of Hydrological Sciences (IAHS) Publication No.170. 313-322.

Boucher, Keith (1975) GLOBAL CLIMATE. The English University Press Ltd. 326 p.

Bowles, Joseph E. (1978) ENGINEERING PROPERTIES OF SOILS AND THEIR MEASUREMENT. McGraw-Hill Book Company, U.S.A. 213 p.

Bozhinsky, A. N.; Krass, M. S.; and Popounin, V. V. (1986) Role of debris cover in the thermal physics of glaciers. JOURNAL OF GLACIOLOGY. V-32, NO.111. 255-266.

Braithwaite, Roger J. (1981) On glacier energy balance, ablation, and air temperature. JOURNAL OF GLACIOLOGY. V-27, No.97. 381-391.

Burbank, Douglas W. and Fort, Monique B. (1985) Bedrock Control on Glacial Limits: Examples from the Ladakh and Zanskar Range, North-Western Himalaya, India. JOURNAL OF GLACIOLOGY. V-31, No.108. 143-149.

Butkovich, T. R. (1955) Density of single crystals of ice from a temperate glacier. JOURNAL OF GLACIOLOGY. 1955 Vol.2 No.18, pp. 553-559.

Cameron Wake (1985) Measurement of Snowcover using Satellite Imagery. SNOW AND ICE HYDROLOGY PROJECT ANNUAL REPORT 1985.

Chorley, Richard J.; Schumm, Stanley A.; and Sugden, David E. (1984) GEOMORPHOLOGY. Methen & Co. Ltd., London. 605 p.

Clayton, Lee and Moran, Stephen R. (1974) A glacial process-form model. GLACIAL GEOMORPHOLOGY. Edited by Donald R. Coates. Publications in Geomorphology State University of New York, Binghamton, New york. 89-120.

Collins, David (1988) Hydrometeorological and Hydrological networks: an introduction. Presentation in the SNOW AND ICE WORKSHOP, 1988 in WLU, Waterloo, Canada.

Dean, Willard W. (1974) Maclure Glacier, California. A contribution to the International Hydrological Decade. Proceedings of the WESTERN SNOW CONFERENCE. 42nd. Annual Meeting, Anchorage, Alaska, April 16-20, 1974. Colorado State University, Colorado. 1-8.

Drewry, David (1986) GLACIAL GEOLOGIC PROCESSES. Scott Polar Research Institute, University of Cambridge. Edward Arnold. 276 p.

Dyson, James L. (1972) THE WORLD OF ICE. Alfred A. Knope, Inc., New York, 292 p.

Echelmeyer, Keith and Kamb, Barclay (1987) Glacier flow in a curving channel. JOURNAL OF GLACIOLOGY. V-33, No.115. 281-292.

Embleton,Clifford (1979) Glacial Processes. PROCESS IN GEOMORPHOLOGY. Edited by Clifford Embleton and John Thrones. John Wiley & Sons, New York.

Embleton, Clifford and King, Cuchlaine A.M. (1975) GLACIAL GEOMORPHOLOGY. Edward Arnold, U.K. 573p.

ENCYCLOPEDIA BRITANNICA (1984) Karakoram Range. V-10, pp.402-403.

Finsterwalder, Richard (1960) German glaciological and geological expedetions to the Batura Mustagh and Karakoram Range. JOURNAL OF GLACIOLOGY. 1960, Vol.3 No.28, pp. 787-788.

Flint, Richard Foster (1957) GLACIAL AND PLEISTOCENE GEOLOGY. John Wiley & Sons, Inc. New York. 553 p.

Flint, Richard Foster (1971) GLACIAL AND QUATERNARY GEOLOGY. John Wiley & Sons, Inc. New York. 892 p.

Folk, Robert L. (1962) PETROLOGY OF SEDIMENTARY ROCKS. Hamphill's Texas. 170 p.

Foutain, Andrew G. and Tangborn Wendell V. (1985) The effect glaciers on streamflow variations. WATER RESOURCES RESEARCH. V-21, No.4. American Geographical Union. 579-586.

Fuggle, R. F. (1970) A Computor Programme for Determine Direct Short-Wave Radiation Income on Slope. CLIMATOLOGICAL BULLETIN NO.7. January, 1970.

Fujii, Yoshiyuki (1974) Field Experiment on Glacier Ablation Under a Layer of Debris Cover. SEPPYO. Journal of the Japanese Society of Snow and Ice. 20-21.

Fujii, Yoshiyuki; and Higuchi, Keiji (1977) Statistical Analysis of thr Form of the Glaciers in the Khumbu Himal. SEPPYO. Journal of the Japanese Society of Snow and Ice. V-39, Special Issue, 1977. 7-14.

Gardner, James (1986) Rakhiot Glacier Research-1986. SNOW AND ICE HYDROLOGY PROJECT ANNUAL REPORT, 1986. Canadian Centre, WLU.

Garnier, B. J. and Ohmura, Atsumu (1968) A method of calculating the direct short-wave radiation income of slopes. JOURNAL OF APPLIED METEOROLOGY, V-7. October, 1968.

Garnier, B. J. and Ohmura, Atsumu (1970) The elevation of surface variation radiation income. SOLAR ENERGY. V-13. 1970, pp. 21-34. Pergamon Press, U.K.

Geiger, R. (1969) Topoclimates. GENERAL CLIMATOLOGY, 2. Edited by H. Flohn.

Glen, J. W. (1952) Experiments on the deformation of ice. JOURNAL OF GLACIOLOGY. V-2, No.12, 111-114.

Glen, J. W. (1963) The rheology of ice. ICE AND SNOW: Properties, Processes, and Applications. Proceedings of a Conference held at the Massachusetts Institute of Technology, February 12-16,1962, Edited by W. D. Kingery. The M. I. T. Press, Cambridge, Massachusetts.

Goudie, Andrew (1984) THE NATURE OF THE ENVIRONMENT. Basil Blackwell Publisher Limited, Oxford, England. 331 p.

Goudie, A.S.; Brunsden, D.; Collins, D.N. and others (1984) The geomorphology of the Hunza Valley, Karakoram mountains, Pakistan. THE INTERNATIONAL KARAKORAM PROJECT VOL-2. Edited by K.J. Miller. Camridge University Press, London. 359-410.

Goudie, A.S.; Jones, David K.C.; and Brunsden, Denys (1984) Recent fluctuations in some glaciers of the western Karakoram mountains, Hunza, Pakistan. THE INTERNATIONAL KARAKORAM PROJECT VOL-2. 411-455.

Gordon, John E.; Birnie, Richard V.; and Timmis, Roger (1978) A major rockfall and debris slide on the Lyell Glacier, South Georgia. ARCTIC AND ALPINE RESEARCH. V-10, No.1. 49-60.

Grove, J. M. (1987) Glacier Fluctuations and Hazards. GEOGRAPHICAL JOURNAL. V-153, No.3, 351-369.

Hewitt, Kenneth (1982) Natural dams and outburst floods of the Karakoram Himalaya. HYDROLOGICAL ASPECTS OF ALPINE AND HIGH MOUNTAIN AREAS (Proceedings of the Exeter symposium, July 1982). IAHS Publ. no.138. 259-269.

Hewitt, Kenneth (1985a) The Snow and Ice Hydrology Project: An Overview. SNOW AND ICE HYDROLOGY PROJECT ANNUAL REPORT 1985.

Hewitt, Kenneth (1985b) Glacier Hydrology Investigations: The Biafo Glacier System, Central Karakoram. S. I. H. P. ANNUAL REPORT 1985. 90-116.

Hewitt, Kenneth (1985c) Experimental Studies: Influence of debris covers on glacier ablation. SYNOPTIC REPORT: FIELD SEASON 1985. Snow and Ice Hydrology Project. W.L.U. Canada., pp.3-5.

Hewitt, Kenneth (1985d) SNOW AND ICE CONDITIONS IN THE UPPER INDUS BASIN: A REVIEW AND BIBLIOGRAPHY. Wilfrid Laurier University, Waterloo, Canada. 55p.

Hewitt, Kenneth (1988a) SNOW AND ICE HYDROLOGY IN REMOTE, HIGH MOUNTAIN REGIONS: THE MIMALAYA SOURCES OF THE RIVER INDUS. S.I.H.P. Working Paper No.1. 29 p.

Hewitt, Kenneth (1988b) The Snow and Ice Hydrology Project: Reasearch and Training for Water Resource Development in the Upper Indus Basin. JOURNAL OF CANADA-PAKISTAN COOPERATION (Special issue on Water Resource Management). Vol.2 No.1, July 1988.

Hoinkes, H. (1955) Measurements of ablation and heat balance on Alpine Glaciers. JOURNAL OF GLACIOLOGY. 1955, Vol.2 No.17, pp.497-501.

Hobson (1972) Surface roughness in topography: A quantitative approach. SPATIAL ANALYSIS IN GEOMORPHOLOGY. Edited by R. J. Chorley. Harper & Row Publishers. 393 p.

Hubley, Richard C. (1954) The problem of short period measurements of snow ablation. JOURNAL OF GLACIOLOGY. 1954, Vol.2 No.16, pp.437-440.

Ikegani, Koichi and Inoue, Jiro (1978) Mass Balance Studies on Kongma Glacier, Khumbu Himal. SEPPYO. Journal of the Japanese Society of Snow and Ice. V-40, Special Issue, 1978. 12-16.

Inoue, Jiro (1977) Mass Budget of Khumbu Glacier. SEPPYO. V-39, Special Issue, 1977. 15-19.

Inoue, Jiro and Yoshida, minoru (1980) Ablation and Heat Exchange over the Khumbu Glacier. SEPPYO. Journal of the Japanese Society of Snow and Ice. V-41, 1980.

Iwata, Shuji; Watanabe, Okitsugu; and Fushimi, Hiroji (1980) Surface morphology in the ablation area of the Khumbu glacier. SEPPYO. Journal of the Japanese Society of snow and Ice. V-41, pp.9-17.

Janes, J. Robert (1976) GEOLOGY AND THE NEW GLOBAL TECTONICS. An Introduction to Physical and Historical Geology. The Macmillan Company of Canada Limited. 468 p.

Kamb, Barclay; Raymond, C. F.; Harrison, W. D.; and others (1985) Glacier Surge Mechanism. SCIENCE. V-227, No.4686. 1985, pp. 469-479.

Kick, W. (1978) Material for a glacier inventory of the Indus drainage basin - The Nanga Parbat Massif. WORLD GLACIER INVENTORY. IAHS-AISH Publ. No.126, 1980, pp. 105-109.

King, Cuchlaine A. M. (1984) GLACIATION: ASPECT OF GEOGRAPHY. Macmillan Education Ltd. USA. 60 p.

Kotlyakov, V. M. and Dolgushin, L. D. (1972) Possibility of artificial augmentation of melting by surface dusting of glaciers (results of Soviet Investigators) THE

ROLE OF SNOW AND ICE IN HYDROLOGY. Proceedings of the Banff Symposium, September 1972. IAHS Piblication No.107, 2 Volumes. 1421-1426.

Krimmel, R. M. and Tangborn, W. V. (1974) South Cascade Glacier: The moderating effect of glaciers on runoff. Proceedings of the WESTERN SNOW CONFERENCE. 42nd Annual Meeting, Anchorage Alaska, April 16-20, 1974. Colorado State University, Colorado. 9-13.

Kuusisto, Esko (1984) SNOW ACCUMULATION AND SNOWMELT IN FINLAND. Publications of the Water Research Institute. Vesihallitus--National Board of Waters, Finland. 149p.

LaChapelle, E. (1959) Errors in ablation measurements from settlement and sub-surface melting. JOURNAL OF GLACIOLOGY. 1959, Vol.3 No.26, pp.458-467.

Lockwood, John G. (1974) WORLD CLIMATOLOGY. Edward Arnold (Publishers) Ltd. Great Britain. 330 p.

Loewe, F. (1961) Glaciers of Nanga Parbat. PAKISTAN GEOGRAPHICAL REVIEW. Vol.16, No.1, 1961, pp. 19-24.

Lewkowicz, Anton G. (1986) Rate of short-term ablation of exposed ground ice, Banks Island, Northwest Territories, Canada. JOURNAL OF GLACIOLOGY. V-32, No.112, 511-519.

Lydolph, Paul E. (1985) THE CLIMATE OF THE EARTH. Rowman & Allanheld Publishers U.S.A. 386 p.

Mani, Anna (1976) Radiation measurements for solar energy applications. SOLAR ENERGY. WMO-No.477. World Meteorological Organization. Geneva-Switzerland.

Mason, K. (1930a) The Glaciers of the Karakoram and Neighbourhood. RECORDS OF THE GEOLOGICAL SURVEY OF INDIA. Vol.63, pt.2, pp. 214-278.

Meier, Mark F. (1962) Proposed definitions for glacier Mass Budget terms. JOURNAL OF GLACIOLOGY. 1962, Vol.4 No.33, pp.252-261.

Middleton, D. (1984) Karakoram history; early exploration. THE INTERNATIONAL KARAKORAM PROJECT VOL-2. 17-31.

Muller, Fritz and Keeler, Charles M. (1969) Errors in short-term ablation measurements on melting ice surfaces. JOURNAL OF GLACIOLOGY. Vol.8 No.52, pp.91-105.

Mercer, J. H. (1975) Glaciers of the Karakoram. MOUNTAIN GLACIERS OF THE NORTHERN HEMISPHERE. Vol.1, Cold Regions Research and Engineering Laboratory, Hanover, New Hampshire, U.S.A. pp.371-409.

Moribayashi, Shigeo; and Higuchi, Keiji (1977) Characteristics of Glaciers in the Khumbu Region and their Recent Variations. SEPPYO. V-39, Special Issue, 1977. 3-6.

Nakawo, Masayoshi and Takahashi, Shuhei (1982) A simplified model for estimating glacier ablation under a debris layer. HYDROLOGICAL ASPECTS OF ALPINE AND HIGH MOUNTAIN AREAS. (Proceeding of the Exeter symposium, July 1982). IAHS Publ. no.138.

Nakawo, M. and Young, G. J. (1981) Field Experiments to Determine the Effect of a Debris Layer on Ablation of Glacier Ice. ANNALS OF GLACIOLOGY 2, 1981. International Glaciological Society. pp.85-91

Nakawo, M. and Young, G. J. (1982) Estimate of Glacier Ablation under a debris layer from surface temperature and meteorological variable. JOURNAL OF GLACIOLOGY. Vol.28, No.98, 1982, pp. 29-34.

Nye, J. F. (1952) The mechanics of glacier flow. JOURNAL OF GLACIOLOGY. V-2, No.12. 81-93.

Nye, J. F. (1969) The effect of longitudinal stress on the shear stress at the base of an ice sheet. JOURNAL OF GLACIOLOGY. V-8, No.53. 207-213.

Ogilvie, I. H. (1904) The effect of superglacial debris on the advance and retreat of some Canadian glaciers. JOURNAL OF GLACIOLOGY. V-12, 722-743.

Ostrem, Gunnar (1972) Runoff forecasts for highly glacierized basins. THE ROLE OF SNOW AND ICE IN HYDROLOGY. Proceedings of the Banff Symposium, September 1972. IAHS Publication No. 107, 2 Volumes. 1111-1132.

Ostrem, G. and Stanley, A. (1969) GLACIER MASS BALANCE MEASUREMENTS; A MANNUAL FOR FIELD AND OFFICE WORK. (Revised edition). The Canadian Development of Energy, Mines and Resourses, Glaciology Subdivision; and The Norwegian Water Resources and Electricity Baord, Glaciology Section. Reprint Series No.66.

Paterson, W. S. B. (1980) Ice sheet and Ice shelves. DYNAMICS OF SNOW AND ICE MASSES. Edited by Colbeck, Samuel C. Academic Press, New York. 1-78.

Paterson, W.S.B. (1981) THE PHYSICS OF GLACIERS. Pergamon Press. 380p.

Pfeffer, W. Tad and Bretherton, Christopher S. (1987) The effect of crevasses on the solar heating of a glacier surface. THE PHYSICAL BASIS OF ICE SHEET MODELLING. Proceedings of the Vancouver Symposium, August, 1987. IAHS Publication No.170. 191-205.

Platt, C.M. (1966) Some observations on the climate of Lewis Glacier, Mount Kenya. JOURNAL OF GLACIOLOGY. Vol.6 No.44.

Posamentier, Henry W. (1977) A new climatic model for glacier behavior of the Austrian Alps. JOURNAL OF GLACIOLOGY. V-18, No.78, 57-65.

Power, J. M. and Young, G. J. (1979) Application of an Operational Hydrologic Forecasting model to a Glacierized Research Basin. Paper presented at THIRD NORTHERN RESEARCH BASIN SYMPOSIUM WORKSHOP, Quebec City, Quebec, June 11-15, 1979.

Raymond, C. F. (1980) Temperate Valley Glaciers. DYNAMICS OF SNOW AND ICE MASSES. Edited by Colbeck, Samuel C. Academic Press, New York. 79-139.

Rice, R. J. (1977) FUNDAMENTALS OF GEOMORPHOLOGY. Longman Group Limited, London & New York. 387p.

Rigsby, G. P. (1960) Crystal orientation in glacier and experimentally deformed ice. JOURNAL OF GLACIOLOGY. V-3, No.27, 1960. 589-606.

Ringenoldus, James C. (1975) Flood Forecasting and Flood Warning Systems. APPRAISAL OF FLOOD MANAGEMENT SYSTEMS IN PAKISTAN VOL-1. Harza Engineering International, Pakistan.

Schytt, Valter (1967) A study of ablation gradient. GEOGRAFISKA ANNALER. 49A (1967), 2-4. pp. 327-332.

Seligman, G. (1950) The specific gravity of ice. JOURNAL OF GLACIOLOGY. Vol.1 No.8, p. 442.

Sharp, Robert P. (1960) GLACIERS. Condon Lectures, Oregon State System of Higher Education, University of Oregan. 78 p.

Shipton, Eric (1940) Karakoram 1939. THE GEOGRAPHICAL JOURNAL. V-95, No.6, June 1940. pp. 409-427.

Sugden, David E. and John, Brian S. (1976) GLACIERS AND LANDSCAPE: A Geomorphological Approach. Edward Arnold, Great Britain. 376 p.

Tahirkhel, R. A. K. and Jan, Q. M. (1984) The geographycal and geological domains of the Karakoram. THE INTERNATIONAL KARAKORAM PROJECT VOL-2. 57-70.

Tarar, Riaz Nazir (1982) Water resources investigation in Pakistan with the help of Landsat imagery - Snow surveys 1975-1978. HYDROLOGICAL ASPECTS OF ALPINE AND HIGH MOUNTAIN AREAS (Proceedings of the Exeter Symposium, July 1982). IAHS Publ. no.138. 177-190.

Tarbuck, Edward J.; and Lutgens, Frederick K. (1976) EARTH SCIENCE. Charles E. Merrill Publishing Company. Columbus, Ohio. 493 p.

Thompson, Russell (1977) THE INFLUENCE OF CLIMATE ON GLACIERS AND PERMAFROST. Geographical Papers. Department of Geography, University of Reading. England. 44 p.

Vohra, C. P. (1981) Himalayan Glaciers. THE HIMALAYA, ASPECTS OF CHANGE.

Edited by Lall, J. S., Oxford University Press.

Wake, Cameron (1985) Preliminary work towards a geographic information systems approach to predicting runoff from the Upper Indus Basin. S.I.H.P. ANNUAL REPORT, 1985. 77-89.

Wake, Cameron (1987) SPATIAL AND TEMPORAL VARIATION OF SNOW ACCUMULATION IN THE CENTRAL KARAKORAM, NORTHERN PAKISTAN. Master Thesis, Wilfrid Laurier University, Waterloo, Ontario. 121 p.

Wake, Cameron and Limnoterra, 1987. ECOBUG AND EPSON MANNUAL. Snow and Ice Hydrology Project. WLU, Waterloo, Ontario, Canada. 31p.

WAPDA (1982) Proposal for a Study of Water, Ice, and Snow Balance of the U.I.B. Pakistan in Collaboration with Canadian Universities, Institutes. HID. Lahore, Pakistan.

Ward, W. H. (1950) The physics of deglaciation in Central Baffin Island. JOURNAL OF GLACIOLOGY. Vol.2 No.11, pp. 9-22.

Watanabe, O.; Iwata, S.; and Fushimi, H. (1986) Topographic characteristics in the ablation area of the Khumbu glacier, Nepal Himalaya. ANNALS OF GLACIOLOGY 8, 1986. pp.177-180. International Glaciology Society.

Wieder, Sol (1982) AN INTRODUCTION TO SOLAR ENERGY FOR SCIENTISTS AND ENGINEERS, John Wiley & Sons, New York.

Wilson, J. Warren (1953) The initiation of dirt cones on snow. JOURNAL OF GLACIOLOGY. Vol.2 No.14, pp. 281-287.

World Meteorological Organization (1977) FLOOD FORECASTING AND WARNING SYSTEM FOR THE INDUS RIVER BASIN PAKISTAN. Aplan for improving Flood Forecasting Networks in Pakistan. Technical Report-1, 1977. United Nations Development Programme, WMO, Geneva.

Wushiki, Hisao (1977) Ice Cliffs and Exposed Stratigraphy of Kongma Glacier, Khumbu. SEPPYO. V-39, Special Issue, 1977. 22-25.

Yafeng, Shi and Xiangsong, Zhang (1984) Some Studies of the Batura Glacier in the Karakoram Mountains. THE INTERNATIONAL KARAKORAM PROJECT. Edited by K.J. Miller, University Press, Cambridge.

Yao, Augustine Y. M. (1981) Agricultural Climatology. GENERAL CLIMATOLOGY,3. Edited by H. E. Landsberg. World Survey of Climatology V-3. Elsvier Scientific Company, New York.

Young, G. J. (1971) Accumulation and ablation patterns as functions of the surface geometry of a glaciar. IAHS-AISH Publ. No. 104, 1975. Proceedings of the Moscow Symposium, August 1971. 134-139.

Young, G. J. (1976) An Approach to Glacier Mass-Balance Analysis Utilizing Terrain Characterization. INLAND WATERS DIRECTORATE, Scietific Sereis No.60, Environment Canada.

Young, G. J. (1977) GLACIAR OUTBURST FLOODS. Paper presented at Canadian Hydrology Symposium. 77-Floods, Edmonton, Alberta. August 1977.

Young, G. J. (1980) Monitoring Glacier Outburst Floods. NORDIC HYDROLOGY. 285-300.

Young, G. J. (1981) Glacier contribution to streamflow in the Himalayan Region. PROFESSIONAL DEVELOPMENT AWARD. International Development Research Centre.

Young, G. J. and Hewitt, K. (1988) HYDROLOGY RESEARCH IN THE UPPER INDUS BASIN, KARAKORAM HIMALAYA, PAKISTAN.

Zotikov, I. A. (1986) THE THERMOPHYSICS OF GLACIERS. Glaciology and Quaternary Geology. D. Reidel Publishing Company, Holland. 275p.

Zotikov, I. A. and Moiseeva, G. P. (1972) A theoretical study of ice surface dusting influence on melting intensity. THE ROLE OF SNOW AND ICE IN HYDROLOGY. Proceedings of the Banff Symposium, September 1972. IAHS Publication No. 107, 2 Volumes. 1410-142.